POLITECNICO
MILANO 1863

SCUOLA DI INGEGNERIA INDUSTRIALE
E DELL'INFORMAZIONE

Integrating Bio-Hydrogen Production for Optimal Hydrogen Supply in Stegra's Fossil-Free Iron and Steelmaking.

Tesi di Laurea Magistrale in
Chemical Engineering - Ingegneria Chimica

Author: **Laura Pesaresi**

Student ID: **248499**
Advisor: **Prof. Flavio Manenti**
Co-advisors: **Klas Engvall** (Division of Process Technology, KTH Royal Institute of Technology),
Marita Nilsson (Hydrogen Technology and Innovation Lead, STEGRA),
Joakim Lundgren (Division of Energy Science, Luleå University of Technology)

Academic Year: **2024-25**

Abstract

The iron and steel sector accounts for a significant share of global greenhouse gas emissions, largely due to fossil-based reduction routes. Achieving deep decarbonization requires alternative solutions, and renewable hydrogen has emerged as a crucial pathway. This thesis, developed in collaboration with Stegra, KTH Royal Institute of Technology, Luleå University of Technology, and Politecnico di Milano, investigates the role of biomass gasification as a complementary pathway to electrolysis for renewable hydrogen production in fossil-free steelmaking.

The work takes Stegra's large-scale Direct Reduced Iron (DRI) facility under construction in Boden, Sweden, as a reference case. A complete plant design was developed, consisting of a circulating fluidized bed gasifier integrated with partial oxidation, water-gas shift, and pressure swing adsorption units. Based on process simulation, the system achieves a hydrogen yield of 40.5 kg per ton of biomass and a thermal efficiency of 58%, supplying up to 17% of the hydrogen demand from the DRI plant.

Economic analysis highlights the strong sensitivity of the Levelized Cost of Hydrogen (LCOH) to biomass price, steam generation strategy, and CO_2 capture. In its most favorable configuration, the process can deliver hydrogen at 3.6 €/kg, making it competitive with electrolysis. At the same time, it offers clear advantages: the chance to reach negative emissions with CO_2 capture, the use of renewable feedstock, and the integration with electrolytic oxygen that enhances overall efficiency. The study also considers innovative technologies such as SATS for H_2S splitting, which could further boost total hydrogen production while improving process efficiency.

Overall, the results show that biohydrogen can play a practical and scalable role in decarbonized steel production. By combining cost-effectiveness, flexibility, and synergies with existing technologies, biomass gasification strengthens the resilience and sustainability of hydrogen supply in the transition toward fossil-free steel.

Keywords: Biohydrogen, Biomass gasification, Fossil-free steel, Direct reduced iron (DRI), Techno-economic analysis, LCOH, CO_2 capture, Electrolysis integration.

Abstract in lingua italiana

Il settore siderurgico è tra le principali fonti globali di emissioni di gas serra, per la forte dipendenza da processi di riduzione fossili. La decarbonizzazione richiede soluzioni alternative, e l'idrogeno rinnovabile si è affermato come soluzione chiave. Questa tesi, sviluppata in collaborazione con Stegra, KTH Royal Institute of Technology, Luleå University of Technology e Politecnico di Milano, analizza il ruolo della gassificazione della biomassa come percorso complementare all'elettrolisi per la produzione di idrogeno destinato alla siderurgia fossile-free.

Il lavoro prende a riferimento la domanda di idrogeno del nuovo impianto DRI di Stegra, in costruzione a Boden, Svezia. È stato sviluppato il design completo dell'impianto, comprendente un gassificatore a letto fluido circolante integrato con ossidazione parziale, water-gas shift e pressure swing adsorption. Le simulazioni mostrano una produzione di 40,5 kg di idrogeno per tonnellata di biomassa, con un rendimento termico del 58%, in grado di coprire fino al 17% della domanda di idrogeno del DRI.

L'analisi economica evidenzia come il costo livellato dell'idrogeno (LCOH) dipenda soprattutto dal prezzo della biomassa, dalla generazione del vapore e dall'adozione di sistemi di cattura della CO_2. Nella configurazione più favorevole, il processo può fornire idrogeno a 3,6 €/kg, risultando competitivo con l'elettrolisi. Al contempo, offre vantaggi significativi: possibilità di emissioni negative con cattura della CO_2, utilizzo di biomassa rinnovabile e integrazione con l'ossigeno da elettrolisi per migliorare l'efficienza. Lo studio considera anche tecnologie innovative come il processo SATS per la scissione dell'H_2S, in grado di aumentare la produzione totale di idrogeno e migliorare le prestazioni del sistema.

Nel complesso, i risultati mostrano come il bioidrogeno possa avere un ruolo concreto e scalabile nella produzione di acciaio decarbonizzato. Grazie a competitività economica, flessibilità e sinergie con tecnologie esistenti, la gassificazione della biomassa rafforza la resilienza e la sostenibilità della fornitura di idrogeno nella transizione verso una siderurgia fossile-free.

Parole chiave: Bioidrogeno, Gassificazione della biomassa, Acciaio fossile-free, Riduzione diretta del minerale di ferro (DRI), Analisi tecno-economica, LCOH, Cattura della CO_2, Integrazione con elettrolisi.

Contents

Introduction

The iron and steel industry is one of the most resource- and energy-intensive sectors globally and contributes significantly to global greenhouse gas (GHG) emissions. Despite considerable improvements in energy efficiency and production technologies, the overall carbon footprint of the industry has continued to grow due to the rising global demand for steel [1]. Globally, the iron and steel industry accounts for 7.2% of global anthropogenic CO_2 emissions [2] and around 7% of global energy-related emissions [3]. Achieving a climate-safe future, as outlined by the Paris Agreement, requires reaching net-zero emissions by 2050 and net-negative thereafter, including in hard-to-abate sectors like steel [4]. A global shift to renewable and alternative energy is needed to cut GHG emissions (mainly CO_2) by 60% by 2050, aiming to limit global warming to below 2 °C [5]. Deep decarbonization of steel production requires a systemic transformation of both the steelmaking process and the broader energy system in which it operates. The technologies required for this transition are not yet commercially available and are currently under development in a series of mostly European innovation projects. However, since 2016, major steel manufacturers have declared their ambitions to pursue deep decarbonization [6]. Several incumbent steel producers have announced the construction of demonstration plants, with some companies communicating plans to introduce 'green' steel to the market within the next decade. Achieving a radical reduction in carbon emissions from iron and steel production requires a combination of measures, particularly the development and deployment of breakthrough technologies with near-zero or zero carbon emissions. The primary strategy involves a shift away from the conventional primary steelmaking route, which relies on the blast furnace followed by the basic oxygen furnace (BF-BOF). This route is the main source of CO_2 emissions in the sector, due to its dependence on fossil carbon in blast furnaces (BFs)[7]. The BF process currently dominates ironmaking technologies and is responsible for around 80% of the total CO_2 emissions from primary iron and steel production [3].

Instead, the industry is moving toward hydrogen-based iron ore reduction. This emerging pathway consists of producing direct reduced iron (DRI) or hot briquetted iron (HBI), followed by melting in electric arc furnaces (EAFs) for final steel production [7]. This

transition represents a fundamental shift in steel manufacturing, requiring substantial advancements in technology, infrastructure, and energy supply. The successful deployment of these innovations will be critical in achieving a low-carbon steel industry.

Scrap-based steelmaking using EAFs is also gaining traction as a decarbonization route; however, concerns over future shortages of high-quality scrap suggest that fossil-free DRI will be essential to supplement scrap availability [3].

Fossil-free ironmaking thus holds the greatest potential for achieving deep emission cuts in the sector. In this context, accelerating the development and deployment of fossil-free DRI technologies becomes crucial. Among the various DRI pathways, biomass-based DRI offers particular promise, especially for countries with ample and sustainably managed biomass resources. Biomass is renewable, versatile, and increasingly recognized as a viable low-carbon alternative to fossil carbon in the steel industry. Accordingly, there is growing interest in expanding biomass utilization in steelmaking processes to support the industry's transition to a sustainable, carbon-neutral future [3].

0.1. GHG Emissions in Steel: A Core Issue

Wang et al. (2021) [1] conducted a comprehensive study analyzing the historical emissions from steel production over the past century (1900–2015) using a combination of Material Flow Analysis (MFA) and Life Cycle Assessment (LCA). The results of this analysis are shown in Figure 1, and it can be stated that the direct emissions from the use of fossil coal and coke in blast furnaces constituting the largest emission source. Their findings, moreover, highlight the stagnation of efficiency improvements in recent decades and emphasize the urgent need for integrated mitigation strategies. The study estimates that approximately 45 gigatonnes (Gt) of steel were produced between 1900 and 2015, resulting in cumulative emissions of around 147 Gt CO_2 -equivalent. While process efficiency improvements have led to a 67% reduction in carbon intensity, the expansion of steel production—by a factor of 44—has driven a 17-fold net increase in annual emissions.

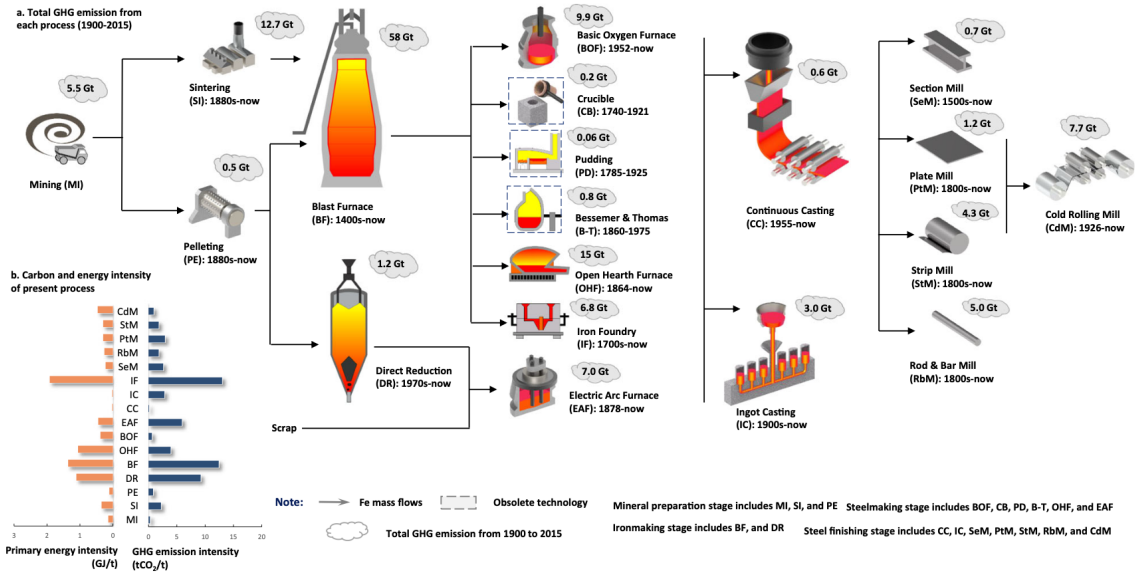

Figure 1: Steel production technologies and their total GHG emissions from 1900 to 2015 (adopted by [1]).

0.2. Biomass Gasification and Hydrogen Production

The transition to low-emission technologies requires a shift to renewable energy sources, reducing reliance on fossil fuels while optimizing existing energy systems. Biomass, as a carbon-neutral energy resource, offers a sustainable alternative with lower environmental impact [8]. Biomass can be converted into energy through various biochemical and thermochemical processes, including combustion, pyrolysis, liquefaction, and gasification. Among these, gasification plays a pivotal role in meeting future energy demands by enabling the production of high-quality syngas, which can be further processed into hydrogen, high-value fuels, or chemical feedstocks [9]. Compared to combustion and pyrolysis, the gasification process allows for higher energy recovery efficiency and generates a cleaner gas, making it particularly suitable for industrial applications [8]. Given its potential to generate hydrogen, biomass gasification presents a key opportunity for decarbonizing industries such as steel manufacturing while contributing to a sustainable energy transition. Research has explored different gasification reactor designs, feedstocks, and operational conditions to optimize hydrogen production. The process can integrate with existing industrial infrastructure, paving the way for large-scale implementation. Further advancements in reactor configurations, syngas upgrading, and techno-economic assessments continue to support the commercial viability of biomass gasification as a cornerstone of the future low-carbon energy system.

0.3. Biomass Integration for Steel Decarbonization

The integration of biomass with carbon capture and storage—commonly referred to as BECCS— is gaining more interest as an effective strategy for achieving net-zero emissions or even creating negative emissions. Countries with ambitious climate targets, such as Sweden, have introduced policy incentives to promote BECCS deployment [10], creating new opportunities for its implementation within the iron and steel industry.

In this context, biomass-based pathways could serve as a complementary route alongside the hydrogen-based direct reduced iron (H_2-DRI) approach. The H_2-DRI pathway holds considerable promise for fossil-free steel production through the use of green hydrogen and renewable electricity. It has gained significant momentum and is currently the main decarbonisation strategy considered by the EU steel industry [11]. Despite the potential, deploying H2-based DRI to decarbonise steelmaking has to overcome several critical challenges, including the need for substantial quantities of renewable electricity, robust grid and hydrogen infrastructure, and the availability of cost-competitive hydrogen [3].

Studies have shown that biochar can be used as a reducing agent to replace coking coal in iron and steel production (for example see [12], [13], [14]). In contrast, fewer studies have focused on the use of biomass-derived gas for DRI production. This represents a promising opportunity, especially considering that current DRI technologies such as MIDREX and HYL-III are gas-based. Biomass gasification is a key technology for producing syngas (biosyngas) from biomass, and it has been extensively studied in the literature, especially regarding process configuration [3].

Biomass gasification is a mature technology, as evidenced by the commercial deployment of biomass gasification plants over the past decades. This suggests a high technology readiness level (TRL) for biomass gasification, typically in the range of 7–9 [3]. Considering the maturity of both gasification and DRI technologies, the integration of the two processes can be seen as a "low-hanging fruit", offering a practical opportunity to facilitate biomass use within the iron and steel industry. When combined with carbon capture, such integration would also enable the production of a pure CO_2 stream suitable for transport or utilisation, thereby creating a significant opportunity for the production of carbon-negative steel.

Furthermore, DRI produced from biosyngas may exhibit similar metallurgical properties to fossil-based DRI, allowing it to be used within existing DRI/EAF routes with minimal need for reconfiguration. Despite its promise, the combined application of biomass gasification, DRI processes, and CCS in steelmaking remains underexplored, primarily

due to the complexity of integrating these technologies, limited industrial demonstration, uncertainties in biomass supply, and the lack of strong economic and policy incentives [3]. While some prior studies have examined the use of biosyngas and bio-based synthetic natural gas (bio-SNG) for heating applications in steel plants, few have addressed its direct role in DRI production within integrated steelmaking systems (for example see [15], [16], [17]).

0.4. Stegra: A Step Toward Green Industry

Stegra, founded in 2020 in Sweden (initially as *H2 Green Steel* and rebranded in 2024 to reflect a broader mission), is one of the most innovative emerging players in the global decarbonization landscape. The name *Stegra*, derived from a Swedish word meaning "to elevate", reflects the company's ambition to accelerate the transition toward sustainable industry. While steel is the starting point, Stegra envisions extending its model to other hard-to-abate sectors such as cement, chemicals, and heavy industry in general. Beyond Sweden, the company is also developing projects in Portugal, Canada, and Brazil, aiming to replicate its green industrial revolution on a global scale.

The initial focus remains steel, one of the most carbon-intensive industries, responsible for roughly 7% of global CO_2 emissions, as already mentioned. Reducing the footprint of this sector is therefore essential to achieving climate targets. Stegra's strategy is based on three integrated technological pillars, which together form the process chain of its new plant in Boden, northern Sweden:

- **Green hydrogen:** one of the world's largest electrolyzers (740 MW installed capacity), powered by low-cost renewable electricity to provide green hydrogen as a reducing agent.
- **Green iron:** a direct reduction iron (DRI) facility where hydrogen replaces coal and coke, producing water instead of CO_2 as a by-product.
- **Green steel:** a fully electrified and digitalized steelmaking facility designed to deliver near-zero emissions steel at large scale.

The Boden site represents the core of Stegra's strategy. Production is planned to start in 2026, and by 2030 the facility is expected to reach a capacity of up to 5 million tonnes of green steel per year, cutting emissions by up to 95% compared to conventional blast furnace processes.

This combination of industrial scale, digitalization, and sustainability makes Stegra's project a pioneering model worldwide. By proving that even one of the hardest sectors

to decarbonize can transition toward low emissions, the company is not only producing clean steel but also setting new benchmarks for the industry of the future, contributing concretely to the creation of a low-carbon economy.

0.5. Project Scope and Objectives

This master's thesis, developed in collaboration with Stegra, explores biomass gasification as a complementary pathway to electrolysis for hydrogen production in the direct reduction of iron ore (DRI). The study takes Stegra's Boden plant in northern Sweden as the reference case and investigates the potential of integrating bio-hydrogen to improve energy efficiency and reduce production costs.

The research focuses on four main objectives: (i) assess mature and cost-effective gasification technologies for hydrogen generation and integration with electrolysis and steelmaking; (ii) identify suitable biomass feedstocks based on regional availability; (iii) conduct a techno-economic evaluation of combined bio- and electrolytic hydrogen supply; and (iv) benchmark the performance and competitiveness of this integrated approach against an electrolysis-only system.

0.6. Expected Contributions

This thesis supports Stegra's goal of producing low-carbon steel by evaluating biomass gasification as an additional source of hydrogen. The study will clarify under which conditions bio-hydrogen can complement or partially replace electrolytic hydrogen, focusing on technical feasibility, energy security, and cost impact. The results are intended to provide concrete guidance for future green hydrogen projects within Stegra and contribute to scaling up sustainable steel production.

Chapter 1 provides an overview of hydrogen production technologies, current global demand, and end-use applications, with a particular focus on the hydrogen production approach adopted by Stegra in their Boden facility. Chapter 2 introduces the theoretical background of biomass gasification, examining its operating principles and exploring strategies to optimize the process for hydrogen production. Chapter 3 presents the designed biomass gasification pathway selected for this study, detailing its configuration and integration within the broader hydrogen production framework. Chapter 4 contains the techno-economic analysis, evaluating the performance, costs, and viability of the proposed pathway based on simulation results. Finally, Chapter 5 offers an overview of existing biomass gasification plants, providing context and benchmarks for comparison.

1 | Hydrogen: Theoretical Background

The widespread use of fossil fuels has led to significant environmental challenges, including global warming, air pollution, and the depletion of finite natural resources. One of the most promising solutions for the future energy transition due to its cleanliness as a carbon-free energy carrier is hydrogen. With a high energy density of 140.4 MJ/kg (approximately three to four times that of conventional hydrocarbon fuels such as coke and gasoline), extensive availability and zero carbon composition hydrogen offers unique advantages for decarbonizing both stationary and mobile energy systems [18, 19].

Hydrogen can be used as a fuel in internal combustion engines and gas turbines, providing high thermal efficiency and ultra-low pollutant emissions [18]. Additionally, hydrogen is considered the optimal fuel for fuel cells, where it reacts with oxygen to produce only water as a byproduct, achieving system efficiencies exceeding 90% [18]. As a result, hydrogen is often described as a potential source of limitless, clean power, contributing to closed-loop energy cycles where water can be recycled to regenerate hydrogen. At present, technological advancements in hydrogen production, storage, and transportation are progressing rapidly worldwide, facilitating the energy sector's transition toward a carbon-neutral future [18, 19].

Nevertheless, the majority of hydrogen produced today still relies on fossil-based methods—such as steam methane reforming (SMR) and coal gasification—which are associated with substantial greenhouse gas emissions. Given the growing urgency of the climate crisis and the global carbon-neutral agenda, there is a strong need to replace these conventional pathways with environmentally friendly and sustainable hydrogen production technologies [18, 19].

In response, researchers have turned to renewable feedstocks such as water and biomass to produce green hydrogen through a variety of processing technologies such as electrolysis, thermo-chemical decomposition, and biological methods. Among these, biomass-based hydrogen production (biohydrogen) is particularly attractive due to the carbon-neutral

nature of biomass and its broad availability in the form of agricultural residues, forestry by-products, and organic waste [18]. Biohydrogen processes also offer relatively high conversion efficiencies and low energy requirements, with the added advantage of resource abundance—examples include corn stover, wheat straw, sawdust, and sugar beet juice [18].

As highlighted in recent global reviews [19], hydrogen has become a key solution for decarbonizing hard-to-abate sectors such as heavy industry, maritime transport, and aviation. The recent energy crisis has only reinforced the urgency of hydrogen deployment, triggering enhanced policy support and investment. However, despite increasing interest, the actual share of low-emissions hydrogen in total production remains limited. Most of today's hydrogen is still used in refining and chemical processes and is produced via unabated fossil-based routes. While production capacity for low-carbon hydrogen is expanding, barriers such as high investment costs and infrastructure limitations persist.

This chapter provides an overview of the current landscape of hydrogen production and utilization, with a particular focus on Stegra's hydrogen production strategy at the Boden plant. The aim is to understand the technical foundation of their project and to introduce the objective of this study: integrating Stegra's system with a proposed biomass gasification pathway to enhance sustainability and diversify hydrogen supply.

1.1. Hydrogen production technology

Hydrogen can be generated from a wide range of renewable and non-renewable sources. Most established technologies involve trade-offs in terms of cost, energy input, carbon emissions, or infrastructure demands [5].

As shown in Figure 1.1, hydrogen is typically classified by color, representing the production method and associated environmental impact. Green hydrogen, produced through water electrolysis powered by renewable energy, is the cleanest form, emitting no greenhouse gases (GHG), but remains the most expensive. In contrast, black hydrogen, derived from coal, is associated with the highest GHG emissions [5].

Today, around 95% of hydrogen is produced from fossil resources: steam methane reforming (SMR), autothermal reforming (ATR), and coal gasification. These processes are technologically mature (TRL 9) and relatively inexpensive, but they cause significant CO_2 emissions unless combined with carbon capture and storage (CCS), which increases costs and reduces efficiency [20].

Electrolysis of water, when powered by renewable energy, is the cleanest option since it produces hydrogen without direct emissions. Alkaline and proton exchange membrane

(PEM) electrolysis are already commercial (TRL 9), while anion exchange membrane (AEM) and solid oxide electrolysis (SOEC) are still emerging (TRL 7). Despite its environmental benefits, electrolytic hydrogen remains costly due to high capital expenditure and electricity demand, making large-scale deployment dependent on cheap renewable power [20].

Alongside these routes, alternative technologies are being developed. Methane pyrolysis (TRL 3–8) avoids CO_2 emissions by producing solid carbon, while natural hydrogen from geological sources (TRL 3) is still at an early stage. Biomass gasification represents a particularly promising pathway: it allows the use of renewable feedstocks, can achieve lower net emissions than fossil-based methods, and offers synergies with electrolysis by diversifying hydrogen supply and improving energy security [20].

Overall, the trade-off between emissions, costs, and maturity highlights the current dominance of fossil-based hydrogen, the growing strategic role of electrolysis, and the need to accelerate the development of emerging low-carbon technologies [5], [20].

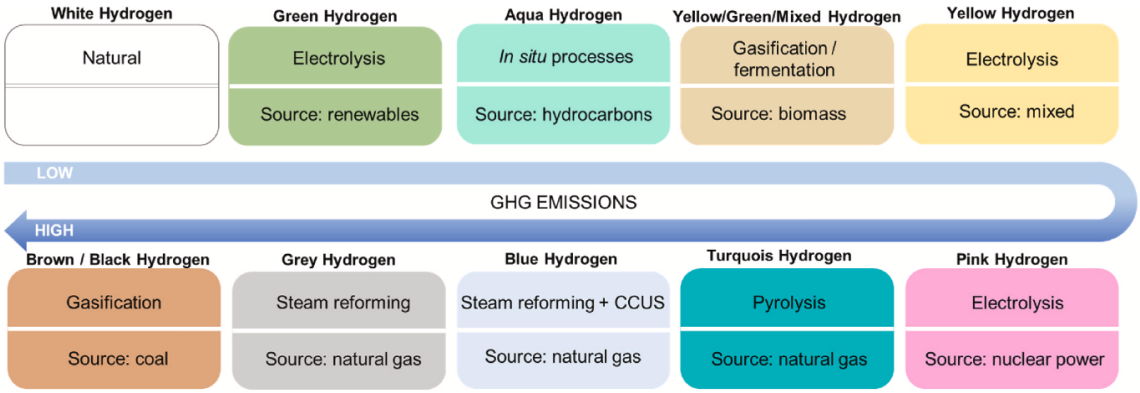

Figure 1.1: Hydrogen color spectrum according to the GHG emissions level (adopted by [5]).

1.2. Low Emission Hydrogen demand

Global hydrogen demand reached a historic high of 97 Mt in 2023, marking a 2.5% increase from 2022. However, its use remains concentrated in traditional sectors such as petroleum refining and the chemical industry, with most supply still derived from unabated fossil fuels, primarily natural gas, as shown in Figure 1.2 [1]. China is the largest producer of hydrogen worldwide [19].

[1]By-product hydrogen from the chlor-alkali industry is not included. CCUS = carbon capture utilisation and storage; RoW = rest of world; 2024e= estimate for 2024. The estimated value for 2024 is a projection based on trends observed until June 2024

To achieve a net-zero energy system, transitioning from unabated hydrogen to low-emission hydrogen is essential [21]. Low-emission hydrogen can significantly reduce carbon emissions in hard-to-abate sectors, including long-distance transport, chemicals, and heavy process industries. While demand for low-emission hydrogen grew by nearly 10% in 2023, it still accounts for only about 1% of total hydrogen consumption (less than 1 Mt) [19].

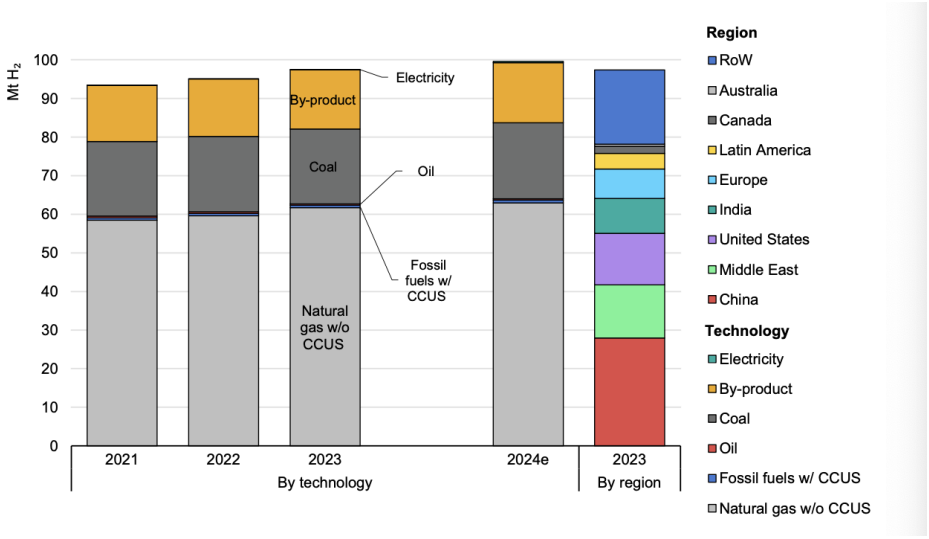

Figure 1.2: Hydrogen production by technology and by region, 2021-2024 (adopted by [19]).

Low-emission hydrogen demand is expected to grow rapidly, particularly in hard-to-abate sectors and energy storage. Announced projects suggest demand could reach 49 Mtpa by 2030 [19], while McKinsey [22] estimates a more moderate 37-38 Mtpa, with most usage in existing industrial applications.

The International Energy Agency [19] estimates that over 70% of low-emission hydrogen will be produced via electrolysis using low-emission electricity, while 26% will come from fossil fuels with carbon capture (CCUS). As water electrolysis is expected to become the dominant technology for future hydrogen production, it will require vast amounts of low-emission electricity. Meeting this growing demand will rely heavily on intermittent renewable sources, particularly wind and solar power. This shift introduces issues related to power stability on the grid, price instability of electricity, and power availability. The large-scale expansion of electricity generation needed for societal electrification—including hydrogen production—also depends on local acceptance, municipal approvals (especially for wind farms and new transmission lines), and the ability of grid operators to scale infrastructure at the necessary pace. Additionally, long permitting processes and limited

land availability could further constrain the speed and scope of this transition. [21].

Alternative production methods for low emission hydrogen, such as biomass gasification, can help mitigate these challenges while offering key [21]:

- Non-intermittent, fossil-free, and scalable production.
- Reduced dependence on low-emission electricity, easing grid constraints.
- Potential process integration with electrolysis, utilizing excess oxygen and heat.
- Generation of a clean CO_2 stream, enabling negative emissions with CCS.
- Production of additional value-added outputs such as biochar, heat, and electricity.
- Potential for *in-situ* CO_2 utilization in bio-electrofuel production when combined with PtX and BtX technologies.

The following chapters outline the study structure. Chapter 2 reviews different gasification technologies for biomass-based hydrogen production and presents relevant commercial initiatives. From these, one technology is selected for further analysis. The selected process is then simulated, and its technical and economic feasibility is assessed, with results reported in Chapters 3 and 4.

1.3. Hydrogen Production Plant and Steelmaking Process at Stegra

As mentioned in Section 0.4, Stegra aims to build one of the greenest steel plants by combining hydrogen-based reduction with traditional methods. While the processes are proven, Stegra stands out by using renewable hydrogen as the main reductant in DRI, marking a major shift toward fossil-free steel.

The traditional steelmaking route predominantly relies on coke-fueled blast furnaces and basic oxygen furnaces (BOF), which contribute significantly to carbon dioxide emissions. In contrast, the Stegra process substitutes these stages with hydrogen-based and electricity-driven technologies, as summarized in Table 1.4. They aim to produce steel with up to 95% lower CO_2 footprint, as shown in Figure 1.3.

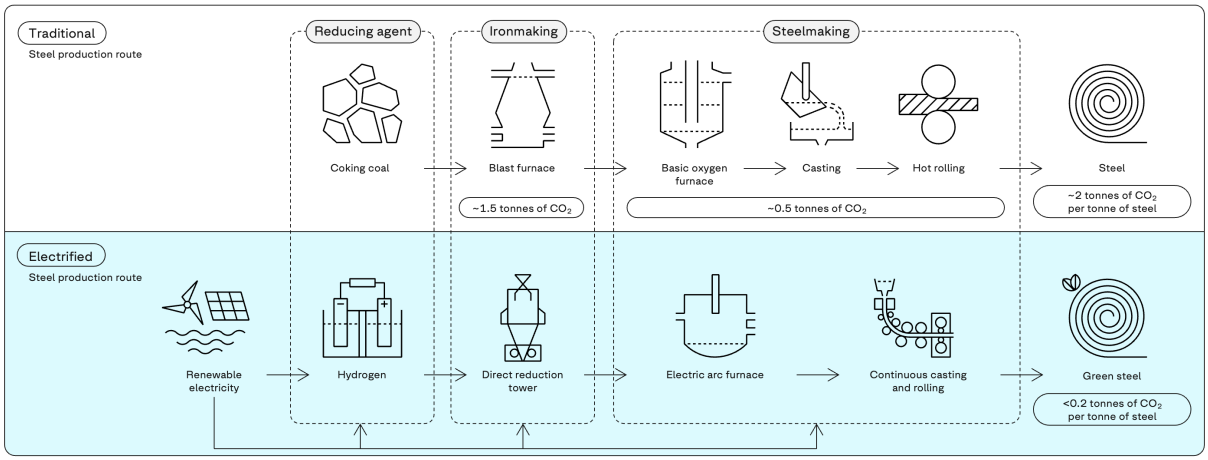

Figure 1.3: Stegra steel production with up to 95% lower CO_2 footprint.

Traditional Process	Description	Stegra Process	Description
Coke Plant	To make steel in a blast furnace, coal must first be turned into coke (coal-based fuel).	**Giga-scale Electrolysis**	Use of electrolysers to produce hydrogen on site using electricity from renewable sources.
Blast Furnace	Blast furnaces produce iron from iron ore. The blast furnace is fuelled by coke.	**Direct Reduction Reactor**	The reducing gas will be hydrogen, to create DRI. This produces hot DRI and Hot Briquetted Iron (HBI) as feedstock for the Electric Arc Furnace using hydrogen as a reductant.
Basic Oxygen Furnace	Uses oxygen to dissolve carbon, giving rise to CO and CO_2.	**Electric Arc Furnace (Meltshop)**	Using electrical energy this provides improved efficiency compared to a traditional blast furnace. Steelmaking will begin with the melting of a mixture of hot DRI and scrap metal.
Casting & Rolling	The liquid steel cools and solidifies. The steel is reheated to be rolled.	**Direct Casting & Rolling**	Integrates casting and hot-rolling of steel, reducing the need to reheat the steel before rolling it.

Figure 1.4: Comparison of traditional steelmaking and the Stegra process.

1.3.1. Stegra Hydrogen Production and Electrolysis Plant

The Stegra hydrogen production plant in Boden will employ Alkaline Water Electrolysis (AWE) technology to produce green hydrogen for the decarbonized steelmaking process.

The installed electrolyser capacity will be 740 MW, corresponding to a nominal production capacity of 148,000 Nm^3/h of hydrogen at full load.

The facility will consist of 37 electrolyser units of 20 MW each, distributed across two dedicated production buildings. The AWE system follows a modular design, scalable from individual elements to gigawatt-scale plants, as illustrated in Figure 1.5. Each unit contains four racks of electrolyser stacks, where demineralized water is split into hydrogen and oxygen. Auxiliary systems provide electrolyte circulation as well as hydrogen and oxygen treatment. After production, the hydrogen is cooled, filtered, and collected in a manifold for downstream use, while oxygen is safely vented to the atmosphere.

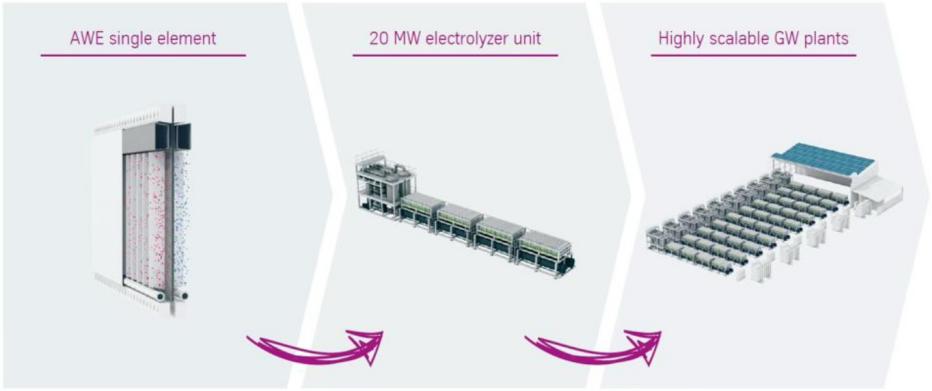

Figure 1.5: Stegra AWE Module set up.

AWE technology was selected for its commercial maturity, lower capital cost, and use of non-precious materials, offering a robust and cost-effective solution compared to alternative technologies such as Proton Exchange Membrane (PEM) or Solid Oxide Electrolysis Cell (SOEC). While AWE presents slightly lower flexibility and efficiency at high loads, it remains the most suitable option for Stegra's large-scale application.

So, the key inputs to the electrolysis plant include demineralized water, nitrogen, cooling water, and instrument air. The outputs consist of hydrogen directed to the manifold, oxygen vented to the atmosphere, and cooling water returned to the site system.

1.3.2. Hydrogen Utilization in the Direct Reduction Plant

The hydrogen produced from the electrolysis is subsequently utilized in the Direct Reduction (DR) plant, where it serves as the primary reducing agent in the production of direct reduced iron (DRI). The DR plant, provided by Midrex Technologies Inc., is based on a hydrogen-based direct reduction process that aligns with Stegra's decarbonized steelmak-

ing strategy. In this process, iron ore pellets are converted into two main products:

- **Hot Direct Reduced Iron (HDRI):** DRI discharged at high temperatures and directly fed into the Electric Arc Furnace (EAF), reducing energy losses during the melting stage.
- **Hot Briquetted Iron (HBI):** DRI compacted at temperatures above 650°C to form dense briquettes, enabling safe storage, transport, or sale to external markets.

In the process, the iron ore pellets are fed into a vertical shaft furnace, while finer particles are screened and recirculated to the feed system. The reducing gas mixture, primarily composed of hydrogen, is preheated in the process gas heater to 950°C before being introduced into the shaft furnace, where it reacts with the iron ore, removing oxygen and yielding metallic iron.

By utilizing hydrogen from renewable and circular sources, the DR plant plays a central role in achieving Stegra's objective of low-carbon steel production, ensuring the integration of clean hydrogen across the entire steelmaking value chain.

1.4. Integration of Electrolysis and Biomass Gasification for Hydrogen Production

It is within this context that the present study focuses on the integration of the electrolysis system with a dedicated biomass gasification process, specifically designed to produce additional hydrogen for the DRI unit and to further enhance the sustainability and flexibility of hydrogen supply at Stegra. In this configuration, part of the oxygen produced in the electrolysis process will be valorized as the oxidant in the gasification unit, enhancing the overall integration and resource efficiency of the hydrogen production system. The design approach, process integration, and performance evaluation of this hybrid hydrogen production concept will be presented and discussed in the following chapters.

2 | Biomass Gasification: Theoretical Background

Biomass, as a renewable and environmentally friendly energy source, plays a crucial role in the future global energy landscape through the production of hydrogen-rich syngas via gasification. While biomass gasification presents a promising pathway to reduce carbon emissions, several technological challenges and knowledge gaps remain before it can be fully implemented on an industrial scale [8]. This chapter provides an overview of the gasification process, with a focus on biomass gasification. It examines different reactor designs and configurations and discusses the key factors that influence performance.

2.1. Gasification Theory

Gasification is a thermochemical process that converts carbonaceous materials (e.g., biomass) into producer gas, biochar, tars, and ash through the action of an oxidizing agent such as air, O_2, steam, CO_2, or their mixtures. The main product, known as producer gas or raw syngas, consists primarily of H_2 and CO, but can also contain CO_2, H_2O, N_2, CH_4, higher hydrocarbons, and impurities, depending on the feedstock, gasifying atmosphere, technology, and operating conditions such as temperature, pressure, and heating rate [23, 24]. The process occurs at high temperatures under substoichiometric conditions, which prevent complete combustion and result in by-products such as char and tar [25], while ensuring efficient energy recovery from solid fuels [21].

Syngas is particularly valuable because, unlike direct combustion products, it can be upgraded via water–gas shift or reforming reactions to obtain high-purity hydrogen, or used as feedstock for chemicals such as methanol, Fischer–Tropsch liquids, and ammonia. This versatility positions gasification not only as an energy recovery route but also as a pathway for material valorization and circular carbon use [26].

The process consists of four main stages: drying, pyrolysis, combustion, and reduction. Figure 2.1 shows the zones and the products that typically occur during that part of the

process. In the drying stage, moisture is removed from the biomass through endothermic evaporation of low-boiling compounds. This step typically occurs at temperatures around 100°C and it significantly reduces the moisture content, improving the efficiency of subsequent reactions. The pyrolysis stage involves the thermochemical decomposition of biomass in an oxygen-free environment at temperatures ranging from 125°C to 500°C. It is endothermic and produces 75 to 90% volatile materials in the form of gaseous and liquid hydrocarbons.([25]). The combustion stage (oxidation stage) is an exothermic process in which a gasification agent is introduced to react with the pyrolysis products. The heat generated at this stage is crucial for sustaining the endothermic reactions required in the next phase of gasification. Finally, in the reduction stage (also known as the gasification zone), the remaining char reacts with hot gases coming from the upper zones, converting into syngas [8].

This multi-step process enables efficient energy conversion from biomass, making gasification a highly effective approach for sustainable energy production.

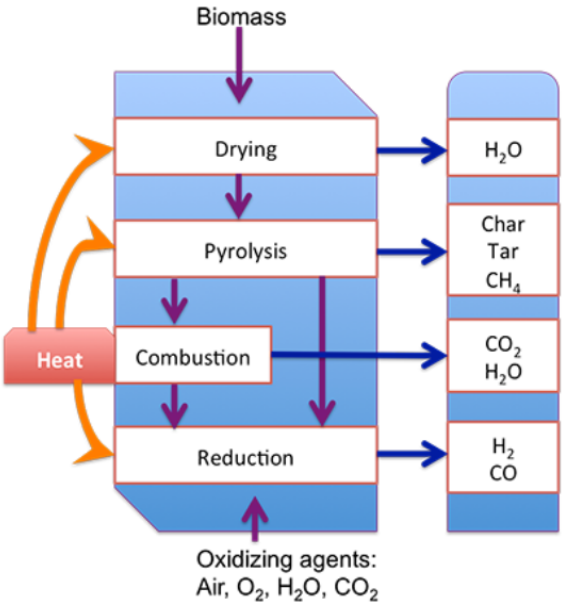

Figure 2.1: General schematic of different regions in a gasifier (adopted by [27]).

Figure 2.2 shows different gasification approaches that can be used for biohydrogen production. Among renewable hydrogen production technologies, biomass gasification is one of the earliest developed and remains one of the most cost-effective options [25].

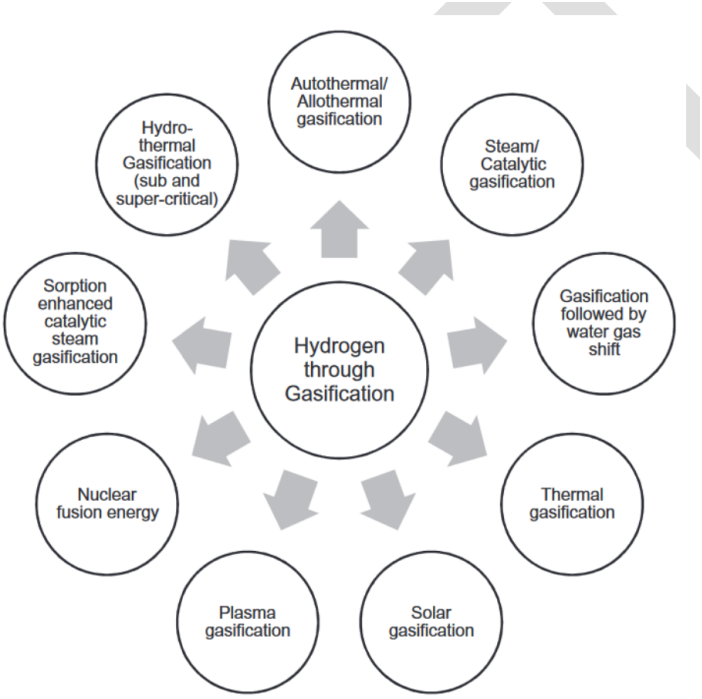

Figure 2.2: Classification of different approaches for H_2 production using biomass gasification (adopted by [25]).

2.2. Gasification Feedstocks

Gasification is a highly flexible process that can convert a wide range of carbonaceous materials into synthesis gas. Typical feedstocks include coal, petroleum residues, biomass, and different waste streams [26]. While coal has historically dominated, its use is declining, and increasing attention is being given to renewable and waste-derived feedstocks, driven by climate policies such as the European Green Deal and the need to reduce CO_2 emissions [25].

According to the Renewable Energy Directive, biomass (Figure 2.3) comprises the biodegradable fraction of products, residues, and wastes of biological origin, including agricultural and forestry residues, animal waste, by-products from industries (e.g., wood, paper, fisheries), and even the biodegradable share of municipal solid waste [24, 26]. Waste-derived feedstocks include sewage sludge, crop residues, plastics, and other by-products, and their gasification contributes to both energy recovery and circular economy strategies by reducing landfill needs and recovering valuable carbon fractions [26].

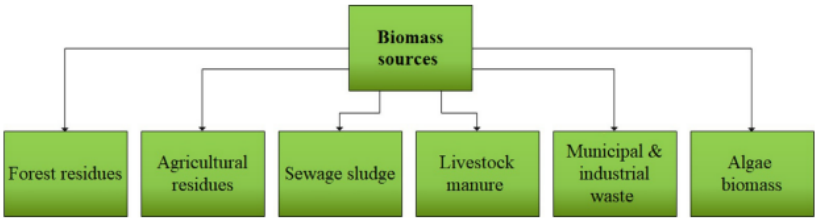

Figure 2.3: Sources of biomass (adopted by [24]).

Feedstock characteristics strongly affect gasification performance. Higher-rank coals, with lower volatile content and H/C ratios, generally produce cleaner syngas, while biomass and waste, due to their higher volatile fraction, favor fast pyrolysis but can lead to higher tar content. Parameters such as moisture, particle size, and bulk density also play a crucial role, making pretreatment steps (e.g., drying, pelletization, removal of inerts) necessary for efficient operation [26].

Overall, the choice of feedstock is central in defining gasification efficiency and syngas quality. Among renewable options, biomass stands out as a cost-effective and sustainable resource, offering both energy security and compliance with environmental targets.

2.3. Gasification Reactions

The gasification process is more complex than simple combustion and is influenced by multiple factors, including the amount and type of oxidant, feedstock composition, gasifier temperature, and reactor geometry. These parameters significantly affect the reaction pathways, syngas composition, and overall efficiency of the process [28].

The biomass gasification mechanism can be expressed by the chemical reactions reported in Table 2.1[1]:

[1]Values of the enthalpy of each reaction (ΔH°) refer to standard conditions (25°C and 1 atm).

Gasification Step	Reaction	Reaction Name	ΔH° (kJ/mol)
Pyrolysis	Biomass → Char + Tar + Volatiles	(1)	
Oxidation	Char(s) + O_2 → CO_2	Carbon Oxidation (2)	−394
	C(s) + $0.5O_2$ → CO	Carbon Partial Oxidation (3)	−110
	CO + $0.5O_2$ → CO_2	Carbon Monoxide Oxidation (4)	−283
	H_2 + $0.5O_2$ → H_2O	Hydrogen Oxidation (5)	−242
Reduction	C(s) + CO_2 ↔ 2CO	Boudouard Reaction (6)	172
	C(s) + H_2O ↔ CO + H_2	Reforming of Char (7)	131
	CO + H_2O ↔ CO_2 + H_2	Water Gas Shift Reaction (8)	−42
	C(s) + $2H_2$ ↔ CH_4	Hydrogasification (9)	−75
	CH_4 + H_2O ↔ CO + $3H_2$	Steam–Methane Reforming (10)	206
Additional Reactions	H_2 + S ↔ H_2S	Hydrogen sulfide formation (11)	−20.6
	0.5 N_2 + 1.5 H_2 ↔ NH_3	Ammonia synthesis (12)	−46.1
	Cl_2 + H_2 ↔ 2 HCl	Hydrogen chloride synthesis (13)	−184.6

Table 2.1: Reactions involved in biomass gasification [9, 28].

2.4. Gasifier types

The gasification process can be carried out using various types of gasifiers, including fixed-bed, fluidized-bed, entrained-flow, and plasma reactors. These gasifiers differ according to several key factors, such as the type of gasifying agent used, operating temperature and pressure, heat supply method, material transport process, and bed material composition. Each type of gasifier is designed to optimize efficiency and syngas production on the basis of specific process conditions and feedstock characteristics [8].
A gasifier typically requires feedstock pretreatment, gas conditioning, and final purification to obtain the desired gas product (hydrogen-rich gas product in this case). Since the hydrogen concentration in gasifier reactors is generally below 50%, various gas conditioning units, along with pre- and post-treatment processes, are implemented to enhance hydrogen purity and achieve higher concentrations [21].

2.4.1. Fixed Bed Gasifier

Fixed bed gasifiers are conventional systems characterized by high carbon conversion, long residence times, low ash carryover, and low gas velocity, operating around 1000 °C. They are widely applied in systems ranging from 10 kW to 100 MW [8]. Based on airflow direction, they are classified as follow and represented in Figure 2.4:

- **Updraft gasifier**: one of the earliest and simplest gasifier designs, operating with

counter-current flow where the oxidant (air, oxygen, or steam) enters from the bottom and the biomass feedstock from the top, while the product gas exits at the top. This configuration is characterized by a simple reactor design, low investment cost, high thermal efficiency, low pressure drop, and easy maintenance. It also shows high tolerance to ash and moisture content, low sensitivity to feedstock size and quantity, and high mass transfer efficiency. However, significant drawbacks include the very high tar content in the product gas (often $> 100\,\mathrm{g/m^3}$), the necessity for extensive gas cleaning, relatively low conversion efficiency of syngas, and limited gasification capacity [8, 24, 29].

- **Downdraft gasifier**: also known as co-current gasifier, it operates with both air (or oxygen/steam) and biomass moving downward through sequential reaction zones, with the product gas exiting at the bottom. This design enables high feedstock conversion rate, good syngas quality with relatively low tar content, high selectivity, and simple processing. It is well suited for small to medium-scale power generation due to its compactness and efficient tar reduction. However, it also presents several limitations, including restriction to dense and uniform feedstock, high exit gas temperature, significant ash accumulation, low overall energy efficiency, and limited scalability to large applications [8, 24, 29].

- **Sidedraft/cross-flow gasifier**: biomass enters from the top, air from the side, with gases exiting laterally. High CO content syngas is produced at high temperatures with high tar levels and low H_2 and CH_4. It offers quick load response, meaning it can rapidly adjust output in response to changes in fuel or air input, making it suitable for dynamic applications like renewable energy integration. However, it suffers from low efficiency, limited scalability, and poor CO_2 reduction in the syngas.[8, 29].

- **Open-Core Gasifier**: operate by introducing air along with biomass fuel from the top, utilizing a downward suction force generated by the vacuum inside the system. This design is a variation of throatless downdraft gasifiers, where both biomass and air move downward simultaneously, enabling efficient gasification [8].

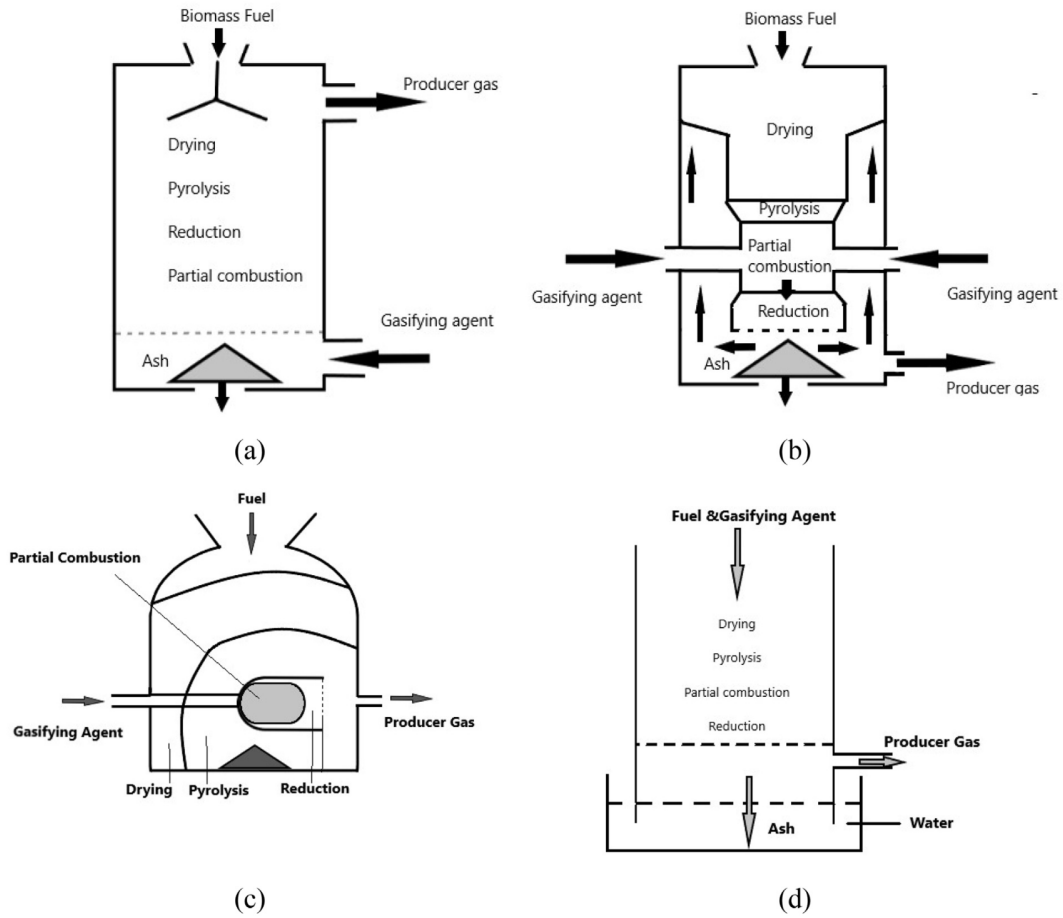

Figure 2.4: Views of fixed bed gasifiers (a) updraft, (b) downdraft, (c) crossflow, (d) open-core (adopted by [29, 30]).

2.4.2. Fluidized bed gasification

Fluidized Bed Gasifiers (FBGs) are efficient, environmentally friendly, and cost-effective systems that convert fuels into syngas through complete mixing with gas and steam at around 1000°C [29]. Biomass and gasification agents are introduced from the top and bottom, respectively, with syngas exiting from the upper bed. Stability can be affected by mineral matter softening. Key parameters impacting efficiency include fluidization rate, biomass ratio, bed material properties, residence time, and gasification equilibrium [8].

Based on fluidization speed, FBGs are classified as follows and represented in Figure 2.5:

- **Bubbling Fluidized Bed Gasifiers (BFBGs)**: characterized by a well-mixed fluidized bed where biomass particles are suspended by the upward flow of air, oxygen, or steam. This configuration ensures uniform temperature distribution,

high carbon conversion efficiency, flexibility in feedstock type and particle size, and suitability for high-moisture feedstocks. It also provides low tar content in the product gas, high energy content of syngas, and prevents ash agglomeration, while allowing the use of catalysts. However, bubbling fluidized bed systems involve higher investment and maintenance costs, and require careful control of gas velocity to avoid inefficiencies related to particle accumulation [8, 24].

- **Circulating Fluidized Bed Gasifiers (CFBGs)**: operate at higher gas velocities compared to bubbling beds, carrying bed particles upward with the product gas, which are then separated in cyclones and recirculated. The lower region remains dense, while the upper region is more dilute and turbulent, ensuring strong gas–solid interaction. This configuration provides uniform conditions, high heat transfer rate from solids to gas, intensive mixing, particle recycling, and high gas–solid contact. CFBGs are highly flexible in fuel composition and moisture content, achieving high conversion efficiency, low emissions (including NO_x), and suitability for large-scale applications exceeding 10 MW (hydrogen production rate 2400 ton/y) without capacity limitations. However, they face challenges such as high investment and operational complexity, as well as possible reduction in bed fluidity due to eutectic formation [8, 24]. .
- **Dual Fluidized Bed (DFB) Gasifiers**: Integrate a gasification reactor (800–850 °C) and a combustion reactor (900–950 °C), where residual char is burned generating the heat required for endothermic steam gasification reactions; this heat is carried by the circulating bed material. This setup produces syngas with high hydrogen content and low tar levels. [8].

The choice of gasifier type depends on operational requirements and desired syngas properties. Figure 2.5 shows the schematic configurations of the three different FBGs types.

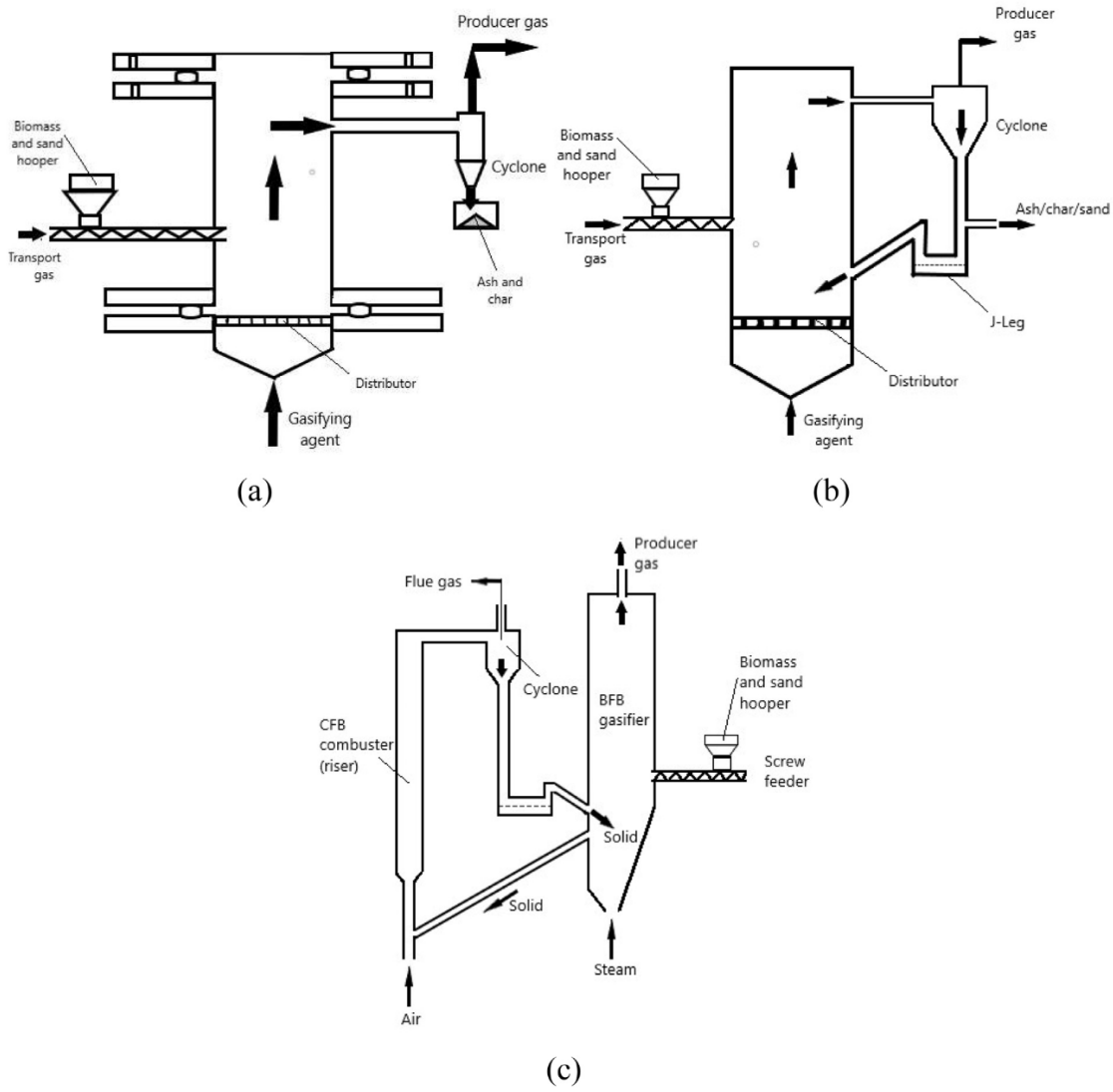

Figure 2.5: Schematic of FBGs (a) bubbling, (b) circulating, and (c) twin-bed/dual (adopted by [29, 30])

2.4.3. Entrained Flow Gasifiers

Entrained Flow Gasifiers operate at high temperature (1250–1600°C) and pressure (20–70 bar), injecting finely ground feedstock together with gasification agents (steam and oxygen) from the top of the reactor. Under these severe conditions, the fuel undergoes rapid heating, achieving very high carbon conversion rates and short residence times of 5–10 s. The resulting syngas is clean, tar-free, and has high energy content, while ash is removed as molten slag. These features, combined with feedstock flexibility and uniform reactor temperature, make entrained flow systems the dominant technology in large-scale syngas production, particularly in Integrated Gasification Combined Cycle (IGCC) plants

[8, 24].

However, several challenges remain: high operational costs, the need for finely pulverized feedstock, large input of gasifying agents, and the requirement for very high heat input to sustain the reaction conditions. In addition, sulfur and chlorine species in the feedstock must be controlled to avoid corrosion and catalyst poisoning [8, 24].

2.4.4. Plasma gasification (PG)

Plasma gasification is an allothermal process in which extremely high temperatures (up to 5000°C) are generated by plasma torches through arc discharges, radio frequency, or microwaves. Unlike autothermal gasification, which relies on redox reactions with oxidants, plasma gasification uses external heat sources, enabling complete decomposition of organic matter, vitrification of inorganic components into inert slag, and the generation of high-purity synthesis gas. Typical syngas composition ranges between 49–65 vol% H_2 and 25–36 vol% CO, depending on feedstock characteristics [8, 24].

Plasma reactors offer several advantages, including high feedstock flexibility (organic and inorganic), no strict material size requirements, reduced production of NO_x, SO_x, chars, and tars compared to conventional gasification, fast start-up and shutdown, steady-state operation, and the possibility of slag valorization in the construction sector. However, they also face significant challenges: short electrode lifetime, very high energy demand leading to high operating and maintenance costs, limited commercial deployment, insufficient understanding of plasma processes, and safety concerns due to limited societal awareness [8, 24].

2.5. Gasification agents

Gasification agents play a crucial role in syngas production by reacting with carbon and hydrocarbons to generate gases like hydrogen (H_2) and carbon monoxide (CO). The choice of agent significantly affects gas composition, heating value, and process efficiency. Common agents include air, steam, oxygen, and their combinations, each with specific advantages and limitations [8]:

- **Air** is a widely used and cost-effective gasification agent. However, due to its high nitrogen (N_2) content, the syngas produced has a relatively low heating value, typically ranging from 4–7 MJ/Nm^3. Despite this limitation, air gasification facilitates heat generation required for the process and helps moderate tar and solid waste formation [8].

- **Oxygen** gasification produces syngas with a higher heating value (12–28 MJ/Nm^3) by avoiding nitrogen dilution occurring in the air case. This improves carbon conversion and reduces tar formation, resulting in a syngas rich in H_2, CO, and CH_4. The main drawback is the high energy cost of oxygen production [8].
- **Steam** gasification generates hydrogen-rich syngas with a calorific value of 10–18 MJ/Nm^3. It improves exergy efficiency, reduces tar content, and enhances coal conversion rates. Compared to oxygen gasification, it offers more economical operation and is considered key for clean energy generation [8].

2.6. Fuel Characteristics and Gasification Temperature

Fuel properties strongly affect hydrogen yield in gasification processes and they can be categorized as follows [21]:

- **Elemental Composition (C, H, O, N, S):** Fuel composition directly influences H_2 yield. High oxygen content binds hydrogen in water, reducing the free H_2 yield. In contrast, for this reason, biomass mixed with plastics enhances hydrogen yield per ton of feedstock [8, 21].
- **Ash Content and Composition:** Ash affects gasifier operation. In fluidized beds, temperatures must stay below ash agglomeration points, while in entrained flow gasifiers, ash composition affects slag formation and conversion efficiency [8, 21].
- **Moisture Content:** Moisture impacts the water-gas shift reaction, enhancing H_2 production. However, an excess moisture increases energy demand, as additional energy is required to evaporate the water, and increases CO_2 formation, reducing H_2 yield. To optimize H2 production, controlled steam addition is preferred over high inherent moisture in the feedstock. For moisture above 35%, hydrothermal gasification is preferable [8, 21].

2.6.1. Gasification Temperature

The operating temperature in gasification is a crucial factor influencing both carbon conversion efficiency and tar production. Fluidized beds operate at 650–950 °C, limited by ash and bed material melting points [21].

From a thermodynamic perspective, exothermic reactions such as partial oxidation to CO and H_2 formation are favored at lower temperatures, while endothermic reactions

including steam reforming, the Boudouard reaction, and the water–gas shift are promoted as temperature increases. Kinetically, however, all reactions accelerate with temperature, with complete combustion to CO_2 and H_2O becoming especially dominant.

As a result, higher temperatures improve carbon conversion and reduce tar, but also increase the risks of agglomeration, sintering, and material degradation, shifting syngas composition toward CO_2, lowering its heating value and H_2 content. These effects are reflected in the strong dependence of equilibrium constants on temperature (Figure 2.6) and in the overall influence on process performance (Figure 2.7) [21, 26].

Temperature is also tied to the equivalence ratio, where higher values reduce cold gas efficiency due to increased oxidation. To control hotspots and maintain heat distribution, oxygen is often diluted with nitrogen, steam, or CO_2, balancing syngas composition while avoiding product dilution [21, 26].

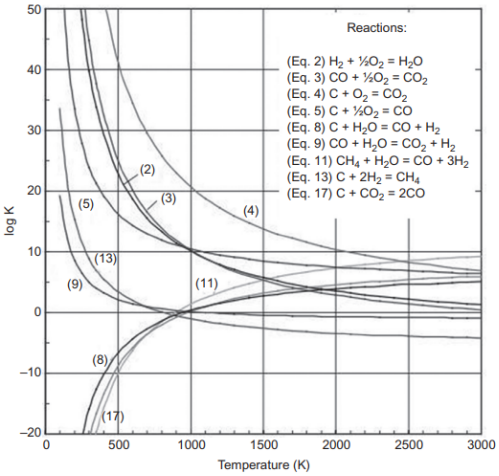

Figure 2.6: Evolution of $\log K$ (equilibrium constant) with temperature for some reactions in Table 2.1 (adopted by [26])

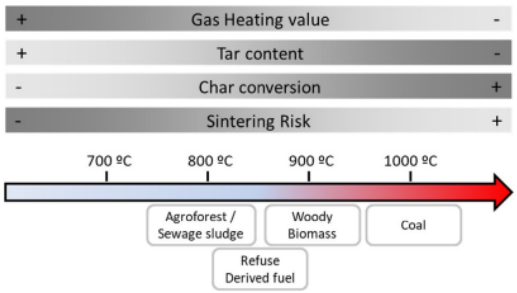

Figure 2.7: Gasification temperature influence (adopted by [26])

2.6.2. Bed Material and Catalysts

In fluidized bed gasifiers, bed materials ensure stable operation by facilitating heat transfer from exothermic to endothermic reactions, maintaining uniform temperatures around 800°C. Quartz sand is common due to its cost and inertness but can cause agglomeration when reacting with alkali metals and chlorine. Alternatives include natural minerals, alumina, and additives like kaolin to prevent agglomeration. Materials such as magnesite and olivine offer improved performance, with magnesite providing better agglomeration resistance and olivine aiding tar cracking.

Catalysts further enhance gasification efficiency. Traditional catalysts include dolomite, alkali metal oxides, and nickel-based compounds. Recent developments feature a Ni-Fe-CaO catalyst (30% Ni, 20% Fe, 50% CaO) boosting hydrogen production, along with carbon-based zinc and Co-Ni/hydrotalcite catalysts, the latter achieving 99% hydrogen purity in sorption-enhanced gasification. Since catalysts are both costly and sensitive to mechanical stress, it's better to use them in a bubbling fluidized bed (BFB) rather than a circulating fluidized bed (CFB), where they are more likely to break.

Catalytic gasification can be conducted at both low and high temperatures to enhance efficiency and optimize syngas production. In low-temperature catalytic gasification (350–600°C), catalysts improve reaction efficiency, lower the degradation temperature of cellulose, and increase gas and oil yields. Metal-based catalysts are particularly effective in promoting the gasification of water-soluble products, leading to early CO_2 and H_2 production, followed by methane formation via methanation.

High-temperature catalytic gasification focuses on optimizing reaction pathways using model compounds such as glucose and cellulose. Studies indicate that biomass concentration significantly affects efficiency, with concentrations above 5–10 wt% reducing hydrogen yield. By operating at around 650°C and keeping biomass concentrations below 3%, nearly complete conversion to hydrogen and carbon dioxide can be achieved [21].

2.7. Gas Cleaning and Upgrading for Hydrogen Production

The syngas produced from biomass gasification contains numerous contaminants, including particulates, tars, sulfur compounds, nitrogen species, chlorine compounds, alkali metals, and heavy metals, which must be removed to avoid catalyst poisoning in downstream units such as the water–gas shift (WGS) reactor [31]. Additionally, the raw syngas has limited hydrogen content and requires further upgrading to meet hydrogen production targets.

To enhance the hydrogen yield, the syngas is typically conditioned via reforming or oxidation steps, such as autothermal reforming (ATR) or partial oxidation (POX), which increase gas reactivity by converting tars and heavier hydrocarbons into lighter species, facilitating higher hydrogen production in the subsequent WGS reactor. After WGS, the syngas can reach a hydrogen content of 65–70 *vol.*%, which is still insufficient for most applications requiring high-purity hydrogen [21].

Final purification is carried out using commercially available technologies, which can

achieve any desired hydrogen purity level depending on the end-use. Pressure swing adsorption (PSA) is widely employed, utilizing molecular sieves to separate gases based on size and offering purities of 99–99.99%, suitable for fuel cell applications. Membrane separation technologies, including polymer, metallic (e.g., Pd-Ag alloys), and ceramic membranes, also offer promising routes for hydrogen purification, although challenges remain regarding durability and scalability. Emerging materials such as graphdiyne membranes have demonstrated hydrogen contents up to 98% with 75% recovery in two-stage systems [32]. Cryogenic separation, although less favored due to its high energy consumption, can be used in combination with membranes to achieve ultra-high purities [21]. Other advanced systems, such as those described in patents by Gaetano et al. [33] and Tawfik [34], integrate multiple syngas cleaning stages—including acid/base scrubbing, wet electrostatic precipitation, and amine-based CO_2 scrubbing—with WGS and PSA units to produce high-purity hydrogen from biomass-derived syngas. Table **??** reports the required purity of hydrogen according to different applications.

Hydrogen purity (%)	**Application**
99.999999	Rocket engine fuel, semiconductor manufacture
99.99	Polymer electrolyte fuel cell On-site hydrogen generating equipment
90	Hydrodesulfurization
70–80	Adjustment of a molecular weight distribution
54–60	Fuel gas

Table 2.2: Required purity of hydrogen for different applications [21].

Thus, achieving efficient and cost-effective hydrogen production from biomass gasification requires a combination of syngas cleaning, reforming or oxidation (ATR/POX), WGS, and purification stages (e.g., PSA, membranes, cryogenics), as consistently reported in literature pathways for biomass-to-hydrogen conversion.

2.8. Negative Carbon Emissions: Technological Opportunities

In global efforts to combat climate change, biomass remains an underutilized resource despite its considerable potential. For example, Torrgas [35] estimates that only 20% of

the corn plant is harvested as food, while the remaining 80% becomes residue. Globally, corn alone generates over 1 billion tonnes of residues annually, with rice, sugarcane, and wheat contributing an additional 860, 264, and 729 million tonnes, respectively [35].

Instead of valorizing this material, open-field burning remains a common practice in many regions, releasing both CO_2 and harmful particulate matter. This not only contributes to greenhouse gas emissions but also causes severe air pollution, with negative health impacts on millions of people. Redirecting these residues toward sustainable biofuel production could significantly reduce emissions while supporting the decarbonization of hard-to-abate sectors [35, 36].

Biomass molecular structure contains carbon that comes from CO_2 absorbed from the atmosphere during plant growth. This means that using biomass can help remove CO_2 from the atmosphere. By capturing the CO_2 released during gasification, the process can achieve negative emissions. Integrating CO_2 capture into biomass gasification is therefore a promising way to make hydrogen production more sustainable and environmentally friendly.

Since CO_2 separation is already an inherent step in gasification processes, the capture can be efficiently integrated at lower costs compared to other sectors. This enables either permanent storage through Carbon Capture and Storage (CCS) or utilization via Carbon Capture and Utilization (CCU), generating additional revenue streams. CCS involves capturing CO_2 from major point sources, such as gasification, power production, or industrial plants, and transporting it via pipelines, ships, or trucks for injection into geological formations like depleted oil and gas reservoirs or saline aquifers. Alternatively, CO_2 can be converted into valuable products, with current global CO_2 utilization reaching approximately 230 million tonnes annually, primarily in urea manufacturing and enhanced oil recovery [19]. In Sweden, the estimated cost for integrating CO_2 capture at biomass-fired combined heat and power plants ranges from 80–180 € per tonne of CO_2, depending on technology, plant size, and transportation logistics [21]. For biomass gasification, these costs are reduced, reinforcing its viability for negative emissions applications. Moreover, biomass-based gasification systems coupled with CCS (BECCS) offer opportunities for deep decarbonization, including sectors like iron and steel production, where BECCS can support carbon-negative steel manufacturing by addressing emissions from iron reduction processes, which represent up to 85% of total CO_2 emissions in these industries [3].

Conceptually, CO_2 capture can be implemented through several approaches: post-combustion capture from flue gases, pre-combustion capture from syngas generated via partial oxidation, and oxy-combustion, where fuel is burned in an oxygen-rich environment to facilitate

CO_2 separation [37]. Among these, pre-combustion capture in gasification offers key advantages due to the high CO_2 partial pressure in the syngas stream, reducing energy and cost penalties compared to post-combustion and oxy-combustion methods, which require significant energy for flue gas treatment or cryogenic oxygen production, respectively [37].

Overall, the integration of BECCS within biomass gasification represents a promising route toward carbon-negative hydrogen production systems.

Certain biomass gasification processes also produce biochar as a co-product. Biochar consists primarily of carbon (approximately 85–90% by weight), with the remainder comprising ashes from the original biomass. Additionally, biochar contains essential nutrients such as nitrogen, phosphorus, and potassium, which contribute to soil improvement. By returning biochar to agricultural soils, carbon depletion in soils is mitigated, and the demand for synthetic fertilizers is reduced. This results in a carbon-negative value chain, further enhancing the sustainability of biomass gasification [21].

3 | Integrated Biomass-to-Hydrogen Process Design

Based on the theoretical background presented in the previous chapters, this chapter presents the design of a biomass gasification process for hydrogen production, considered as a complementary pathway to the electrolysis plant currently under construction by Stegra in Boden. The most suitable units are selected and modeled, and the resulting mass and energy balances are analyzed to evaluate syngas composition, hydrogen yield, and overall process performance.

3.1. Plant Description

Figure 3.1 illustrates the simplified block flow diagram (BFD) of the integrated biomass gasification and hydrogen production system. The plant is designed to produce hydrogen from biomass using a circulating fluidized bed gasifier (CFBG), and to integrate this with hydrogen produced by alkaline electrolyzers, following the configuration of the Stegra green hydrogen production plant in Boden.

The main process units include a biomass dryer, CFBG gasifier, high-temperature filtration unit, partial oxidation (POX) reactor, syngas cleaning section, two-stage water-gas shift reactors (HT WGS and LT WGS), a CO_2 capture and drying section, and a pressure swing adsorption (PSA) unit for hydrogen purification and compression.

The integration is realized not only by combining the produced hydrogen streams at the storage level, but also by utilizing the oxygen by-product from the electrolyzers as the oxidant in the gasification and partial oxidation steps, improving process efficiency and system synergy.

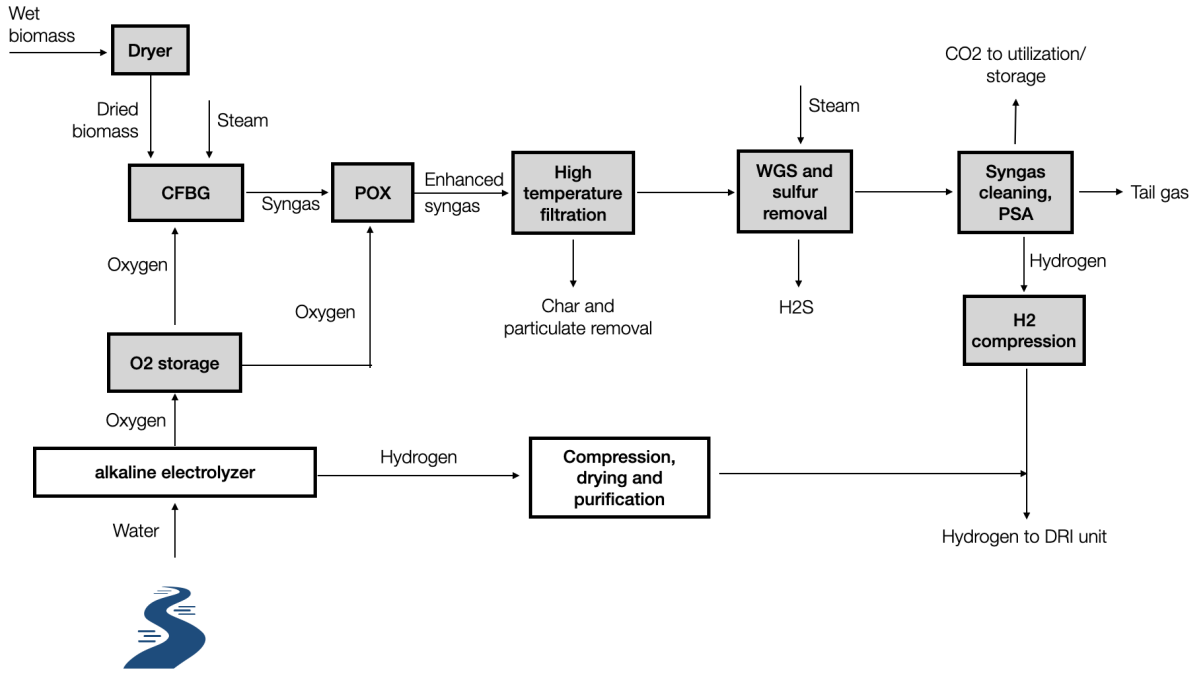

Figure 3.1: Simplified block flow diagrams for biomass-to-H2 process.

Table 3.1 summarizes the required specifications of the hydrogen stream produced by the integrated gasification and electrolysis system, intended for direct use in the DRI process for green iron production.

Parameter	Requirement
Pressure	> 8 bar
H_2 content	$> 99.8\ \%_{\text{dry}}$
O_2 content	$< 0.2\ \%_{\text{dry}}$
H_2O content	$< 0.5\ \%$
Impurities content	$< 5\ ppm$

Table 3.1: Specifications of hydrogen flow for DRI production.

According to the Boden plant project, the hydrogen demand for injection into the DRI unit is approximately 150,000 Nm^3/h. It's expected from the start that gasification alone won't cover the full hydrogen demand, mainly due to limited biomass and lower hydrogen yield.

3.1.1. Choice of Biomass

Sweden is largely covered by forests, as illustrated in Figure 3.2. Approximately 70% of Sweden's land area is forested, compared to only 31% in Italy [38]. As a result, woody biomass represents the primary biomass resource in this context [39]. The composition of the woody biomass considered in this study is based on the work of Rajaee et al. [40] and is presented in Table 3.2.

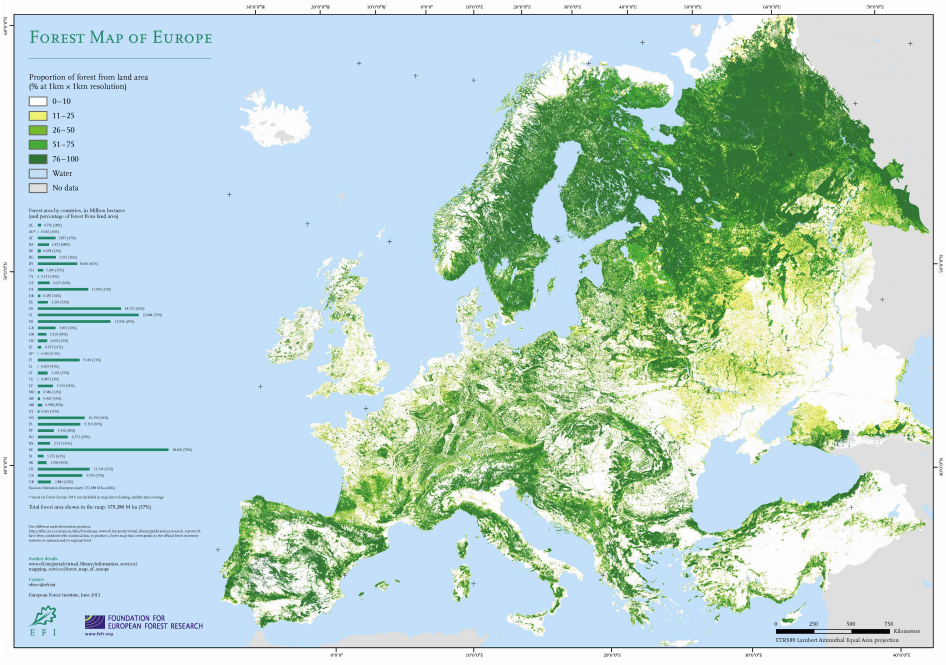

Figure 3.2: Forest Map of Europe (adopted by [39])

Property	Parameter	Value
Lower Heating Value	LHV (MJ/kg_{AR})	9.74
Moisture Content	Moisture (%wt)	45
Proximate Analysis (dry basis)	Fixed Carbon (FC, %wt)	18.84
	Volatiles (V, %wt)	80.00
	Ash (%wt)	1.16
Ultimate Analysis (dry basis)	Carbon (C, %wt)	51.19
	Hydrogen (H, %wt)	6.08
	Nitrogen (N, %wt)	0.20
	Chlorine (Cl, %wt)	0.05
	Sulfur (S, %wt)	0.02
	Oxygen (O, %wt)	41.30
	Ash (%wt)	1.16

Table 3.2: As-received biomass composition and properties [40].

3.1.2. Biomass Pre-Treatment

A belt dryer is utilized to lower the moisture content of the incoming woody biomass from 45% to 15%. Moisture removal is driven by thermal energy, which is transferred through a stream of drying air heated by a hot water circuit operating between 90°C and 30°C. The process requires approximately 1 MWh of thermal energy per tonne of water evaporated. In addition to thermal input, the belt dryer also consumes around 32 kWh of electricity per tonne of dried biomass [40]. The dried biomass exits the dryer and is fed to the CFBG. Its composition is reported in Appendix A

3.1.3. Steam-oxygen blown circulating fluidized bed gasifier

The use of a circulating fluidized bed (CFB) gasifier combined with steam-oxygen as the gasifying agent is particularly suitable for this hydrogen production process. The CFB configuration, as also already reported in Section 2.4.2, offers excellent fuel flexibility, high throughput, and uniform temperature distribution, which are essential for efficient conversion of woody biomass with relatively low heating value. Its ability to enhance char conversion through solid recirculation improves overall gasification efficiency. Moreover, CFB gasification is a proven and commercially available technology, already offered by several equipment manufacturers, which eliminates the need for custom construction. It is especially well-suited for the chosen feedstock—woody biomass—and supports scalable,

continuous operation. Compared to other gasifier types, CFB provides better mixing, heat and mass transfer, and can operate effectively at lower equivalence ratios, contributing to higher hydrogen yields after downstream processing.

The choice of steam-oxygen, rather than air, avoids nitrogen dilution of the syngas, increasing its heating value and simplifying downstream processing. Moreover, steam promotes the water-gas shift reaction, which is critical for maximizing hydrogen yield, while oxygen supplies the necessary heat through partial oxidation. According to Sher et al.[36] steam is ideal for both small and large-scale systems, producing syngas with high H_2 content and lower CO_2 and CH_4. This combination supports a syngas composition optimized for hydrogen production and CO_2 capture, making it a technically sound and efficient choice.

The simulation of biomass gasification and degradation is inherently complex due to multiple interacting phenomena at various levels: (1) it is a multi-component problem, given the intrinsic variability in biomass composition; (2) a multi-phase process, involving reactions in both condensed and gas phases that yield bio-char, bio-oil, and syngas; (3) a multi-scale system, requiring consideration of intra- and inter-phase transport phenomena at both particle and reactor scales; and (4) a multi-dimensional problem, with system evolution dependent on variables such as particle radius, bed structure, and time. This complexity is further compounded by the necessity of a coupled treatment of transport phenomena and detailed kinetic schemes in both solid and gas phases [41].

To model the operation of the circulating fluidized bed gasifier (CFBG), the simulation approach was based on the study by Rajaee et al.[40], which focuses on the Varkaus demonstration plant with a thermal biomass input of 100 MW. Their system employs a pressurized CFBG that converts woody biomass into syngas using a mixture of steam and oxygen as the gasifying agents. The reactor operates at a temperature of 870 °C and a pressure of 4 bar. Rajaee et al. provide detailed compositions for both the inlet and outlet streams of the gasifier.

For the purpose of this simulation, certain simplifications were adopted. Trace impurities were neglected; chlorine in the biomass was assumed to be fully converted into hydrogen chloride (HCl), sulfur into hydrogen sulfide (H_2S), and 10% of the nitrogen content was assumed to form ammonia (NH_3).

The core gas-phase reactions were characterized using the following atomic balance matrix:

	C	H_2O	H_2	CH_4	CO	CO_2	O_2
C	1	0	0	1	1	1	0
H	0	2	2	4	0	0	0
O	0	1	0	0	1	2	2

Based on this matrix, the number of independent reactions required to define the system thermodynamically is calculated as $NR = N_{species} - rank_{matrix} = 4$.

Consequently, the extent of the following four reactions was determined using the syngas composition data reported by Rajaee et al.:

$$C + O_2 \rightleftharpoons CO_2$$
$$C + H_2O \rightleftharpoons CO + H_2$$
$$C + 2H_2 \rightleftharpoons CH_4$$
$$C + CO_2 \rightleftharpoons 2CO$$

Using the reaction extents obtained, the results were scaled to match the case study under consideration, which assumes a thermal input of 150 MW. The resulting syngas composition is presented in Appendix A.

GASDS simulation

GASDS is a kinetic-based simulation package designed for the gasification of biomass and coal, developped by Politecnico of Milan. It is particularly suited for analyzing pyrolysis, gasification, and combustion processes, incorporating detailed kinetic schemes across multiple scales. The software takes into account the heterogeneous and homogeneous reactions and the transport phenomena inside the reactor. The dynamic behavior of the system is originally described by a set of partial differential equations (PDEs), accounting for gradients with respect to time, longitudinal direction, and radial coordinate. However, through appropriate approximations, the system is reduced to a set of ordinary differential equations (ODEs), where only temporal gradients are considered [42]. These ODEs are solved using advanced numerical techniques available in the BzzMath library [43], which are especially effective for stiff systems and are based on the Gear multivalue method [44] [42].

In this study, GASDS is employed to simulate the gasifier under the same input conditions as those reported by Rajaee et al. [40], and scaled up by a factor of 1.5—from a thermal input of 100 MW to 150 MW. The results obtained from the simulation, reported in Table 3.3 demonstrate good agreement in syngas composition, thereby validating the reliability

of the overall calculation approach.

Component	%mol OUT		%wt OUT	
	GASDS simulation	Calculated	GASDS simulation	Calculated
CO	13.91	14.64	18.31	19.54
H_2O	38.45	40.38	32.55	34.64
CO_2	19.57	17.31	40.46	36.30
H_2	19.29	20.11	1.83	1.92

Table 3.3: Comparison of GASDS simulation and calculated values for gas composition (%mol and %wt OUT).

The obtained results show that the syngas composition is mainly characterized by H_2 and CO, CO_2 and CH_4. Other species such as higher hydrocarbons, tars, or nitrogen compounds are not reported, since they are typically present in smaller amounts or require detailed kinetic modeling that goes beyond the scope of this convalidation study. Compared to literature values, the hydrogen content is slightly lower, while CO_2 is higher, indicating a shift in the equilibrium at the selected operating conditions. This discrepancy may be attributed to the specific assumptions made in the model, such as complete tar cracking and simplified kinetics.

The distribution of products also reflects the strong influence of temperature and equivalence ratio: higher temperatures enhance hydrogen yield but simultaneously increase CO_2 formation due to more complete oxidation. Such trade-offs are consistent with findings from other studies and highlight the importance of carefully tuning operating parameters to maximize hydrogen production while limiting carbon losses.

3.1.4. Partial Oxidation unit (POX)

Partial oxidation (POX) is used after gasification to reduce tar content in syngas by promoting radical-driven reforming reactions through controlled oxygen injection [45]. In this study, POX is preferred over autothermal reforming (ATR) due to the availability of oxygen from the upstream electrolysis process, eliminating the need for additional oxygen production units and reducing overall system cost. While ATR is more commonly found in literature, it requires costly catalysts, making POX more economically viable in this context. Although the benefits of POX are evident, experimental data on its application to real gasifier producer gas are scarce, with most studies relying on simulated syngas.

Due to the complexity of species and reaction pathways involved, comprehensive radical kinetic models are needed for accurate prediction of reactor outlet compositions [45].

As reference unit, the partial oxidation (POX) unit developed at LRGP is taken into consideration. It is installed downstream of the gasyfier and included four main sections: a pre-heating chamber, a gas-centered non-premixed swirl coaxial burner, a reaction chamber, and a cooling zone (as shown in Figure 3.3). Producer gas from the gasyfier entered the pre-heating chamber at near-atmospheric pressure, then flowed through the central tube of the coaxial burner. Simultaneously, oxygen is injected tangentially via a swirl mechanism.

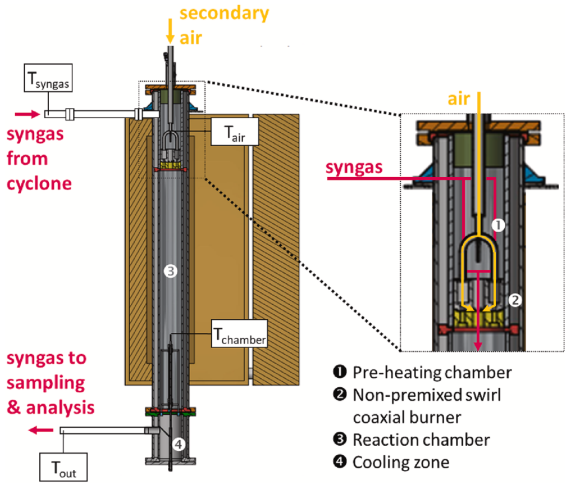

Figure 3.3: Scheme of the POX unit (adopted by [45])

In their work, Demol et al.[45] developed the SYNPOX model (SYNgas Partial OXidation), which comprises 742 species and 5093 reactions. The model was validated using experimental data from Tanoh's study [46], with results showing satisfactory overall agreement. Among the various cases analyzed, the authors identified case 0.1-1100 (ER-$T_{chamber}$) as the most reliable. For this reason, the parameters reported in Table 3.4, corresponding to case 0.1-1100, are used as the reference in this thesis.

To gain insight into the key reactions involved in the partial oxidation process, the work of Rößger et al.[47] was used as an additional reference. The main reactions derived from this study are summarized in Table 3.5.

Parameter	Value
Oxygen preheating set-point (°C)	500
Oxygen inlet T_{O2} (°C)	565
Producer gas inlet T_{syngas} (°C)	691
POX external oven set-point (°C)	1200
Reaction chamber $T_{chamber}$ (°C)	1100
Cooling chamber exit T_{out} (°C)	668
ER	0.1

Table 3.4: Operating parameters for POX (adopted by [45]).

No.	Reaction
(1)	$CH_4 + H_2O \leftrightarrow CO + 3H_2$
(2)	$CO + H_2O \leftrightarrow CO_2 + H_2$
(3)	$2CO + O_2 \leftrightarrow 2CO_2$
(4)	$C + CO_2 \leftrightarrow 2CO$
(5)	$C_2H_2 + 2.5O_2 \leftrightarrow 2CO_2 + H_2O$
(6)	$C_2H_4 + 3O_2 \leftrightarrow 2CO_2 + 2H_2O$
(7)	$C_2H_6 + 3.5O_2 \leftrightarrow 2CO_2 + 3H_2O$
(8)	$C_3H_8 + 5O_2 \leftrightarrow 3CO_2 + 4H_2O$
(9)	$n\text{-}C_4H_{10} + 3.5O_2 \leftrightarrow 4CO_2 + 5H_2O$
(10)	$i\text{-}C_4H_{10} + 3.5O_2 \leftrightarrow 4CO_2 + 5H_2O$
(11)	$N_2 + 3H_2 \leftrightarrow 2NH_3$
(12)	$NH_3 + CO \leftrightarrow HCN + H_2O$
(13)	$H_2 + S \leftrightarrow H_2S$
(14)	$H_2S + CO_2 \leftrightarrow COS + H_2O$

Table 3.5: Main reactions involved in the POX process (adopted by [47]).

The outlet gas composition, along with the water and acid gas yields reported by Demol et al.[45], were used as references and adapted to the specific process conditions considered in this study. The resulting output composition is provided in Appendix A.

3.1.5. High Temperature (HT) filtration

Syngas from biomass gasification contains contaminants such as particulates, tars, sulfur, nitrogen, chlorine compounds, and metals, which can severely impact sensitive downstream catalysts (e.g., WGS). High-temperature gas cleaning improves overall efficiency by avoiding syngas cooling. Metallic filters have emerged as a robust alternative to ceramic filters, offering similar filtration efficiency with improved durability. Depending on the alloy used, these filters can operate at temperatures up to 1000 °C, though values between 400 and 700 °C are more commonly reported [31].

In this study, the filtration temperature is set equal to the syngas outlet temperature from the partial oxidation (POX) unit, thereby eliminating the need for an additional heat exchanger and simplifying the system layout. Following Villot et al.[31], a filter efficiency of 99.9% for particles <0.5µm is assumed in the simulation. The filtered gas is then cooled through cold traps to condense water and tars.

3.1.6. Water-Gas Shift Units

The Water-Gas Shift (WGS) reaction, shown in Eq.3.1, is essential for increasing hydrogen production by converting carbon monoxide and steam into hydrogen and carbon dioxide. As hydrogen enrichment is a primary goal of this process, the WGS unit is a critical step. The reaction is moderately exothermic and is typically implemented in two stages: a high-temperature stage that favors reaction kinetics, and a low-temperature stage that benefits from improved thermodynamic equilibrium [48]. The WGS section consists of two fixed-bed catalytic reactors. The first stage operates at 310–450 °C and uses a Fe–Cr-based catalyst, which enables rapid CO conversion (around 80%) and can tolerate sulfur concentrations in the range of 100–500 ppm [49]. The second stage, operating at 180–250°C, utilizes a Cu–ZnO–Al_2O_3 catalyst to drive the reaction further toward equilibrium. However, this catalyst is highly sensitive to sulfur, with a tolerance of less than 0.1 ppm [49]. To protect it, a sulfur guard bed is placed between the two stages to remove hydrogen sulfide (H_2S) generated upstream [50]. According to the work of Dehimi at al.[49], both reactors and all product-gas-carrying piping are equipped with electric heating elements, enabling independent temperature control at the reactor inlets and minimizing heat losses [50]. This configuration ensures that the low-temperature reactor can achieve a final CO conversion of up to 97%, thereby maximizing hydrogen yield [50].

In the present process, the syngas exiting the gasifier contains insufficient steam to allow effective CO conversion in the WGS reactors. To address this, additional steam is

introduced to increase the steam-to-carbon monoxide ratio (STCO), enhancing reaction efficiency and preventing carbon deposition on the catalyst surface [50]. The STCO ratio—defined in Eq.3.3—is a critical design parameter. Steam is added in excess in order to shift the equilibrium toward the product side (since it is a reversible reaction [25]), and, in particular, values above 2 are recommended to thermodynamically suppress carbon formation [50].

The overall CO conversion, (X_{CO}), is calculated using Eq.3.4, serving as a basis for evaluating reactor performance and optimizing process conditions. In this study, a CO conversion of 97% and a fixed STCO ratio of 2 are assumed. Under these conditions, the resulting product gas composition has been calculated and is presented in Appendix A.

$$\mathrm{CO} + \mathrm{H_2O} \rightleftharpoons \mathrm{H_2} + \mathrm{CO_2} \qquad \Delta H_0^{\mathrm{reaz}} = -41 \ \frac{\mathrm{kJ}}{\mathrm{mol}} \tag{3.1}$$

$$STCR = \frac{\dot{n}_{H_2O,in}}{\dot{n}_{C,in}} \quad \text{in } \mathrm{mol}_{H_2O}\ \mathrm{mol}_{C}^{-1} \tag{3.2}$$

$$STCOR = \frac{\dot{n}_{H_2O,in}}{\dot{n}_{CO,in}} \quad \text{in } \mathrm{mol}_{H_2O}\ \mathrm{mol}_{CO}^{-1} \tag{3.3}$$

$$X_{CO} = \frac{\dot{n}_{CO,in} - \dot{n}_{CO,out}}{\dot{n}_{CO,in}} \cdot 100 \quad \text{in } \% \tag{3.4}$$

3.1.7. Gas cleaning units

To protect the downstream Rectisol unit and ensure efficient CO_2 absorption, a condenser is placed after the WGS reactors to remove excess water vapor. This step also helps dissolve and remove acid gases such as HCl and NH_3, reducing their concentrations below the thresholds specified in Table 3.1.

Then, the pre-cleaned syngas enters the Rectisol unit for advanced purification. The Rectisol process provides a comprehensive "5-in-1" gas treatment solution [51], including: (1) trace contaminant removal, (2) deep desulfurization with total sulfur content reduced below 80 ppb, (3) bulk CO_2 removal of up to 100%, (4) CO_2 purification to $>98.5 vol\%$ with residual sulfur below 5ppmv, and (5) acid gas enrichment with sulfur content exceeding $25 vol\%$.

The Rectisol process is a low-temperature physical absorption system that uses refriger-

ated methanol to selectively absorb acid gases such as H_2S, COS, and CO_2 [52]. It typically operates around –70°C. Due to the strong dependence of CO_2 solubility in methanol on both temperature and pressure, the process achieves high efficiency at low temperatures and elevated pressures. This behavior is illustrated in Figures 3.4 and 3.5, which show that solubility increases sharply below -40 °C and with rising CO_2 partial pressure [53]. Regeneration of the solvent is achieved through either a temperature swing (raising the temperature) or a pressure swing (lowering the pressure), both of which decrease CO_2 solubility and release the absorbed gas [53].

Due to the upstream installation of a ZnO guard bed, most of the H_2S is removed before the syngas enters the Rectisol unit. Consequently, the acid gas stream exiting the unit consists primarily of CO_2, with only trace amounts of sulfur species. For the sake of simplification in the simulation and calculations, the presence of residual sulfur traces has been neglected. The resulting CO_2 stream is therefore assumed to be fully purified and can either be directly vented or directed to a carbon capture and storage (CCS) system, with the alternative option of being sold as a marketable byproduct. These scenarios are evaluated from an economic perspective in the subsequent chapter.

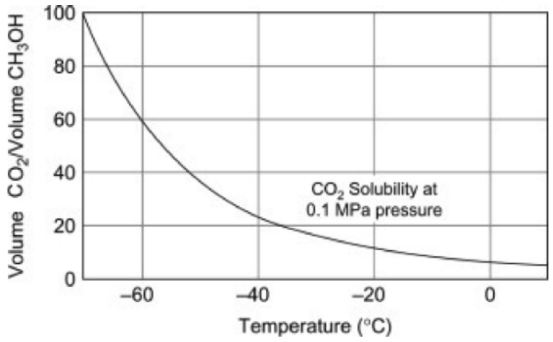

Figure 3.4: Temperature dependence of CO_2 solubility in methanol (adopted by [53])

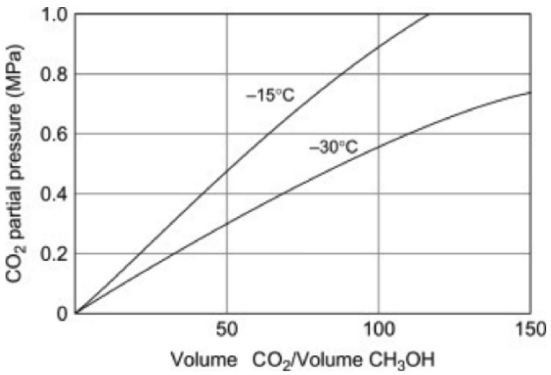

Figure 3.5: Partial-pressure dependence of CO_2 solubility in methanol (adopted by [53])

3.1.8. Pressure swing adsorption (PSA) unit

The gas is then introduced into the pressure swing adsorption (PSA) unit. In this unit, hydrogen (raffinate) is separated from other gaseous components (tail gas), including CO_2, residual CO, N_2, CH_4, Ar, and higher hydrocarbons [50].

According to the study by Gubin et al.[50], continuous PSA operation is achieved using four adsorber vessels operating in a 7-step cycle. Each vessel contains a multilayer bed of adsorbents composed of activated carbon (Norit® RB2), carbon molecular sieve (Neca|cms®260), and 5Å zeolite (Köstrolith® 5ABFK).

The PSA cycle consists of the following seven sequential steps across all vessels: (1) adsorption, (2) pressure equalization, (3) blowdown, (4) vacuum desorption, (5) purge regeneration, (6) pressure equalization, and (7) repressurization. The hydrogen recovery (Rec_{H_2}) is calculated using Eq. 3.5.

$$Rec_{H_2} = \frac{\dot{n}_{H_2,out}}{\dot{n}_{H_2,in}} \cdot 100 \quad \text{in \%} \tag{3.5}$$

In the experimental conditions reported by Gubin et al.[50], a hydrogen purity of at least 99.9vol.% and a recovery rate of 79.0% were achieved. CO levels remained below the detection limit (LOD = 0.5ppmv), while CO_2 concentrations were measured at approximately 5ppmv. Their system operated at an adsorption pressure of 6.5bar_a, an equalization pressure of 4.75bar_a, and an adsorption duration of 480 seconds. For this study, an adsorption pressure of 8 bar_a is selected; however, the performance data reported by Gubin et al. have been verified to remain applicable at this pressure and are therefore used as the basis for simulation and calculation. All the specifications reported in Table 3.1 are then verified.

The main results are presented in Section 4.4

4 | Techno-Economic Assessment (TEA)

In this section, the metrics in terms of energy, environmental and economic performance are defined [54]. The H_2 production plant concept can be schematically represented as shown in Figure 4.1.

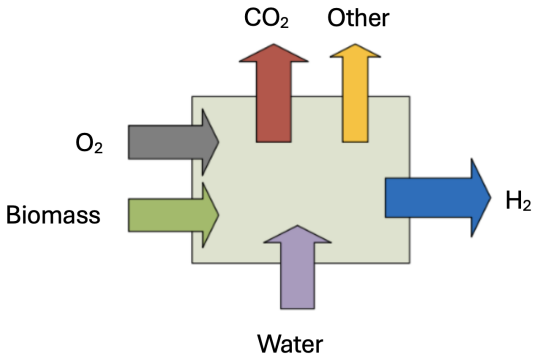

Figure 4.1: Schematic representation of the H_2 plants (aodpted by [54])

The economic and energetic performance of such systems depends on several factors, including biomass availability and logistics, as well as the capital and operating costs of the plant [36]. Technologies for biomass gasification vary widely in their maturity, ranging from early-stage concepts to commercially available systems, typically evaluated using the Technology Readiness Level (TRL) framework.

Techno-Economic Assessment (TEA) is a key tool to evaluate both technical and economic feasibility. It enables performance benchmarking and supports informed decision-making for future deployment [36]. Common economic indicators used in TEA include capital expenditure (CAPEX), operational expenditure (OPEX), total capital investment (TCI), production cost (PC), levelized cost of hydrogen (LCOH) [36].

Two general approaches are used in techno-economic studies. The first relies on adapting data from previous research, adjusted for inflation and currency updates. The second

employs simulation tools like Aspen Plus to derive mass and energy balances, which are then used to calculate investment and production costs. The first method mentioned is adopted in this study.

4.1. Assessment of the Technology Readiness Level (TRL)

TRL is a point-based system used to assess the maturity of a technology based on a scale ranging from 1 to 9, with higher numbers indicating greater maturity. Originally developed by NASA in the 1970s, it has become a standard framework in research and innovation, including in the energy sector. TRLs are grouped into three stages: concept to lab scale (TRL 1–4), lab to pilot scale (TRL 4–6), and pilot to commercial scale (TRL 6–9) [36]. Table 4.1 summarizes the meaning of each scale number.

TRL	Description
TRL 1	Basic principles observed
TRL 2	Technology concept formulated
TRL 3	Experimental proof of concept
TRL 4	Technology validated in lab
TRL 5	Technology validated in relevant environment (industrially relevant environment in the case of key enabling technologies)
TRL 6	Technology demonstrated in relevant environment (industrially relevant environment in the case of key enabling technologies)
TRL 7	System prototype demonstration in operational environment
TRL 8	System complete and qualified
TRL 9	Actual system proven in operational environment (competitive manufacturing in the case of key enabling technologies; or in space)

Table 4.1: European Union Horizon 2020 TRL Scale (European Commission, 2014).

For biomass gasification applied to hydrogen production, the TRL is considered relatively high. Depending on the assessment method, estimates range from TRL 5 to TRL 9. For instance, using the *Weighted Average* method, Lundgren et al.[21] estimate a TRL of 7, while the *Weakest Link* approach suggests TRL 5. Lepage et al.[55] report TRL 7, Buffi et al.[56] estimate TRL 9, and Sher et al.[36] assign a TRL of 8–9.

4.2. Methodology and Economic Indicators

Following process modeling and simulation, the main techno-economic indicators were derived using overall mass and energy balances [37].

Technical Performance Metrics

- **Biomass thermal input** (Q_{Biomass}) was computed using biomass flow rate and its lower heating value (LHV):

$$Q_{\text{Biomass}} = \dot{m}_{\text{Biomass}} \cdot LHV_{\text{Biomass}} \quad [\text{MW}] \tag{4.1}$$

- **Hydrogen thermal output** (Q_{Hydrogen}) was calculated similarly:

$$Q_{\text{Hydrogen}} = \dot{m}_{\text{Hydrogen}} \cdot LHV_{\text{Hydrogen}} \quad [\text{MW}] \tag{4.2}$$

Economic Indicators

- **Capital expenditure (CAPEX)** was estimated for each plant subsystem (e.g., biomass preparation, gasification, syngas treatment, acid gas removal, hydrogen purification, carbon management). The capital cost for each unit was derived using reference cost data and the following scaling law:

$$C_E = C_B \cdot \left(\frac{Q}{Q_B}\right)^M \quad [€] \tag{4.3}$$

  where C_B is the base cost, Q_B is the reference capacity, and M is the scaling exponent [37]. Used reference data for CAPEX calculation are presented in Table 4.2 and Table 4.3.
- **Operational and maintenance (O&M) costs** include both fixed and variable components. Fixed costs account for maintenance, labor, administration, and overhead. Variable costs include process-related consumables such as biomass, catalysts, solvents, membranes, and utilities [37]. Key assumptions are detailed in Table 4.4.
- **Levelized Cost of Hydrogen (LCOH)** is computed as ratio of annualized CAPEX and O&M costs to the combined hydrogen production:

$$LCOH = \frac{Annualized\ CAPEX + O\&M\ cost}{annual\ H_2\ production} \quad \left[\frac{€}{\text{kg}}\right] \tag{4.4}$$

The methodology used to estimate capital expenditures (CAPEX) and operational ex-

penses (OPEX) is based on the work of Cormos [37]. In accordance with techno-economic studies on biomass gasification, a high plant capacity factor of 90% is assumed. This assumption reflects the need for continuous operation to ensure the economic viability of capital-intensive technologies such as biomass-based hydrogen production [40].

The key assumptions adopted in this analysis, consistent with prior literature, are summarized in Table 4.4. A detailed breakdown of the fixed capital investment (FCI) is provided in Table 4.3; note that FCI values exclude working capital.

Plant component	Cost scaling parameter	Reference capacity	Scaling exponent	Reference purchase cost [M€]	Ref
Biomass-to-syngas island					
Feedstock handling	Biomass feed [MWth]	157.00	0.31	6.94	[40]
Belt dryer	Water evaporated [kg/s]	0.34	0.28	2.49	[40]
Pressurized O_2 CFBG	Dry biomass [kg/s]	17.8	0.75	49.38	[40]
POX	Inlet syngas [Nm^3/h]	1000.00	0.65	1.00	
Metal hot-gas filter	Inlet syngas [Nm^3/h]	50000.00	0.60	1.60	
HT WGS	Inlet syngas flow rate [kg/h]	160763.9	0.56	0.4666	[57]
LT WGS	Inlet syngas flow rate [kg/h]	160763.9	0.56	0.323	[57]
Cleaning					
Sulfur removal (ZnO bed)	Inlet syngas flow rate [kg/h]	81371.7	0.56	0.037	[57]
Condenser	Duty [kW]	1000.00	0.60	0.05	
Rectisol unit	Inlet syngas [Nm^3/h]	200000.0	0.65	20.00	[58]
Waste water treatment	Waste water [m^3/h]	22.56	0.67	0.45	[40]
CO_2 processing unit	Captured CO_2 flow [ton/h]	550.00	0.80	36.30	[37]
Syngas-to-H_2 island					
PSA	Inlet gas molar flow rate [kmol/h]	17069	0.60	27.96	[57]
Compression					
Syngas compressor	Compressor power [MWel]	7.01	0.67	7.50	[40]
CO_2 compressor	Compressor power [MWel]	0.64	0.67	0.75	[57]
H_2 compressor	Compressor power [MWel]	0.64	0.67	0.75	[40]
Heat exchanger (rule of thumb)					
Syngas cooler	Heat duty [kW], exchange area [m^2]	–	–	–	[59, 60]

Table 4.2: Cost scaling parameters and reference costs for plant components.

Items	Ratio factor	Ref
Direct cost		
Purchased equipment (delivered)	1	[61]
Equipment installation	0.4	[61]
Instrumentation & controls	0.2	[61]
Piping	0.15	[61]
Electrical systems	0.15	[61]
Buildings	0.3	[61]
Yard improvements	0.1	[61]
Service facilities (waste treatment, receiving, shipping, packaging, storage, offices, etc.)	0.2	[61]
Indirect capital cost		
Engineering and supervision	0.25	[61]
Contingency	0.3	[61]
Contractors fees/overheads/profits	0.1	[61]
Start-up	0.1	[61]
Additional investment		
Working capital	30 days' supply	[37]
Fixed capital investment (FCI) = direct costs + indirect costs		
Total capital investment (TCI) = FCI + WC		

Table 4.3: Capital cost breakdown of the project.

Item	Value	Unit	Ref
Variable operational cost			
Biomass feedstock cost	80.6	[€/t]	[62]
Electricity price	Boden data	[€/MWh]	
Sulfur (by-product) price	120	[€/t]	[37]
Cost for ash disposal	16	[€/t]	[37]
Capture CO_2 transport and storage cost	15	[€/t]	[37]
Steam	30	[€/t]	[63]
CO_2 emission tax	0	[€/t]	[37]
Fixed operational cost			
Number of direct personnel	96	persons	[37]
Average annual direct personnel cost	48	[k€/person/y]	[37]
Administrative costs	35	% of labour cost	[37]
Maintenance costs	4	% of annual capital cost	[37]
Working capital	30	days' supply	[37]
Operational assumptions			
Plant operational factor	90	%	[37]
Interest rate	8	%	[37]
Plant erection time	3	[y]	[37]
Productive operational time	25	[y]	[37]

Table 4.4: Operational and maintenance cost breakdown.

4.3. Results and discussions of green hydrogen production from biomass gasification

Overall mass and energy balances were utilized to quantify the most relevant plant performance indexes (as defined in section 4.2). In the next sections, all the main results are reported and discussed.

4.4. Technical Performance

Based on the assumptions made and data from literature, the system achieves a hydrogen production rate of 0.63 kg/s (0.31 kmol/s). This output corresponds to about 17% of the hydrogen flow required for the DRI unit, according to the Stegra specifications reported in Table 3.1 and Section 3.1.

From an energy perspective, assuming a lower heating value (LHV) of 140.4 MJ/kg for hydrogen [18], the hydrogen stream provides a thermal output of 87.4 MW. Compared to the biomass thermal input of 150 MW at the gasification stage, this results in an overall thermal efficiency of 58.3%. The hydrogen yield, defined as the ratio of hydrogen mass flow to the mass flow of the biomass feedstock, is 40.5 $kg_{H_2}/t_{biomass}$.

When scaled to annual operation (8000 h/y), the plant processes approximately 437,000 t/y of biomass, producing 17,500 t/y of hydrogen. Furthermore, with the implementation of carbon capture (CCUS), about 318,400 t/y of CO_2 can be stored, significantly improving the environmental performance of the process.

A summary of these results is reported in Table 4.5. The produced hydrogen is subsequently compressed to the target pressure of 10 bar and is assumed to be mixed and stored together with the hydrogen supplied from the electrolysis unit.

Parameter	Value
Biomass input	437,000 t/y
Hydrogen production rate	0.63 kg/s
Annual hydrogen production	17,500 t/y
Share of H_2 required for DRI	17%
Hydrogen LHV [18]	140.4 MJ/kg
Hydrogen thermal output	87.4 MW
Biomass thermal input	150 MW
Thermal efficiency	58.3%
Hydrogen yield	40.5 kg $H_2/t_{biomass}$
Captured CO_2 (with CCUS)	318,400 t/y

Table 4.5: Summary of technical performance results for the biomass-to-hydrogen system.

4.4.1. Reference Yields and Efficiencies from Literature

According to the International Energy Agency [19], thermochemical processes such as gasification, pyrolysis, and reforming typically achieve high hydrogen yields, generally ranging from 40 to 190 kg of hydrogen per tonne of feedstock. The thermal efficiency of these processes, based on the lower heating value (LHV), is commonly reported in the range of 40–67%. The values found in these study are within those ranges.

Previous studies on hydrogen production via biomass gasification demonstrate a wide variability in technical performance, with reported energy efficiencies ranging from 35% to 75%. This variation is primarily due to differing assumptions regarding prerequisites, definitions of energy products, technology configurations, and operational conditions.

Hydrogen yield from biomass gasification is influenced by several factors, including process design, operating parameters, and upgrading strategies such as water-gas shift (WGS) and steam methane reforming (SMR).

Turn et al. [64] reported that, in theory, hydrogen yields as high as 165 kg per tonne of biomass can be achieved under optimized conditions involving steam gasification combined with WGS and SMR. In practice, their experiments reached a maximum yield of 128 kg $H_2/t_{biomass}$, which corresponds to approximately 2.1 times the hydrogen content originally present in the biomass (assuming a hydrogen content of 6% on a dry ash-free mass basis) [21].

Sher et al. [36] evaluated an energy efficiency of 37.88% for the BTH (biomass to hydrogen) system studied.

4.5. Economic performance

This section introduces the economic evaluation, including capital and operating costs, in order to assess the feasibility of integrating biomass gasification with hydrogen production. The data used for the calculations are reported in Tables 4.2, 4.3, and 4.4.

4.5.1. Overview of Key Variables and Assumptions

The techno-economic assessment of the hydrogen production pathway from biomass gasification was conducted by analyzing the impact of three key variables:

Biomass feedstock price: based on the data provided by the Swedish Energy Agency [62] for woodchips in 2024, reported at 324 SEK/MWh, which corresponds to approximately 80.6 €/ton (as reported in Table 4.4) assuming a lower heating value (LHV) of 9.74 MJ/kg [40]. This elevated price reflects the market conditions currently affected by geopolitical instability. Nevertheless, similar values have been reported in literature; for instance, Rajaee et al. [40] adopted a biomass price of 72.40 €/ton in their techno-economic evaluation of biomass-to-methanol pathways.

CO_2 handling strategy: two alternative strategies were considered in this study: (i) direct venting of CO_2 to the atmosphere without capture and (ii) capture, compression,

transport, and permanent storage of CO_2 with potential revenue from negative emissions credits (CCUS).

In the baseline scenario without capture, CO_2 is emitted directly to the atmosphere. This approach requires no additional capture infrastructure, resulting in lower capital expenditures (CAPEX) and operating expenditures (OPEX). However, it implies a direct emission of fossil-equivalent CO_2, potentially incurring carbon taxes or forgoing potential revenues from the sale of negative emission certificates.

In the CCUS scenario, the CO_2 capture rate was computed considering the ratio between the molar flow of captured CO_2 ($\dot{n}_{CO2,captured}$) and the molar flow of carbon input from biomass ($\dot{n}_{C,biomass}$) as shown in Equation 4.5 [37]:

$$CO_2 \text{ capture rate} = \frac{\dot{n}_{CO2,captured}}{\dot{n}_{C,biomass}} \cdot 100 \quad [\%] \tag{4.5}$$

According to Lundgren et al. [21], an overall CO_2 capture rate of 85 % was assumed. The captured CO_2 is sold at a negative emissions certificate price of 100 €/ton CO_2. The on-site CO_2 handling and compression, as well as transportation via truck to an intermediate storage hub, were estimated at 50 €/ton CO_2 (the downstream ship transport and permanent storage of CO_2 are assumed to cost between 35 €/ton CO_2 and 55 €/ton CO_2, based on the techno-economic assessment by Beiron et al. [65]).

Consequently, while the implementation of CCUS leads to an increase in CAPEX due to the installation of capture units, compressors, the process can benefit from a net credit of approximately 50 €/ton CO_2, which can effectively help the hydrogen production cost by reducing the net OPEX. This dual impact—higher CAPEX with a potential reduction in net OPEX—makes the CCUS scenario economically attractive under certain policy frameworks and carbon pricing conditions.

Steam supply strategy: two alternative steam supply strategies were considered in this study: (i) purchasing steam from an external utility provider and (ii) generating steam internally through a combination of heat recovery and additional biomass combustion.

In the first case, steam is assumed to be supplied at 20 bar saturated pressure from an external utility network, which is a common practice in industrial sites located within energy clusters or integrated utility hubs. Based on published data by Industry Economics Worldwide [63] and the study of Pérez-Urest et al. [66], a price of 30 €/t_{steam} was adopted, as reported in Table 4.4.

In the second case, an integrated strategy was assessed in which steam is generated in-

ternally. Excess heat recovered from syngas cooling stages, combustion flue gases, and exothermic reactions is first utilized to produce medium-pressure steam via heat recovery steam generators (HRSG). Since process heat alone is insufficient to meet the total demand, the remaining steam requirement is covered by firing additional biomass in a dedicated boiler. This increases OPEX, due to higher biomass consumption, and also requires additional CAPEX for the installation of the steam generation section and auxiliary equipment. Nevertheless, this configuration reduces dependence on external utilities, valorizes waste heat, and improves overall energy integration within the plant.

4.5.2. Base Case Analysis: Current High Biomass Price (80.6 €/ton)

In the base case, the biomass feedstock cost was fixed at 80.6 €/t (see Table 4.4). The analysis considers an annual hydrogen production of about 17,500 t/y and evaluates four scenarios obtained by combining the steam supply strategy with the CO_2 handling option, explained in Section 4.5.1. The corresponding CAPEX, OPEX, and LCOH values are summarized in Table 4.6, while the detailed calculations are reported in Appendix B.

Scenario	Annualized CAPEX [M€/y]	Net OPEX [M€/y]	LCOH [€/kg H_2]
1) No CCUS + Purchased Steam	29.4	53.9	4.7
2) No CCUS + Internal Steam	30.9	48.4	4.5
3) CCUS + Purchased Steam	30.3	37.9	3.8
4) CCUS + Internal Steam	31.8	32.4	3.6

Table 4.6: Base case results for different combinations of CO_2 handling and steam supply strategies at a biomass price of 80.6 €/ton.

In all scenarios, the differences in LCOH reflect the cost trade-offs already discussed in Section 4.5.1. In the case steam is fully purchased from external suppliers. This solution does not require additional CAPEX but increases OPEX due to the procurement cost (30 $/t_{steam}$, as reported in Table 4.4). In the second case, steam is generated internally: part of the demand is covered through process heat recovery, while the remainder is produced by firing additional biomass. This increases CAPEX, due to the installation of a steam generation unit, and raises OPEX, due to the higher biomass consumption.

For CO_2 handling, if CO_2 is vented, no capture-related investment is required and no penalties are applied, since Sweden does not currently tax biogenic emissions. Conversely,

if CO_2 is captured and sold, additional CAPEX is needed for the capture and compression unit, and OPEX rises due to capture-related utilities. However, these costs are partially offset by revenues from CO_2 sales, leading to a net credit of 50 /t_{CO_2} [21], which contributes to lowering the hydrogen cost.

As expected, the scenarios with CCUS display higher CAPEX but lower OPEX compared to the no CCUS ones, due to the contribution of CO_2 revenues. Similarly, when comparing steam supply options, internal generation slightly increases CAPEX but reduces OPEX, as it avoids the recurring cost of purchased steam. Among all cases, the configuration with CCUS and internal steam generation shows the highest CAPEX, reflecting the combined cost of the CO_2 unit and the steam generator, but also the lowest OPEX, thanks to avoided steam purchases and CO_2 sales revenues. This scenario results in the lowest LCOH, equal to 3.6 €/kg_{H_2}, as reported in Table 4.6.

The Levelized Cost of Hydrogen (LCOH) was calculated according to the following general expression:

$$\text{LCOH} = \frac{\text{CRF} \cdot \text{CAPEX} + \text{OPEX} - \text{credits}}{\dot{m}_{\text{H}_2} \cdot t_{\text{op}}} \tag{4.6}$$

where CAPEX and OPEX represent the annualized capital and operational expenditures, respectively, while *credits* account for revenues from CO_2 sales and other by-products. The denominator refers to the annual hydrogen production, obtained by multiplying the hydrogen production rate by the operating hours reported in Table 4.5.

The annualized CAPEX was derived using the capital recovery factor (CRF), which converts the total investment cost into an equivalent annual value:

$$\text{CRF} = \frac{\frac{i}{100} \cdot \left(1 + \frac{i}{100}\right)^n}{\left(1 + \frac{i}{100}\right)^n - 1} \tag{4.7}$$

where $i = 8\%$ is the interest rate and $n = 25$ years is the productive life of the plant [37] (Table 4.4).

For clarity, the results in Table 4.6 are expressed as *annualized CAPEX* (i.e., already multiplied by the CRF) and *net OPEX* (OPEX after deducting CO_2 revenues). This representation provides a direct comparison across scenarios, highlighting how costs vary depending on the steam supply strategy and CO_2 handling option.

4.5.3. Sensitivity Analysis on LCOH: CAPEX and OPEX Variations

A sensitivity analysis was conducted by varying the target LCOH between 3 €/kg and 5 €/kg to determine the corresponding ranges of CAPEX and OPEX under the assumption of high biomass prices (80.6 €/ton, as reported in Table 4.4). This type of analysis is crucial for evaluating the economic feasibility of the project under different market scenarios and financing structures.

LCOH [€/kg H_2]	Annual CAPEX+OPEX [M€/y]
3.00	52.48
5.00	87.47

Table 4.7: Annual CAPEX+OPEX at different LCOH.

Table 4.7 shows the starting range to consider for the analysis.

Scenario 1: Steam fully purchased and CO2 emitted

LCOH [€/kg H_2]	Net OPEX [M€/y]	Annualized CAPEX [M€/y]
3.00	53.85	-1.37
4.76	53.85	29.37
5.00	53.85	33.62

Table 4.8: Relationship between annualized CAPEX and LCOH under fixed OPEX conditions (Scenario 1).

LCOH [€/kg H_2]	Net OPEX [M€/y]	Annualized CAPEX [M€/y]
3.00	23.12	29.37
4.76	53.85	29.37
5.00	58.10	29.37

Table 4.9: Relationship between net OPEX and LCOH under fixed CAPEX conditions (Scenario 1).

Table 4.8 shows the CAPEX range required to achieve different LCOH values while maintaining OPEX constant. Table 4.9 presents the OPEX range that enables reaching the target LCOH while keeping CAPEX fixed.

Scenario 3: Steam fully purchased and CO2 captured and sold

LCOH [€/kg H_2]	Net OPEX [M€/y]	Annualized CAPEX [M€/y]
3.00	37.93	14.56
3.85	37.93	30.33
5.00	37.93	49.54

Table 4.10: Relationship between annualized CAPEX and LCOH under fixed OPEX conditions (Scenario 3).

Similarly, Table 4.10 reports the CAPEX variation needed to reach the desired LCOH while keeping OPEX fixed. Due to the CO_2 sales revenue, OPEX is lower in this scenario, leading to a higher feasible CAPEX range compared to Scenario 1.

This type of analysis is particularly valuable from an investor or company perspective, as it provides insights into the flexibility of CAPEX and OPEX values required to achieve a specific LCOH target. Since capital costs are often more uncertain than operational costs, the CAPEX-focused sensitivity (Table 4.8 and Table 4.10) is of particular interest, as it helps identify the acceptable investment cost range for economic viability.

Comparing the results with Table 4.10, it is evident that the acceptable CAPEX range is higher for Scenario 3, thanks to the lower OPEX achieved by capturing and selling CO_2, thereby making this configuration more economically attractive.

4.5.4. Sensitivity Analysis on Biomass Price: LCOH Reduction Potential

Given the strategic importance of biomass price in the overall process economy, a further sensitivity analysis was performed by varying the biomass price from 30 €/ton to 50 €/ton, which reflects possible future scenarios assuming market stabilization or increased biomass availability.

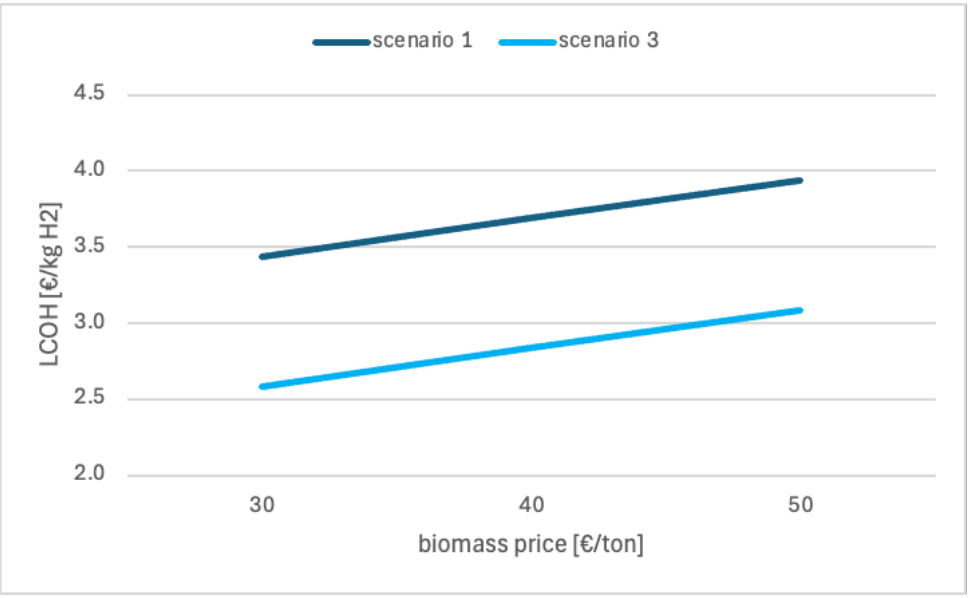

Figure 4.2: LCOH at different biomass price for scenario 1 and 3.

Biomass price [€/ton]	Annualized CAPEX [M€/y]	Net OPEX [M€/y]	LCOH [€/kg H_2]
30	29.1	32.0	3.4
40	29.1	36.4	3.7
50	29.1	40.7	3.9

Table 4.11: LCOH at different biomass price - Scenario 1.

Biomass price [€/ton]	Annualized CAPEX [M€/y]	Net OPEX [M€/y]	LCOH [€/kg H_2]
30	30.3	16.0	2.6
40	30.3	20.5	2.8
50	30.3	24.8	3.1

Table 4.12: LCOH at different biomass price - Scenario 3.

Figure 4.2 and the relative Tables 4.11 and 4.12 presents the impact of the reduction in biomass price on the achievable LCOH, for both Scenario 1 (steam purchased, CO_2 emitted) and Scenario 3 (steam purchased, CO_2 captured and sold), highlighting the critical importance of the competitiveness of the cost of feedstock.

As expected, the LCOH shows a positive correlation with biomass price in both scenarios, underlining the significant impact of feedstock costs on the overall hydrogen production cost.

Scenario 3 consistently achieves a lower LCOH compared to Scenario 1 across the entire biomass price range, mainly due to the additional revenue from CO_2 sales, which offsets part of the OPEX.

Lower biomass prices are clearly advantageous, leading to lower LCOH values and improving the overall economic feasibility of both configurations. However, the relative economic advantage of Scenario 3 becomes even more pronounced at higher biomass prices, emphasizing the role of CO_2 sales revenue in mitigating feedstock price risks. Thus, ensuring access to low-cost biomass feedstock or securing CO_2 offtake agreements becomes critical to improve project competitiveness, especially under volatile biomass market conditions.

4.5.5. Cost Breakdown Analysis

To better assess the economic drivers of the proposed configuration, a cost breakdown analysis was performed for Scenario 3, corresponding to the case with CCUS implementation and purchased steam supply. Figure 4.3(a) reports the capital expenditure (CAPEX) distribution among the main process sections. The results show that more than half of the total investment (52%) is associated with the biomass-to-syngas island, highlighting the high capital intensity of the gasification and syngas conditioning units. Compressors account for about 20% of the CAPEX, while cleaning sections and syngas-to-hydrogen units contribute 11% and 9%, respectively. Heat exchangers represent a marginal share of the investment (8%).

A more detailed breakdown of the biomass-to-syngas island (Figure 4.3(b)) confirms that the circulating fluidized bed gasifier (CFBG) and the partial oxidation (POX) reactor together dominate the section, contributing approximately 69% of the total. Feedstock handling and drying account for 14%, while the metal hot-gas filter and the HT/LT water-gas shift units contribute 5% and 12%, respectively. This distribution underlines the crucial role of the CFBG and POX units in determining the overall investment cost of the plant.

Regarding operating expenditures (OPEX), Figure 4.3(c) shows that the biomass feedstock represents the dominant contribution (65%), confirming that feed supply is the key cost driver in biomass-based hydrogen production. Electricity accounts for 7% of the OPEX, mainly due to compression requirements, while purchased steam contributes 15%. Fixed costs, including labor, maintenance, and overheads, amount to 13% of the total.

These results highlight how the economic performance of the process is strongly influenced by the cost of biomass and the capital requirements of the gasification and oxidation units. Consequently, future optimization should focus on improving the efficiency of the biomass-to-syngas conversion and on exploring strategies to reduce feedstock supply costs.

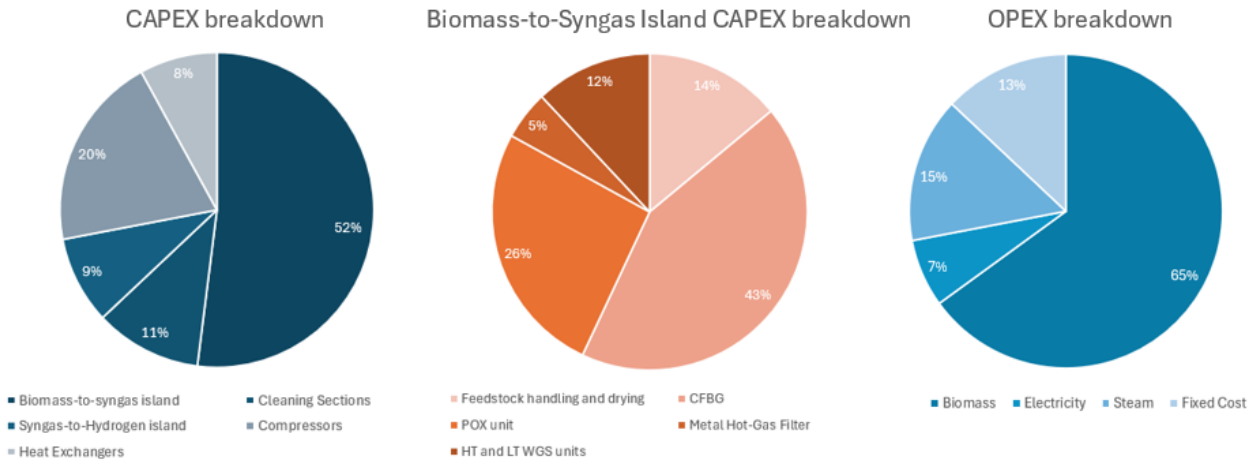

Figure 4.3: Economic breakdowns for Scenario 3: (a) CAPEX Breakdown, (b) Biomass-to-Syngas Island CAPEX Breakdown, (c) OPEX Breakdown

4.5.6. CO_2 Emissions Contribution

An analysis of the contribution of each process section to the overall CO_2 balance was carried out for Scenario 3 (CCUS with purchased steam). The main source of direct CO_2 generation is the biomass-to-syngas island, where carbon is partially oxidized in the CFBG and POX units. These reactors account for the majority of the raw CO_2 produced in the system ($\approx$ 374600 ton/y).

The syngas conditioning and cleaning sections (WGS, ZnO guard bed, SATS, AGR) do not release significant amounts of CO_2 directly, but they contribute indirectly through energy consumption for heating, cooling, and auxiliary operations. Similarly, the H_2 purification (PSA) and compression units are essentially neutral in terms of carbon conversion, yet they require considerable amounts of electricity. The same holds for purchased steam, whose carbon footprint would depend on the upstream steam generation technology.

Thanks to the implementation of CCUS, most of the CO_2 generated in the gasification and POX units is captured and compressed for storage, thereby preventing its release to the atmosphere. As a result, the residual carbon footprint of the plant is mainly associated with indirect emissions from electricity and steam supply. However, since Stegra relies on renewable energy sources, these indirect contributions do not translate into additional

fossil CO_2 emissions, further strengthening the decarbonization potential of the process.

4.6. Integration of SATS Technology for H_2S Splitting

The Sulfidric Acid Thermal Splitting (SATS) technology, developed at *Politecnico di Milano* in collaboration with *ITT SpA*, represents an innovative approach to recovering hydrogen from toxic hydrogen sulfide (H_2S) waste gases [67]. The process is based on the endothermic decomposition of H_2S into hydrogen and elemental sulfur, according to the reaction:

$$H_2S \longrightarrow H_2 + 0.5\,S_2 \qquad \Delta H_r = +20.4 \text{ kJ mol}^{-1} \tag{4.8}$$

followed by a purification stage in which the hydrogen-rich stream is cooled, condensed sulfur is separated, and purified hydrogen is recovered [67]. Unlike the conventional Claus process, which focuses exclusively on sulfur production, SATS simultaneously enables the valorization of H_2S and the generation of high-value hydrogen, which can then be reintegrated into the main production line of the plant.

From a general technological perspective, the process can be integrated into existing industrial facilities, such as natural gas sweetening units using amine washing or waste-to-fuel processes like tire pyrolysis, where H_2S is present in significant concentrations [67, 68].

The endothermic splitting of H_2S is thermodynamically promoted at high temperature and low pressure [67]. At sufficiently high temperature and residence time the reaction is highly selective to elemental products, so intermediates are negligible [67].

Significant conversion is only achieved above 900 °C, where high temperature activates the splitting and markedly increases conversion, especially at low pressure. Yet, a mechanical limit of about 1200 °C, dictated by the thermal resistance of common materials, prevents further increases. Under these conditions the maximum per-pass conversion is therefore restricted to about 38% [67]. Consequently, recycling unreacted H_2S is essential to raise overall yield. In its current TRL 6 configuration, SATS operates in the 1000 °C to 1200 °C window with typical per-pass conversions of ∼25–30%, while catalytic routes (e.g., MoS_2) are being explored to reduce the required temperature and improve kinetics [67, 68].

Overall, integrating SATS into hydrogen production pathways based on gasification or other carbonaceous feedstocks offers a promising strategy to increase efficiency, reduce emissions, and valorize sulfur-containing waste streams by recovering additional hydrogen

directly into the main production chain.

4.6.1. SATS Technology Simulation Results

A simulation analysis was carried out to evaluate the performance of the SATS technology under three reactor temperature conditions: 900 °C, 1100 °C, and 1200 °C. The process was modeled at atmospheric pressure, assuming ideal separation conditions and a constant H_2S feed of 10.43 kg h^{-1} from the ZnO bed. The SATS reactor was represented as an ideal Plug Flow Reactor (PFR), externally heated to ensure isothermal operation [67]. In this analysis, pressure drops along the reactor were neglected, while the design parameters, including a residence time of 0.5 s, were selected to ensure equilibrium conditions at the outlet and to maximize conversion.

The modeling of the SATS unit was performed with `DSmoke`, a dedicated software developed at *Politecnico di Milano* for the simulation of sulfur-containing systems. The tool is specifically designed to describe pyrolysis and thermal degradation pathways, and it includes more than 150 reactions and about 50 species related to sulfur chemistry. When extended to hydrocarbon oxidation, the framework encompasses over 2000 reactions and 150 species, enabling a detailed kinetic representation of the system. This level of description allowed reliable prediction of the reactor behavior under the selected conditions, providing insights into the effect of temperature on conversion and hydrogen recovery [67].

The results, reported in Table 4.13, show that increasing the reactor temperature significantly enhances the H_2S conversion (from 12.9% at 900 °C to 37.5% at 1200 °C). As a consequence, the amount of H_2S that needs to be recycled decreases considerably. The hydrogen output remains constant at 0.6169 kg h^{-1}, since no purge stream was considered in the system. As a result, all unreacted gases are fully recycled, and the overall H_2 production remains unchanged across all cases.

Energy demands—both for heating and compression—decrease with increasing temperature, reflecting more efficient conversion and lower recycling needs. These results confirm the thermodynamic favorability of the H_2S splitting reaction at elevated temperatures and support the integration of a recycle loop to maximize hydrogen recovery.

T react [°C]	Conversion [%]	Heating [kW]	Reactor [kW]	Cooling [kW]	Compression [kW]	H_2 Out [kg/h]	Recycle H_2S [kg/h]
900	12.9	15.42	24.91	26.95	5.344	0.6169	70.42
1100	28.3	10.27	24.95	18.97	2.452	0.6169	26.42
1200	37.5	9.044	24.96	17.14	1.858	0.6169	17.38

Table 4.13: Simulation results of the SATS technology at different reactor temperatures.

In this case, the increase in H_2 production is minimal, less than 1% compared to the previous scenario, and the revenue from sulfur sales is also relatively low. Assuming a sulfur selling price of 120 €/ton [37], as reported in Table 4.4, the amount of sulfur produced in the three scenarios is 1.27 kg/h, 2.8 kg/h, and 3.7 kg/h, corresponding to additional annual revenues of approximately 1,216 €, 2,668 €, and 3,535 €, respectively.

Although the increase in H_2 production achieved through this technology is relatively modest, the SATS technology remains advantageous, particularly when compared to implementing a separate Claus process for H_2S treatment. This is because the same reactor unit can be used, with only different operating parameters applied to handle H_2S. Instead of fully combusting it, the process involves selectively cracking H_2S, enabling the recovery of both hydrogen and elemental sulfur. Therefore, while the economic benefit naturally increases with higher H_2S concentrations in the syngas, the technology can still be favorable even at lower concentrations due to the minimal additional CAPEX required.

4.7. Comparison with Literature Studies

Several studies in the literature have estimated hydrogen production costs from biomass gasification, varying by technology type, plant scale, and feedstock cost. Table 4.14 summarizes selected examples, highlighting production costs in both €/MWh and €/kg H_2, across different gasification technologies.

Technology	H_2 output (MW)	Biomass cost [€/MWh]	Production cost [€/MWh]	Production cost [€/kg]	Ref.
Dual Fluidised Bed (DFB)	3	19.4	222	7.4	Yao et al. (2017)
Dual Fluidised Bed (DFB)	145	17.6	120	4.0	Awgustow et al. (2023)
Dual Fluidised Bed (DFB)	50	18.0	66	2.2	Binder et al. (2018)
O_2-blown Entrained Flow (EF)	630	18.0	141	4.7	Salkuyeh et al. (2018)
O_2-blown Circular Fluidised Bed (CFB)	59	10.0	137	4.6	Hannula et al. (2021)

Table 4.14: Comparison of biomass gasification technologies for hydrogen production.

Ahlström [69] reported biohydrogen production costs from thermochemical processes ranging 2.6–7.0 €/kg (78-210 €/MWh), while Borges et al. [70] reported a LCOH ranging 3.1-3.5 USD/kg (with biomass price of 42.2 UUSD/ton); both data align well with the estimates presented in Table 4.14. Biomass feedstock price plays a critical role in these costs. Lundgren et al.[21] reported that production costs can range from 2.7–4.0 €/kg (82 to 120€/MWh) assuming a biomass price of 20 €/MWh (54 €/ton), and noted that cost reductions of 10–20% are possible due to economies of scale and efficiency improvements.

The same study also evaluated the impact of CO_2 sales at 50 €/ton (same assumption reported in section 4.5.1), which would reduce the cost range to 2.2–3.5 €/kg H_2 (67–105 €/MWh).

The average hydrogen production cost from fossil-based steam methane reforming (SMR) in Europe has historically been around 2 €/kg (or 60 €/MWh). However, in 2022, due to a spike in natural gas prices, costs surged to 5.7 €/kg. By 2023, the average SMR-based hydrogen cost had declined to 3.8 €/kg as natural gas prices stabilized [21].

International Energy Agency ([19]) estimated geospatially explicit costs of the production of hydrogen from electrolysis from solar cells as well as from onshore wind power after 2040–2050, presented in Figure 4.4. It can be seen that the production cost range of biomass gasification-based hydrogen estimated in this report is highly competitive to cost ranges of various kinds of renewable electrolytic hydrogen in most parts of the world.

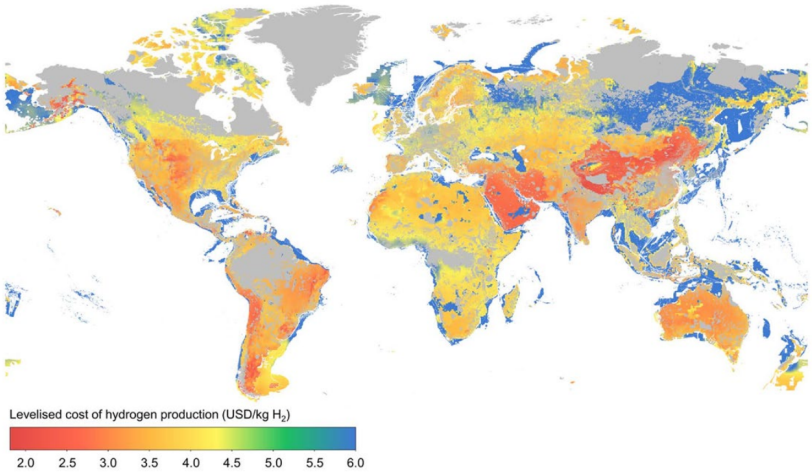

Figure 4.4: Estimated cost of hydrogen based on solar cells and onshore wind power beyond 2040–2050 (adopted by [19]).

4.8. Insights and Critical Considerations

Economic Drivers

The techno-economic analysis highlights several key insights. The choice of a CO_2 handling strategy (CCUS) strongly impacts both CAPEX and OPEX due to the additional capture and storage infrastructure. Nevertheless, it also opens the possibility of generating revenues through CO_2 utilization. Internal steam generation by recovering process excess heat proves economically favorable, especially in scenarios with high biomass prices. Among all parameters, the cost of biomass feedstock emerges as the most influential: reducing its price directly decreases the levelized cost of hydrogen (LCOH), underlining the importance of supply chain optimization and policy measures that ensure stable and affordable biomass availability.

These findings are consistent with previous techno-economic studies on biohydrogen production, which identify feedstock cost and process integration as the main drivers for achieving competitive hydrogen prices.

Hydrogen Yield Limitations

From a technical standpoint, the hydrogen yield obtained in this study is approximately 41%. Although this value may appear relatively low compared to theoretical yields or alternative process configurations, it is mainly constrained by two fundamental aspects:

(i) the low hydrogen-to-carbon ratio intrinsic to biomass compared to fossil feedstocks, and (ii) the thermodynamic limitations of the gasification and water–gas shift (WGS) reactions. Despite the application of both high- and low-temperature WGS units, the conversion of CO to H_2 remains restricted by equilibrium conditions, leading to a syngas mixture containing significant amounts of CO_2, CO, CH_4, and N_2.

Role of Steam-to-Biomass Ratio

An additional critical parameter is the steam-to-biomass ratio (S/B). Increasing this ratio enhances the extent of the WGS reaction, thereby favoring higher H_2 yields. However, it simultaneously raises the demand for steam generation, which implies greater energy consumption and operational complexity. Hence, optimizing the S/B ratio requires a careful balance between thermodynamic benefits and economic feasibility. Economically, a higher hydrogen yield would translate into more efficient utilization of biomass, a reduction in the required size of downstream equipment, and improved overall process efficiency. On the other hand, achieving such improvements would likely necessitate additional investments (e.g., in steam generation systems or advanced catalytic materials) and could increase operating costs. Although these trade-offs are not quantified in the present work, they represent relevant aspects for future techno-economic assessments.

Impact of Operating Hours

It is important to note that the annual operational time of the gasifier strongly influences the overall economics. If the annual operational time of the gasifier is reduced, the levelized cost of hydrogen (LCOH) increases. This is primarily due to the fixed capital expenditures (CAPEX) and operational expenditures (OPEX) being distributed over a smaller quantity of hydrogen produced. Since these costs do not scale down proportionally with reduced operating hours, a shorter uptime leads to a higher cost per unit of hydrogen. High utilization rates, close to the design capacity (e.g., 8000 h/year), are therefore essential to ensure economic viability in hydrogen production systems based on biomass gasification.

4.9. Why This Integration Matters for Stegra: Project Outcomes

4.9.1. Advantages of Biomass Gasification Over Electrolysis for Hydrogen Production

While both biomass gasification and water electrolysis are viable methods for hydrogen production, biomass gasification presents several distinct advantages that are particularly relevant in the context of this study.

Firstly, biomass gasification enables the use of residual and low-value feedstocks such as forestry residues, wood chips, and agricultural waste. This contributes to a circular economy by transforming waste materials into a valuable energy carrier while also supporting sustainable forest management practices. In regions like Sweden, where such biomass is abundant, this approach leverages local resources effectively.

A major advantage of gasification is its significantly lower reliance on electricity. Electrolysis is electricity-intensive and so highly dependent on electricity availability and price. In contrast, biomass gasification primarily depends on thermal energy, much of which can be internally supplied by combusting part of the biomass or syngas. Electricity consumption is limited to auxiliary systems such as pumps and compressors. This makes gasification particularly attractive in contexts where clean electricity is limited, expensive, or better used elsewhere in the energy system [71, 72].

Another key benefit is the potential for carbon-negative hydrogen production. Since biomass absorbs CO_2 from the atmosphere during its growth, combining gasification with carbon capture and storage (CCS) can result in net removal of CO_2. This contrasts with electrolysis, which is only carbon-neutral when powered by renewable electricity and does not inherently allow for negative emissions.

The use of biomass also enhances regional energy security by reducing dependence on imported fuels and centralized electricity grids. Locally sourced biomass can support decentralized hydrogen production systems that are more resilient to supply disruptions and more aligned with rural development goals.

Economically, in areas with plentiful and inexpensive biomass, gasification can offer lower operational costs than electrolysis, especially when electricity prices are volatile or high. This improves the economic feasibility of hydrogen production projects, particularly for industrial or off-grid applications [71, 72].

Additionally, although not the focus of this study, the literature notes that biomass gasification may enable the co-production of other valuable outputs, such as heat, power, or biochar. These by-products could offer added value and improve overall system efficiency in certain applications. In comparison, electrolysis yields oxygen as a by-product, which

typically has limited commercial relevance.

Finally, while not explored in this work, other studies have examined the possibility of integrating gasification-based hydrogen production with downstream synthesis of chemicals such as methanol or ammonia. Such integration may offer additional flexibility and alignment with existing industrial processes, depending on regional and economic conditions.

In summary, biomass gasification provides a robust, locally adaptable, and potentially carbon-negative route for hydrogen production. It complements the long-term role of electrolysis, particularly in biomass-rich regions and applications where thermal integration and by-product valorization are advantageous.

4.9.2. Integration of Biomass Gasification and Electrolysis for Hydrogen Production

A central focus of this work is the integration of biomass gasification and water electrolysis for hydrogen production. While each pathway has individual merits, their combination into a hybrid system offers several technical, environmental, and economic advantages that strengthen the overall feasibility and strategic value of the project.

The integration leverages the complementary nature of the two technologies. Biomass gasification provides a thermochemical route that utilizes locally available, renewable solid feedstocks such as forestry residues. It enables base-load hydrogen production and offers the potential for carbon-negative outcomes when combined with carbon capture and storage (CCS). Electrolysis, in contrast, provides a highly flexible, electrically driven route that can absorb excess renewable electricity and respond rapidly to fluctuating power markets. When operated together, the two technologies can produce hydrogen more efficiently, reliably, and sustainably than either system alone. [71].

One of the key advantages is improved operational flexibility. The gasifier can provide steady hydrogen output, while the electrolyzer can be operated dynamically based on electricity price signals or grid availability. This duality enables the system to respond to both biomass supply and electricity market conditions, enhancing its robustness and economic performance [71–73].

Another significant advantage lies in the utilization of oxygen produced during electrolysis. Oxygen, generated as a byproduct at the anode of the electrolyzer, is often vented to the atmosphere in many research and industrial applications, including, at present, in the Stegra project in Boden. However, utilizing this oxygen as a gasification agent in the

biomass gasifier and in the partial oxidation (POX) unit can enhance the quality of the produced syngas while significantly reducing the cost associated with the treatment of unwanted gases. Furthermore, eliminating the need for dedicated oxygen supply equipment, such as cryogenic air separation units, can substantially lower hydrogen production costs [72].

Environmentally, the hybrid system maximizes carbon mitigation potential. Biomass gasification, when paired with CCS, can deliver negative emissions by permanently storing biogenic CO_2. Electrolysis powered by renewable electricity produces zero-carbon hydrogen. Together, these pathways contribute to a deep decarbonization strategy aligned with long-term climate targets. From a strategic perspective, integrating these technologies enhances energy security by diversifying input resources and creating a resilient, decentralized hydrogen supply [71–73].

5 | Commercial Developments in Biomass Gasification for Hydrogen Production

Currently, no commercial-scale biomass gasification plants dedicated to hydrogen production are in operation globally. However, several technology providers offer biomass gasification solutions, and the number of announced projects for hydrogen production is growing worldwide. This reflects the increasing interest in biomass-based hydrogen as part of decarbonization strategies [21].

Selected ongoing activities and projects are summarized in the following sections, with examples shown in Figure 5.1.

Figure 5.1: Examples of technology providers and projects on gasification based biohydrogen production (adopted by [21]).

5.1. Torrgas Technology (The Netherlands)

Torrgas addresses the underutilization and harmful disposal of agricultural residues by offering a solution that transforms these wastes into valuable products, reducing pollution and enabling sustainable biofuel and chemical production. Through its innovative process, Torrgas turns biomass waste into clean syngas and biochar, contributing to climate change mitigation and circular economy strategies.

The Torrgas process, reported in Figure 5.2, starts with a mobile torrefaction unit that converts residual biomass into torrified briquettes known as *Torquettes*. These Torquettes have a significantly increased energy density, storing up to 30 times more energy than the original feedstock, which allows for highly efficient transportation [35].

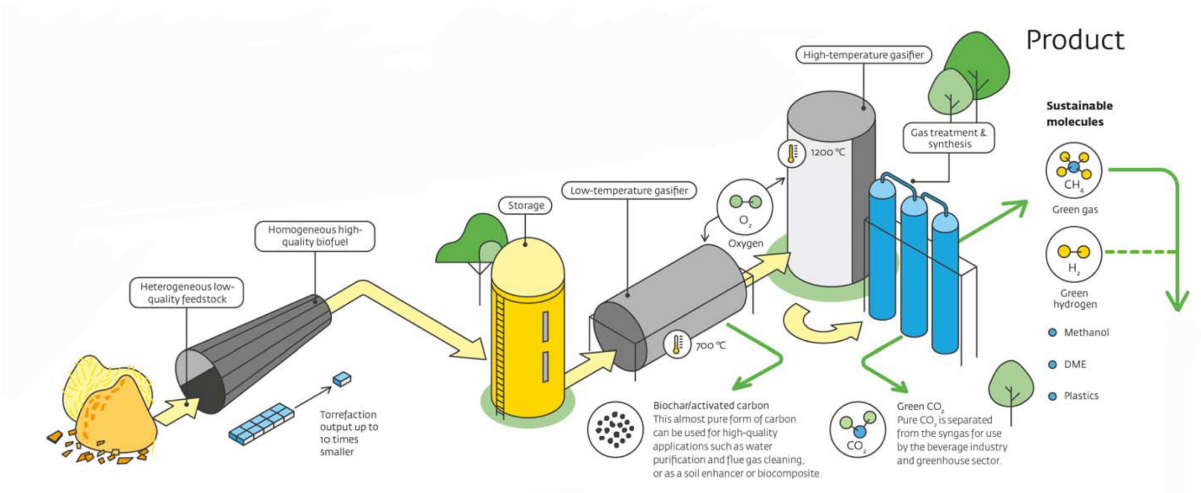

Figure 5.2: Torrgas process (adopted by [35]).

The Torquettes then enter a two-step gasification process designed by Torrgas.

In the first stage, known as low-temperature gasification, the torrefied biomass undergoes controlled thermal decomposition. This is followed by high-temperature gasification, where the remaining solids are further converted into syngas and solid by-products. This two-stage approach is specifically designed to avoid common issues associated with traditional gasification technologies, such as tar and slag formation. The resulting syngas is exceptionally clean and suitable for the production of a wide range of green chemicals and biofuels, including biomethanol, hydrogen, dimethyl ether (DME), and renewable plastics. Additionally, the process separates high-purity carbon dioxide, which can be utilized in industrial applications such as beverage production and greenhouse enrichment. The solid by-product, biochar or activated carbon, can be used for soil improvement, water purification, flue gas cleaning, or further valorized as a biocomposite material [35].

Torrgas' process thus offers a decentralized, flexible, and scalable solution to biomass valorization. By converting problematic waste streams into high-value products while minimizing environmental harm, Torrgas presents an innovative pathway that supports the transition to a low-carbon, circular economy.

5.2. Mote Process and Carbon-Negative Hydrogen Production (USA)

Mote, a U.S.-based company, is developing a first-of-a-kind technology that converts woody waste biomass into carbon-negative hydrogen while permanently sequestering CO_2 underground. This approach addresses climate goals, improves air quality, and helps mitigate wildfire risks [21].

The process, shown in Figure 5.3, begins with woody biomass that is chopped and reacted with pure oxygen in an oxygen-blown fluidized bed gasifier with temperatures of approximately 1500°F. The output of the gas mixture is separated and cleaned up to generate high-purity biohydrogen and a concentrated CO_2 stream, which is permanently stored in geological formations. Additionally, residual ash is recovered for use by fertilizer industries [74].

Mote's system captures nearly all carbon from the feedstock, ensuring no emissions while achieving high energy efficiency. Compared to alternatives like water electrolysis and Direct Air Capture, Mote's process requires significantly less capital, land, water, and electricity [74].

The company's first large-scale facility will process more than 300,000 tons of wood residue per year, producing around 21,000 tons of hydrogen and sequestering more than 450,000 tons of CO_2. This hydrogen is intended for applications in transportation and energy storage, providing a scalable pathway to carbon-negative fuels and enabling deep decarbonization of hard-to-abate sectors [74].

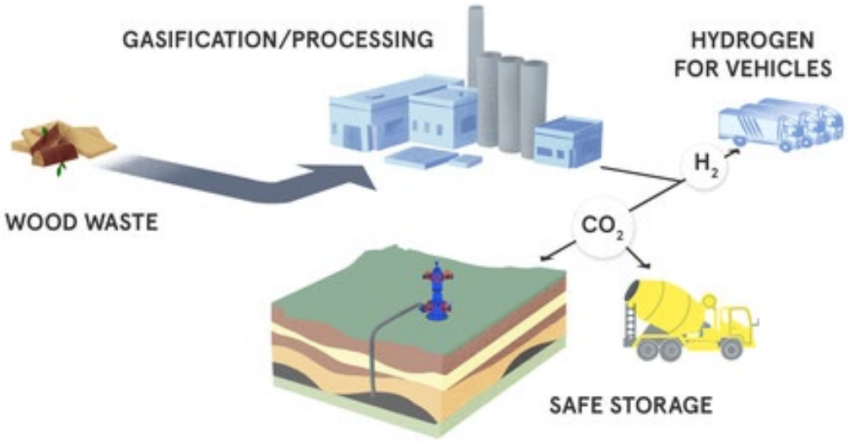

Figure 5.3: Mote hydrogen production process based on biomass gasification and CCS (adopted by [21]).

5.3. Haffner Energy Process and Biohydrogen Production

Haffner Energy, a French technology provider, aims to accelerate decarbonization through local biomass valorization, targeting the avoidance of 200 million tons of CO_2 emissions by 2034. The company's approach emphasizes short supply chains, enabling the conversion of local biomass residues into renewable hydrogen and energy for immediate use in industries and mobility applications, fostering local virtuous ecosystems[75].

Central to Haffner Energy's offering is its proprietary gasification technology, *Gasiliner®*, which distinguishes itself by its flexibility to handle diverse biomass feedstocks and its resistance to ash-related issues common in conventional gasifiers. The process involves the gasification of biochar at high temperatures (around 1000°C) with steam injection, promoting the reaction between carbon and steam to yield hydrogen and carbon monoxide ($C + H_2O \longrightarrow H_2 + CO$). The high specific surface area of biochar allows for nearly complete conversion of carbon, resulting in high process yields and minimizing ash to its inert inorganic fraction[75].

The resulting syngas, branded as *Hypergas®*, is characterized by a hydrogen content exceeding 45% by volume, a high heating value, and low impurity levels, making it a superior alternative to conventional syngases. This, after appropriate gas treatment and conversion, it is transformed into renewable hydrgen, renewable syngas, renewable methanol and sustainable aviation fuel (SAF). For practical deployment, Haffner Energy offers the

HYNOCA® solution, a turnkey package encompassing engineering, construction, and operation support to produce renewable hydrogen without reliance on electricity [75]. Figure 5.4 and 5.5 show the process design the company relies on.

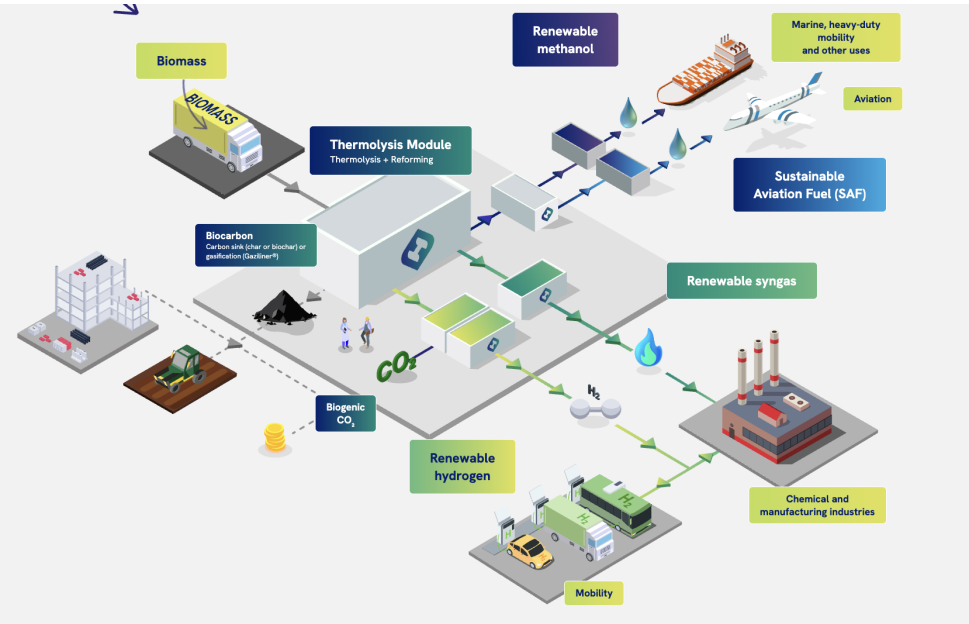

Figure 5.4: Haffner Energy Technology (adopted by [75]).

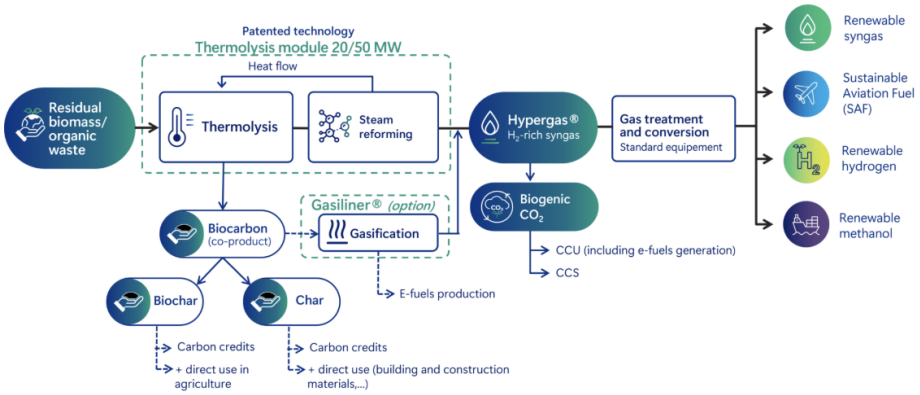

Figure 5.5: Haffner Energy simplified production process (adopted by [75]).

Haffner Energy has announced plans to establish three smaller-scale biohydrogen plants in Europe. Facilities in Gloveller (Switzerland) and Alkmaar (Netherlands) are each expected to produce 720 kg/day of hydrogen, with operations scheduled to commence in 2026. A third plant in Montbéliard (France) aims for a larger capacity exceeding 1,000 kg/day, with planned start-up in early 2027 [21].

5.4. Cortus Energy and the WoodRoll® Process (Sweden)

Founded in 2006, Cortus Energy AB, a Swedish technology company, has developed the patented WoodRoll® gasification technology to provide renewable, ultra-clean syngas as a replacement for fossil fuels in climate-intensive sectors such as the steel and transport industries. The company's goal is to support the transition to a low-carbon economy by converting low-grade biomass and waste into high-purity hydrogen-rich syngas, significantly reducing the carbon footprint of hard-to-abate sectors [76].

The WoodRoll® process is characterized by its versatility and ability to handle a wide range of biomass and waste feedstocks, including forest residues, energy crops, agricultural wastes, and industrial by-products like fiber sludge and construction waste. The process operates in a series of steps designed to ensure high efficiency and product purity [76].

Initially, the biomass is dried at around 100°C, followed by pyrolysis at approximately 400°C, producing pyrolysis gas and char. The pyrolysis gas is combusted to supply heat for both the pyrolysis and drying steps, with the resulting steam fed into the gasifier. In the high-temperature gasification stage, finely ground char reacts with steam at about 1100°C, producing a clean syngas with a hydrogen content between 55% and 60% [76].

To further maximize the hydrogen yield, a dual pressure swing adsorption (PSA) system is integrated. The first PSA extracts hydrogen directly from the syngas, while the tail gas undergoes a water-gas shift reaction to convert remaining carbon monoxide into additional hydrogen, which is recovered in the second PSA stage [21].

The technology has been demonstrated in the 6 MW WoodRoll® plant located at the Höganäs steel plant in Sweden, schematically showed in Figure 5.6.

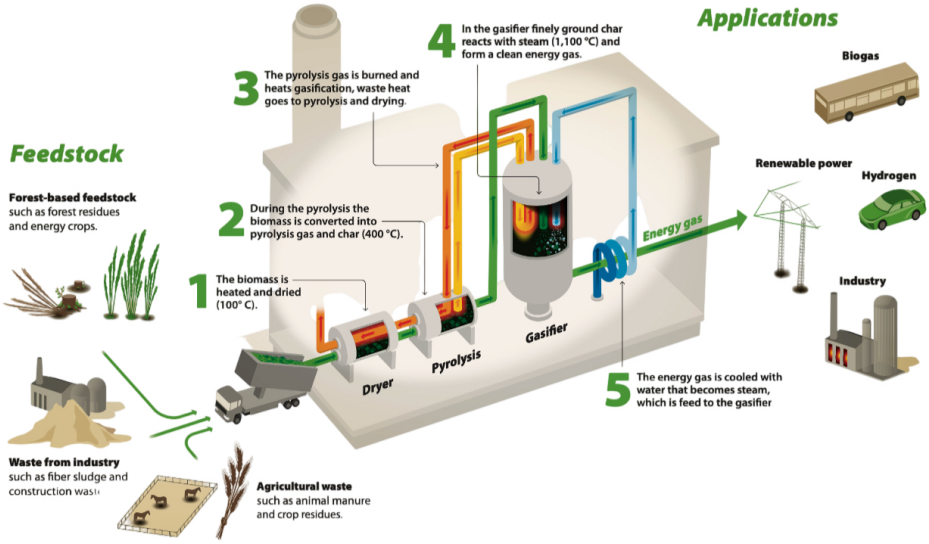

Figure 5.6: Cortus Energy process (adopted by [76]).

5.5. BtX energy GmbH (Germany)

AHT Syngas Technology NV and BtX energy GmbH are collaborating to develop a containerized solution for the production of hydrogen from pelletized biogenic residues. The project builds upon BtX's established gasification technology, known for producing clean product gas, and the Ferro-Hy-Tunnel (FHT) hydrogen separation technology, which has been successfully tested at laboratory scale but not yet applied at technical scale (Figure 5.7) [21, 77].

The objective is to optimize hydrogen content in wood-derived syngas, ensure gas purity suitable for downstream applications, and enable efficient separation of high-purity hydrogen from the product gas. Depending on the gas quality, the system is expected to produce 1 kg of hydrogen from 12–15 kg of pelletized wood residues. Upon successful demonstration, the project will deliver a mobile, containerized plant capable of producing green hydrogen from wood pellets, offering a flexible and decentralized energy solution based on a widely available renewable feedstock [21, 77].

Figure 5.7: BtX Energy test facility (adopted by [21]).

6 | Conclusions

This thesis has evaluated the techno-economic potential of integrating biomass gasification as a complementary hydrogen production route for fossil-free steelmaking, with specific reference to Stegra's DRI plant in Boden, Sweden. The results show that woody biomass gasification in a circulating fluidized bed, coupled with partial oxidation, water-gas shift, and PSA, can provide a technically viable and economically competitive supplement to electrolysis. The modeled system achieves a hydrogen yield of 40.5 kg per ton of biomass at a thermal efficiency of 58.3%, supplying around 17% of the hydrogen required by the DRI unit. The produced hydrogen meets high-purity specifications (>99.8%), making it suitable for direct use in iron reduction. Emerging technologies such as the SATS process may also enhance overall efficiency by increasing hydrogen recovery and creating additional opportunities for byproduct valorization.

From an economic perspective, the Levelized Cost of Hydrogen (LCOH) is found to be strongly dependent on biomass price, steam generation strategy, and CO_2 handling. The most favorable case—internal steam production combined with CO_2 capture and sale—achieves an LCOH of 3.6 €/kg H_2, while less favorable scenarios fall in the range of 4.5–4.7 €/kg H_2. High utilization rates (close to 8000 h/year) and secure access to affordable biomass emerge as essential conditions for competitiveness.

Although the cost of biohydrogen is slightly above that of electrolysis for Stegra, the technology brings several system-level advantages: it reduces dependence on large-scale electricity supply, allows the valorization of woody and potentially waste biomass, and can even enable carbon-negative hydrogen production when combined with CCUS. In hybrid systems, it can provide stable hydrogen output, exploit electrolytic oxygen, and increase overall flexibility.

These outcomes align with benchmarks from the literature, reinforcing the potential role of biohydrogen as a competitive and complementary low-emission pathway. Future analyses could focus on practical testing and gradual optimization of the process configuration.

Overall, this work provides evidence that biomass gasification can play a strategic role in decarbonized steelmaking, complementing electrolysis and strengthening energy sys-

tem resilience. Unlocking its full potential will require careful process integration, stable resource supply chains, and strong policy support. Within these conditions, biohydrogen can become not only a technically viable option, but also a practical enabler of the industrial energy transition.

Bibliography

[1] Peng Wang, Morten Ryberg, Yi Yang, Kuishuang Feng, Sami Kara, Michael Hauschild, and Wei-Qiang Chen. Efficiency stagnation in global steel production urges joint supply- and demand-side mitigation efforts. *Nature Communications*, 12 (2066), 2021. doi: 10.1038/s41467-021-22245-6. URL `https://doi.org/10.1038/s41467-021-22245-6`.

[2] Hannah Ritchie, Pablo Rosado, and Max Roser. Breakdown of carbon dioxide, methane and nitrous oxide emissions by sector. *Our World in Data*, 2020. https://ourworldindata.org/emissions-by-sector.

[3] Ilman Nuran Zaini, Anissa Nurdiawati, Joel Gustavsson, Wenjing Wei, Henrik Thunman, Rutger Gyllenram, Peter Samuelsson, and Weihong Yang. Decarbonising the iron and steel industries: Production of carbon-negative direct reduced iron by using biosyngas. *Energy Conversion and Management*, 281:116806, 2023. ISSN 0196-8904. doi: https://doi.org/10.1016/j.enconman.2023.116806. URL `https://www.sciencedirect.com/science/article/pii/S0196890423001528`.

[4] V. Masson-Delmotte, P. Zhai, H.-O. Pörtner, D. Roberts, J. Skea, P.R. Shukla, A. Pirani, W. Moufouma-Okia, C. Péan, R. Pidcock, S. Connors, J.B.R. Matthews, Y. Chen, X. Zhou, M.I. Gomis, E. Lonnoy, T. Maycock, M. Tignor, and T. Waterfield, editors. *Global Warming of 1.5°C. An IPCC Special Report on the impacts of global warming of 1.5°C above pre-industrial levels and related global greenhouse gas emission pathways, in the context of strengthening the global response to the threat of climate change, sustainable development, and efforts to eradicate poverty*. Cambridge University Press, Cambridge, UK and New York, NY, USA, 2018. doi: 10.1017/9781009157940.001.

[5] Pavel Afanasev, Aysylu Askarova, Tatiana Alekhina, Evgeny Popov, Strahinja Markovic, Aliya Mukhametdinova, Alexey Cheremisin, and Elena Mukhina. An overview of hydrogen production methods: Focus on hydrocarbon feedstock. *International Journal of Hydrogen Energy*, 78:805–828, 2024. ISSN 0360-3199. doi: https:

//doi.org/10.1016/j.ijhydene.2024.06.369. URL https://www.sciencedirect.com/science/article/pii/S0360319924026090.

[6] Max Åhman Valentin Vogl and Lars J. Nilsson. The making of green steel in the eu: a policy evaluation for the early commercialization phase. *Climate Policy*, 21 (1):78–92, 2021. doi: 10.1080/14693062.2020.1803040. URL https://doi.org/10.1080/14693062.2020.1803040.

[7] Robert Lundmark, Elisabeth Wetterlund, and Elias Olofsson. On the green transformation of the iron and steel industry: Market and competition aspects of hydrogen and biomass options. *Biomass and Bioenergy*, 182:107100, 2024. ISSN 0961-9534. doi: https://doi.org/10.1016/j.biombioe.2024.107100. URL https://www.sciencedirect.com/science/article/pii/S0961953424000539.

[8] Özgün Tezer, Nazlıcan Karabağ, Atakan Öngen, Can Özgür Çolpan, and Azize Ayol. Biomass gasification for sustainable energy production: A review. *International Journal of Hydrogen Energy*, 47(34):15419–15433, 2022. ISSN 0360-3199. doi: https://doi.org/10.1016/j.ijhydene.2022.02.158. URL https://www.sciencedirect.com/science/article/pii/S0360319922007728. GREEN HYDROGEN FOR GLOBAL DECARBONIZATION.

[9] Ahmed AlNouss, Gordon McKay, and Tareq Al-Ansari. A comparison of steam and oxygen fed biomass gasification through a techno-economic-environmental study. *Energy Conversion and Management*, 208:112612, 2020. ISSN 0196-8904. doi: https://doi.org/10.1016/j.enconman.2020.112612. URL https://www.sciencedirect.com/science/article/pii/S0196890420301503.

[10] Swedish Energy Agency. State aid for beccs 2022. http://www.energimyndigheten.se/en/sustainability/carbon-capture-and-storage/state-aid-for-beccs/, 2022. Accessed September 28, 2022.

[11] J. Somers. *Technologies to decarbonise the EU steel industry*. EUR 30982 EN. Publications Office of the European Union, Luxembourg, 2022. doi: 10.2760/069150. URL https://doi.org/10.2760/069150.

[12] Hannu Suopajärvi, Eva Pongrácz, and Timo Fabritius. Bioreducer use in finnish blast furnace ironmaking – analysis of co2 emission reduction potential and mitigation cost. *Applied Energy*, 124:82–93, 2014. ISSN 0306-2619. doi: https://doi.org/10.1016/j.apenergy.2014.03.008. URL https://www.sciencedirect.com/science/article/pii/S030626191400230X.

[13] H. Suopajärvi and T. Fabritius. Towards more sustainable ironmaking—an analysis

of energy wood availability in finland and the economics of charcoal production. *Sustainability*, 5:1188–1207, 2013. doi: 10.3390/su5031188. URL https://doi.org/10.3390/su5031188.

[14] H. Han, D. Duan, P. Yuan, and D. Li. Biomass reducing agent utilisation in rotary hearth furnace process for dri production. *Ironmaking & Steelmaking*, 42:579–584, 2015. doi: 10.1179/1743281215Y.0000000001. URL https://doi.org/10.1179/1743281215Y.0000000001.

[15] M. M. Carvalho, M. Cardoso, and E. K. Vakkilainen. Bio-sng production in brazil: Applications in the iron and steel industry. In *Proceedings of the 9th Japan-Brazil Symposium on Dust Processing in the Metallurgical Industry*, 2013.

[16] Duleeka Sandamali Gunarathne, Pelle Mellin, Weihong Yang, Magnus Pettersson, and Rolf Ljunggren. Performance of an effectively integrated biomass multi-stage gasification system and a steel industry heat treatment furnace. *Applied Energy*, 170:353–361, 2016. ISSN 0306-2619. doi: https://doi.org/10.1016/j.apenergy.2016.03.003. URL https://www.sciencedirect.com/science/article/pii/S0306261916303142.

[17] Chinedu M. Nwachukwu, Andrea Toffolo, and Elisabeth Wetterlund. Biomass-based gas use in swedish iron and steel industry – supply chain and process integration considerations. *Renewable Energy*, 146:2797–2811, 2020. ISSN 0960-1481. doi: https://doi.org/10.1016/j.renene.2019.08.100. URL https://www.sciencedirect.com/science/article/pii/S096014811931287X.

[18] Xianxian Xu, Quan Zhou, and Dehai Yu. The future of hydrogen energy: Bio-hydrogen production technology. *International Journal of Hydrogen Energy*, 47(79):33677–33698, 2022. ISSN 0360-3199. doi: https://doi.org/10.1016/j.ijhydene.2022.07.261. URL https://www.sciencedirect.com/science/article/pii/S0360319922033961.

[19] International Energy Agency. Global hydrogen review 2024. Technical report, IEA, Paris, 2024. URL https://www.iea.org/reports/global-hydrogen-review-2024. Licence: CC BY 4.0.

[20] Herib Blanco Emanuele Taibi, Raul Miranda (IRENA), Marcelo Carmo (Forschungszentrum Jülich). The study was supervised by Dolf Gielen, and Roland Roesch (IRENA). Green hydrogen cost reduction: Scaling up electrolysers to meet the 1.5°c climate goal, 2020. URL https://www.irena.org/publications.

[21] Joakim Lundgren, Berend Vreugdenhil, Yadi Ganjkhanlou, and Robert Baldwin.

Biomass gasification for hydrogen production. Technical report, IEA Bioenergy: Task 33, February 2025. URL https://www.ieabioenergy.com/. Copyright © 2025 IEA Bioenergy.

[22] McKinsey Energy Solutions. Global energy perspective 2023: Hydrogen outlook. Report, McKinsey & Company, 2024. URL https://www.mckinsey.com/industries/oil-and-gas/our-insights/global-energy-perspective-2023-hydrogen-outlook.

[23] Vittoria Giannini, Claudia Oehmke, Nicola Silvestri, Wendelin Wichtmann, Federico Dragoni, and Enrico Bonari. Combustibility of biomass from perennial crops cultivated on a rewetted mediterranean peatland. *Ecological Engineering*, 97:157–169, 2016. ISSN 0925-8574. doi: https://doi.org/10.1016/j.ecoleng.2016.09.008. URL https://www.sciencedirect.com/science/article/pii/S0925857416305195.

[24] Dovilė Gimžauskaitė and Andrius Tamošiūnas. Chapter 3 - biofuels production by biomass gasification. In Mejdi Jeguirim and Antonis A. Zorpas, editors, *Advances in Biofuels Production, Optimization and Applications*, pages 39–62. Elsevier, 2024. ISBN 978-0-323-95076-3. doi: https://doi.org/10.1016/B978-0-323-95076-3.00009-0. URL https://www.sciencedirect.com/science/article/pii/B9780323950763000090.

[25] Thallada Bhaskar, Bhavya Balagurumurthy, Rawel Singh, and Mukesh Kumar Poddar. Chapter 12 - thermochemical route for biohydrogen production. In Ashok Pandey, Jo-Shu Chang, Patrick C. Hallenbecka, and Christian Larroche, editors, *Biohydrogen*, pages 285–316. Elsevier, Amsterdam, 2013. ISBN 978-0-444-59555-3. doi: https://doi.org/10.1016/B978-0-444-59555-3.00012-X. URL https://www.sciencedirect.com/science/article/pii/B978044459555300012X.

[26] Virginia Pérez, Manuel Bailera, and Pilar Lisbona. Chapter 2 - syngas production by gasification processes. In Mohammad Reza Rahimpour, Mohammad Amin Makarem, and Maryam Meshksar, editors, *Advances in Synthesis Gas : Methods, Technologies and Applications*, volume 1, pages 17–46. Elsevier, 2023. ISBN 978-0-323-91871-8. doi: https://doi.org/10.1016/B978-0-323-91871-8.00020-9. URL https://www.sciencedirect.com/science/article/pii/B9780323918718000209.

[27] Pennsylvania State University. Egee 439: Alternative fuels from biomass sources. https://courses.ems.psu.edu/egee439/node/607, 2025.

[28] Mateus Paiva, Admilson Vieira, Helder T. Gomes, and Paulo Brito. Simulation of a downdraft gasifier for production of syngas from different biomass

feedstocks. *ChemEngineering*, 5(2), 2021. ISSN 2305-7084. doi: 10.3390/chemengineering5020020. URL https://www.mdpi.com/2305-7084/5/2/20.

[29] Jamison Watson, Yuanhui Zhang, Buchun Si, Wan-Ting Chen, and Raquel de Souza. Gasification of biowaste: A critical review and outlooks. *Renewable and Sustainable Energy Reviews*, 83:1–17, 2018. ISSN 1364-0321. doi: https://doi.org/10.1016/j.rser.2017.10.003. URL https://www.sciencedirect.com/science/article/pii/S1364032117313758.

[30] S.K. Sansaniwal, K. Pal, M.A. Rosen, and S.K. Tyagi. Recent advances in the development of biomass gasification technology: A comprehensive review. *Renewable and Sustainable Energy Reviews*, 72:363–384, 2017. ISSN 1364-0321. doi: https://doi.org/10.1016/j.rser.2017.01.038. URL https://www.sciencedirect.com/science/article/pii/S1364032117300394.

[31] Audrey Villot, Yves Gonthier, Evelyne Gonze, Alain Bernis, Serge Ravel, Maguelone Grateau, and Jacques Guillaudeau. Separation of particles from syngas at high-temperatures with an electrostatic precipitator. *Separation and Purification Technology*, 92:181–190, 2012. ISSN 1383-5866. doi: https://doi.org/10.1016/j.seppur.2011.04.028. URL https://www.sciencedirect.com/science/article/pii/S1383586611002528. Papers presented at European Conference on Fluid-Particle Separation (FPS 2010),.

[32] Ravneet Kaur, Poonam Gera, Mithilesh Kumar Jha, and Thallada Bhaskar. Chapter 8 - thermochemical route for biohydrogen production. In Ashok Pandey, S. Venkata Mohan, Jo-Shu Chang, Patrick C. Hallenbeck, and Christian Larroche, editors, *Biohydrogen (Second Edition)*, Biomass, Biofuels, Biochemicals, pages 187–218. Elsevier, second edition edition, 2019. ISBN 978-0-444-64203-5. doi: https://doi.org/10.1016/B978-0-444-64203-5.00008-3. URL https://www.sciencedirect.com/science/article/pii/B9780444642035000083.

[33] I. Gaetano, S. Annarita, and A. Elena. Process and apparatus for producing pure hydrogen from a syngas originated from waste gasification, 2019. International patent publication.

[34] Tamer Tawfik. System and method for production of ultra-pure hydrogen from biomass, 2019. Granted patent.

[35] Torrgas BV. Technology, 2024. URL https://www.torrgas.nl/technology/.

[36] Farooq Sher, Saman Hameed, Narcisa Smječanin Omerbegović, Alexander Chupin, Irfan Ul Hai, Bohong Wang, Yew Heng Teoh, and Magdalena Joka Yildiz. Cutting-

edge biomass gasification technologies for renewable energy generation and achieving net zero emissions. *Energy Conversion and Management*, 323:119213, 2025. ISSN 0196-8904. doi: https://doi.org/10.1016/j.enconman.2024.119213. URL https://www.sciencedirect.com/science/article/pii/S0196890424011543.

[37] Calin-Cristian Cormos. Green hydrogen production from decarbonized biomass gasification: An integrated techno-economic and environmental analysis. *Energy*, 270:126926, 2023. ISSN 0360-5442. doi: https://doi.org/10.1016/j.energy.2023.126926. URL https://www.sciencedirect.com/science/article/pii/S0360544223003201.

[38] Skogsforum. Forest map for europe - discussion on biomass gasification, 2017. URL https://skogsforum.se/viewtopic.php?f=15&t=28608. Forum post.

[39] Fredrik Hansson. Forestry meets steel. a technoeconomic study of the possible dri production using biomass. Master's thesis, Luleå University of Technology, 2015. URL https://www.diva-portal.org/smash/get/diva2:1001437/FULLTEXT01.pdf. Accessed March 27, 2025.

[40] Fatemeh Rajaee, Giulio Guandalini, Matteo C. Romano, and Jouni Ritvanen. Techno-economic evaluation of biomass-to-methanol production via circulating fluidized bed gasifier and solid oxide electrolysis cells: A comparative study. *Energy Conversion and Management*, 301:118009, 2024. ISSN 0196-8904. doi: https://doi.org/10.1016/j.enconman.2023.118009. URL https://www.sciencedirect.com/science/article/pii/S0196890423013559.

[41] Eliseo Ranzi, Michele Corbetta, Flavio Manenti, and Sauro Pierucci. Kinetic modeling of the thermal degradation and combustion of biomass. *Chemical Engineering Science*, 110:2–12, 2014. ISSN 0009-2509. doi: https://doi.org/10.1016/j.ces.2013.08.014. URL https://www.sciencedirect.com/science/article/pii/S0009250913005575. Mackie-2013 "Pushing the boundaries".

[42] L. Cabianca, Andrea Bassani, Andre Amaral, Francesco Rossi, Giulia Bozzano, Eliseo Ranzi, Dries Telen, Filip Logist, Jan Van Impe, and Flavio Manenti. Gasds: a kinetic-based package for biomass and coal gasification. *Chemical Engineering Transactions*, 50:247–252, 01 2016. doi: 10.3303/CET1650042.

[43] Guido Buzzi-Ferraris and Flavio Manenti. BzzMath: Library overview and recent advances in numerical methods. *Computer Aided Chemical Engineering*, 30(2):1312–1316, 2012.

[44] C. W. Gear. *Numerical Initial Value Problems in Ordinary Differential Equations*. Prentice Hall PTR, 1971.

[45] Rémi Demol, Miguel Ruiz, Adam Schnitzer, Olivier Herbinet, and Guillain Mauviel. Experimental and modeling investigation of partial oxidation of gasification tars. *Fuel*, 351:128990, 2023. ISSN 0016-2361. doi: https://doi.org/10.1016/j.fuel.2023.128990. URL https://www.sciencedirect.com/science/article/pii/S0016236123016034.

[46] Koyo Norinaga, Tetsuya Shoji, Shinji Kudo, and Jun ichiro Hayashi. Detailed chemical kinetic modelling of vapour-phase cracking of multi-component molecular mixtures derived from the fast pyrolysis of cellulose. *Fuel*, 103:141–150, 2013. ISSN 0016-2361. doi: https://doi.org/10.1016/j.fuel.2011.07.045. URL https://www.sciencedirect.com/science/article/pii/S0016236111004819.

[47] Philip Rößger, Ludwig Georg Seidl, Fred Compart, Johannes Hußler, Martin Gräbner, and Andreas Richter. Integrating biomass and waste into high-pressure partial oxidation processes: Thermochemical and economic multi-objective optimization. *Journal of Cleaner Production*, 358:132053, 2022. ISSN 0959-6526. doi: https://doi.org/10.1016/j.jclepro.2022.132053. URL https://www.sciencedirect.com/science/article/pii/S0959652622016602.

[48] Vincenzo Palma, Antonio Ricca, Biagio Addeo, Maurizio Rea, Gaetano Paolillo, and Paolo Ciambelli. Hydrogen production by natural gas in a compact atr-based kw-scale fuel processor. *International Journal of Hydrogen Energy*, 42(3):1579–1589, 2017. ISSN 0360-3199. doi: https://doi.org/10.1016/j.ijhydene.2016.06.049. URL https://www.sciencedirect.com/science/article/pii/S0360319916312599. The 6th European Fuel Cell Technology Applications Piero Lunghi Conference Exhibition (EFC15), 16-18 December 2015, Naples, Italy.

[49] Leila Dehimi, Oualid Alioui, Yacine Benguerba, Krishna Kumar Yadav, Javed Khan Bhutto, Ahmed M. Fallatah, Tanuj Shukla, Maha Awjan Alreshidi, Marco Balsamo, Michael Badawi, and Alessandro Erto. Hydrogen production by the water-gas shift reaction: A comprehensive review on catalysts, kinetics, and reaction mechanism. *Fuel Processing Technology*, 267:108163, 2025. ISSN 0378-3820. doi: https://doi.org/10.1016/j.fuproc.2024.108163. URL https://www.sciencedirect.com/science/article/pii/S0378382024001334.

[50] V. Gubin, D. Kadlez, A. Bartik, L. Steiner, J. Zeitlhofer, F. Thelen, H. Hofbauer, and S. Müller. Hydrogen production from woody biomass via fixed-bed gasification

at pilot-scale. *International Journal of Hydrogen Energy*, 114:462–474, 2025. ISSN 0360-3199. doi: https://doi.org/10.1016/j.ijhydene.2025.02.357. URL https://www.sciencedirect.com/science/article/pii/S0360319925009358.

[51] Air Liquide Global E&C Solutions US Inc. Lurgi Rectisol™ – The "5 in 1" Solution. https://www.engineering-airliquide.com, n.d. Flyer, Air Liquide Global E&C Solutions US Inc., 9807 Katy Freeway, Houston, TX 77024, USA.

[52] Richard A. Newby, Francis S. Lau, Rachid B. Slimane, and Suresh C. Jain. Development of the ultra-clean dry cleanup process for coal-based syngases. Technical report, Siemens Westinghouse Power Corporation and Gas Technology Institute, supported by U.S. Department of Energy, National Energy Technology Laboratory, 2002. DOE/NETL project report.

[53] Steve Rackley. Co_2 absorption. In *Negative Emissions Technologies for Climate Change Mitigation*, chapter 7, pages 109–131. Elsevier, 2023. doi: 10.1016/B978-0-12-819663-2.00009-5. URL https://doi.org/10.1016/B978-0-12-819663-2.00009-5.

[54] Carlos Arnaiz del Pozo, Schalk Cloete, and Ángel Jiménez Álvaro. Carbon-negative hydrogen: Exploring the techno-economic potential of biomass co-gasification with co2 capture. *Energy Conversion and Management*, 247:114712, 2021. ISSN 0196-8904. doi: https://doi.org/10.1016/j.enconman.2021.114712. URL https://www.sciencedirect.com/science/article/pii/S0196890421008888.

[55] Thibaut Lepage, Maroua Kammoun, Quentin Schmetz, and Aurore Richel. Biomass-to-hydrogen: A review of main routes production, processes evaluation and techno-economical assessment. *Biomass and Bioenergy*, 144:105920, 2021. ISSN 0961-9534. doi: https://doi.org/10.1016/j.biombioe.2020.105920. URL https://www.sciencedirect.com/science/article/pii/S0961953420304530.

[56] Marco Buffi, Matteo Prussi, and Nicolae Scarlat. Energy and environmental assessment of hydrogen from biomass sources: Challenges and perspectives. *Biomass and Bioenergy*, 165:106556, 2022. ISSN 0961-9534. doi: https://doi.org/10.1016/j.biombioe.2022.106556. URL https://www.sciencedirect.com/science/article/pii/S0961953422002185.

[57] Mónica P.S. Santos and Dawid P. Hanak. Techno-economic feasibility assessment of sorption enhanced gasification of municipal solid waste for hydrogen production. *International Journal of Hydrogen Energy*, 47(10):6586–6604, 2022. ISSN

0360-3199. doi: https://doi.org/10.1016/j.ijhydene.2021.12.037. URL https://www.sciencedirect.com/science/article/pii/S0360319921047376.

[58] Eric D. Larson, Haiming Jin, and Fuat E. Celik. Supporting information to "large-scale gasification-based co-production of fuels and electricity from switchgrass", 2009. URL https://doi.org/your-doi-if-available. Supporting information document to a paper in Biofuels, Bioproducts and Biorefining.

[59] Syntia L. Cotrim, Edwin V.C. Galdamez, Kennedy B. Matos, and Mauro A.S.S. Ravagnani. Heat exchanger networks synthesis considering the rigorous equipment design and distinct parameters for capital cost estimation. *Energy Conversion and Management: X*, 11:100099, 2021. ISSN 2590-1745. doi: https://doi.org/10.1016/j.ecmx.2021.100099. URL https://www.sciencedirect.com/science/article/pii/S2590174521000246.

[60] Gavin Towler and Ray Sinnott. Capital cost estimating. In *Chemical Engineering Design*, pages 239–278. Elsevier, 3rd edition, 2022. doi: 10.1016/B978-0-12-821179-3.00007-8.

[61] Zhihai Zhang, Benoit Delcroix, Olivier Rezazgui, and Patrice Mangin. Simulation and techno-economic assessment of bio-methanol production from pine biomass, biochar and pyrolysis oil. *Sustainable Energy Technologies and Assessments*, 44:101002, 2021. ISSN 2213-1388. doi: https://doi.org/10.1016/j.seta.2021.101002. URL https://www.sciencedirect.com/science/article/pii/S2213138821000126.

[62] Swedish Energy Agency. Biofuel and peat prices - swedish energy agency statistics database. https://pxexternal.energimyndigheten.se/pxweb/en/Energimyndighetens_statistikdatabas/Energimyndighetens_statistikdatabas__Officiell_energistatistik__Tradbransle_och_torvpriser/2_EN0307_2.px/, 2024.

[63] Intratec Solutions LLC. Steam cost - industry economics worldwide, 2024. URL https://www.intratec.us/products/industry-economics-worldwide/utility/steam-cost-sweden. Accessed: 2025-05-12.

[64] S. Turn, C. Kinoshita, Z. Zhang, D. Ishimura, and J. Zhou. An experimental investigation of hydrogen production from biomass gasification. *International Journal of Hydrogen Energy*, 23(8):641–648, 1998. ISSN 0360-3199. doi: https://doi.org/10.1016/S0360-3199(97)00118-3. URL https://www.sciencedirect.com/science/article/pii/S0360319997001183.

[65] Johanna Beiron, Fredrik Normann, and Filip Johnsson. A techno-economic assess-

ment of co2 capture in biomass and waste-fired combined heat and power plants – a swedish case study. *International Journal of Greenhouse Gas Control*, 118:103684, 2022. ISSN 1750-5836. doi: https://doi.org/10.1016/j.ijggc.2022.103684. URL https://www.sciencedirect.com/science/article/pii/S1750583622001025.

[66] Salvador I. Pérez-Uresti, Mariano Martín, and Arturo Jiménez-Gutiérrez. Estimation of renewable-based steam costs. *Applied Energy*, 250:1120–1131, 2019. ISSN 0306-2619. doi: https://doi.org/10.1016/j.apenergy.2019.04.189. URL https://www.sciencedirect.com/science/article/pii/S0306261919308529.

[67] Simone Caspani and Flavio Manenti. Hydrogen recovery from end-of-life tire pyrolysis gas via h2s splitting. *International Journal of Hydrogen Energy*, 144:1292–1298, 2025. ISSN 0360-3199. doi: https://doi.org/10.1016/j.ijhydene.2025.02.059. URL https://www.sciencedirect.com/science/article/pii/S036031992500624X.

[68] Politecnico di Milano, SUPER Project. Technology – super, 2024. URL https://super.chem.polimi.it/technology-3/.

[69] Johan M. Ahlström. Renewable hydrogen production from biomass. Technical report, RISE Research Institutes of Sweden, 2021. Funded by the European Union's Horizon 2020 research and innovation programme under grant agreement No 825179.

[70] Pedro Tavares Borges, Electo Eduardo Silva Lora, Osvaldo José Venturini, Marcelo Risso Errera, Diego Mauricio Yepes Maya, Yusuf Makarfi Isa, Alexander Kozlov, and Shu Zhang. A comprehensive technical, environmental, economic, and bibliometric assessment of hydrogen production through biomass gasification, including global and brazilian potentials. *Sustainability*, 16(21), 2024. ISSN 2071-1050. doi: 10.3390/su16219213. URL https://www.mdpi.com/2071-1050/16/21/9213.

[71] L. Romero-Piñeiro, A.L. Villanueva Perales, and P. Haro. Low-emission hydrogen supply chain for oil refining: Assessment of large-scale production via electrolysis and gasification. *International Journal of Hydrogen Energy*, 97:338–349, 2025. ISSN 0360-3199. doi: https://doi.org/10.1016/j.ijhydene.2024.11.448. URL https://www.sciencedirect.com/science/article/pii/S0360319924051450.

[72] Dohee Kim, Taehyun Kim, Yungeon Kim, and Jinwoo Park. Integration of biomass gasification and water electrolysis: Importance of sweep gas selection. *Applied Energy*, 393:126069, 2025. ISSN 0306-2619. doi: https://doi.org/10.1016/j.apenergy.2025.126069. URL https://www.sciencedirect.com/science/article/pii/S0306261925007998.

[73] Wenwu Xu, Lili Yang, Ziqiang Niu, Shuai Wang, Yinglong Wang, Zhaoyou Zhu,

and Peizhe Cui. Thermodynamic and economic analysis of a novel dme-power polygeneration system based on the integration of biomass gasification and alkaline electrolysis of water for hydrogen production. *Energy*, 314:134185, 2025. ISSN 0360-5442. doi: https://doi.org/10.1016/j.energy.2024.134185. URL https://www.sciencedirect.com/science/article/pii/S036054422403963X.

[74] Mote Hydrogen. Technology - mote hydrogen, 2024. URL https://www.motehydrogen.com/technology. Company website, accessed September 2025.

[75] Haffner Energy. Our expertise: Thermolyse, 2024. URL https://www.haffner-energy.com/our-expertise. Company website.

[76] Cortus Energy AB. Green technology for a sustainable future, 2024. URL https://cortus.se/. Company website.

[77] BtX energy GmbH. Bidrogen project, 2024. URL https://btx-energy.de/projekte/bidrogen/. Company website.

A | Appendix A: Inlet and Outlet Stream Compositions

This appendix provides the detailed molar composition (in mol%) and molar flow (in kmol/s) of the process streams entering and exiting each major unit operation involved in the hydrogen production process from woody biomass gasification.

A.1. Circulating Fluidized Bed Gasifier (CFBG)

Inlet Streams to the CFBG

Component	Molar Flow [kmol/s]	Molar Fraction [-]
C	0.361	0.451
H_2	0.258	0.322
O_2 (in biomass)	0.109	0.137
N_2	0.00061	0.00076
H_2O (in biomass)	0.071	0.089
S	5.29×10^{-5}	6.61×10^{-5}
Cl	0.00012	0.00015
Ash	0.00131	0.0016
Total Biomass	**0.8**	**1.0**
Additional O_2	**0.085**	**1.0**
Additional H_2O (steam)	**0.288**	**1.0**

Table A.1: Inlet molar composition to the CFB gasifier, including separately added oxygen and steam.

Gasification Reactions and Reaction Extents

To model the operation of the circulating fluidized bed gasifier (CFBG), the simulation approach was based on the study by Rajaee et al.[40], which focuses on the Varkaus

demonstration plant with a thermal biomass input of 100MW. The set of main reactions considered in the simulation is derived from the atomic matrix analysis presented in Section 3.1.3. The extent of four independent gasification reactions was evaluated from this reference, and a scaling factor of 1.5 was subsequently applied to match the 150 MW thermal input considered in this work.

Gasification Reaction	Extent of Reaction (λ)
$C + O_2 \rightarrow CO_2$	0.2459
$C + H_2O \rightarrow CO + H_2$	0.0194
$C + 2H_2 \rightarrow CH_4$	0.0254
$C + CO_2 \rightarrow 2CO$	0.1475

Table A.2: Gasification reactions and corresponding extents used in the simulation.

Outlet Stream from the CFBG (Raw Syngas)

Component	Molar Flow [kmol/s]	Molar Fraction [-]
Char	0.0165	
Ash	0.0013	
H_2	0.171	0.20
N_2	0.009	0.011
CO	0.125	0.147
CO_2	0.148	0.173
H_2O	0.344	0.404
CH_4	0.038	0.045
C_2H_4	0.0171	0.020
H_2S	8.52×10^{-5}	0.0001
HCl	8.52×10^{-5}	0.0001
NH_3	8.52×10^{-6}	0.00001
Total Syngas	**0.87**	**1.00**

Table A.3: Outlet molar composition from the CFB gasifier (raw syngas).

A.2. Partial Oxidation Unit (POX)

The partial oxidation reactor receives the raw syngas from the gasifier and a stream of pure oxygen. The table below reports the molar flow rates and molar fractions of each stream involved in the POX unit, assuming an equivalence ratio (ER) of 0.1. The other operating parameters are taken from the study of Demol et al. [45], as discussed in Section 3.1.4.

Oxygen Injection

Component	Molar Flow [kmol/s]	Molar Fraction [-]
O_2	0.0914	1.00

Table A.4: Composition of oxygen stream injected into the POX unit.

Outlet Stream from the POX Unit (Reformed Syngas)

Component	Molar Flow [kmol/s]	Molar Fraction [-]
H_2	0.179	0.185
O_2	0.010	0.010
N_2	0.054	0.056
CO	0.149	0.156
CO_2	0.158	0.164
H_2O	0.370	0.384
CH_4	0.037	0.038
C_2H_4	0.0085	0.0089
H_2S	8.52×10^{-5}	8.85×10^{-5}
HCl	8.52×10^{-5}	8.85×10^{-5}
NH_3	8.52×10^{-6}	8.85×10^{-6}
Total Syngas Out	**0.963**	**1.00**

Table A.5: Outlet molar composition from the POX unit (reformed syngas).

A.3. Water-Gas Shift Unit (HTWGS + LTWGS Combined)

The combined high-temperature and low-temperature water-gas shift reactors convert CO and H_2O to CO_2 and H_2. The following tables report the molar compositions of the streams entering and exiting the WGS unit. The CO conversion was assumed to be 97%, while the STCO equal to 2, as explained in Section 3.1.6.

Inlet Streams to the WGS Unit

Syngas Inlet

Component	Molar Flow [kmol/s]	Molar Fraction [-]
H_2	0.179	0.186
O_2	0.010	0.010
N_2	0.054	0.057
CO	0.149	0.157
CO_2	0.158	0.165
H_2O	0.370	0.390
CH_4	0.037	0.039
H_2S	8.52×10^{-3}	8.93×10^{-5}
HCl	8.52×10^{-4}	8.93×10^{-6}
NH_3	8.52×10^{-6}	8.93×10^{-6}
Total Syngas In	**0.955**	**1.00**

Table A.6: Molar composition of syngas entering the WGS unit.

Steam Inlet

Component	Molar Flow [kmol/s]	Molar Fraction [-]
H_2O	0.299	1.00

Table A.7: Molar composition of steam entering the WGS unit.

Outlet Stream from the WGS Unit

Component	Molar Flow [kmol/s]	Molar Fraction [-]
H_2	0.31	0.25
O_2	0.015	0.011
N_2	0.054	0.043
CO	0.0045	0.004
CO_2	0.303	0.242
H_2O	0.529	0.422
CH_4	0.038	0.029
HCl	8.52×10^{-4}	6.79×10^{-6}
NH_3	8.52×10^{-6}	6.79×10^{-6}
Total Syngas Out	**1.255**	**1.00**

Table A.8: Outlet molar composition from the WGS unit (after 97% CO conversion).

A.4. Main Outlet Species

Table A.9 reports the outlet molar flow rates of the main compounds leaving the process. In particular, H_2 is sent to the DRI unit, H_2S is treated in the SATS unit, CO_2 is either captured and stored or directly emitted, and H_2O is sent to treatment.

Species	Molar Flow [kmol/s]	Source
H_2	0.31	from PSA unit
CO_2	0.30	from AGR unit
H_2S	8.52×10^{-5}	from ZnO guard bed
H_2O	0.53	from condenser

Table A.9: Final molar flows of the main species and their origin.

B | Appendix B: Calculation of Steam Generation via Generator, Associated Costs, and CO_2 Capture Scenario

B.1. Case Assumption - Steam Generation

In this scenario, the steam required for the process is assumed to be generated using a biomass-fired generator. The purpose of the following calculations is not to provide a detailed design of the steam system, but rather to estimate, with sufficient accuracy, the additional biomass demand as well as the associated CAPEX and OPEX contributions.

Heat and Biomass Demand for Steam Production

The first step was to determine the thermal energy required to cover the steam demand if no heat recovery was applied. As shown in Table B.1, the steam production would require about 31.7 MW of thermal energy. Considering a boiler efficiency of 80% [37] and a biomass LHV of 9.74 MJ/kg (Table 3.2), this corresponds to a biomass consumption of about 4.1 kg/s. This value provides an upper bound of the potential biomass requirement.

Parameter	Value	Unit
Heat needed to produce steam	31.7	MW
Generator efficiency	0.8	–
Specific heat capacity of syngas (c_p)	1.2	kJ/kg·K
Biomass lower heating value (LHV)	9.74	MJ/kg
Heat input if no heat recovery	39.6	MWth
Equivalent biomass consumption	4.1	kg/s

Table B.1: Heat demand and biomass consumption for steam production without recovery.

Heat Recovery Contributions

In practice, part of the steam demand can be satisfied through process heat recovery. Table B.2 reports the estimated contributions: approximately 12.6 MW are recovered after partial oxidation and 6.2 MW from the high- and low-temperature water-gas shift (WGS) stages. This reduces the net duty to be supplied by the biomass boiler to 12.9 MW.

Heat Recovery Step	Recovered Heat	Unit
After partial oxidation (POX)	12.6	MW
From HT and LT water-gas shift (WGS)	6.2	MW
Remaining heat to be provided by generator	12.9	MW

Table B.2: Heat recovered at different process steps.

Biomass Input for Remaining Heat

To supply the remaining duty of 12.9 MW, a thermal input of about 16.2 MWth is required when considering the boiler efficiency. This translates into an additional biomass consumption of approximately 1.7 kg/s, as shown in Table B.3. This value is the incremental demand that must be sustained compared to the base case without steam generation.

Parameter	Value	Unit
Thermal input required	16.2	MWth
Equivalent biomass consumption	1.7	kg/s

Table B.3: Biomass demand for remaining heat to be generated.

CAPEX Estimation of Steam Generator

The capital cost of the biomass-fired generator was estimated using a standard scaling correlation, reported in Equation B.1. A reference cost of 6.0 M€ for a 10 MWth unit and a scaling exponent of 0.65 were assumed [40]. Scaling to the required capacity of 16.2 MWth results in a generator cost of approximately 8.2 M€ (Table B.4). This provides a rough order-of-magnitude estimation of the additional CAPEX associated with this option.

Parameter	Value	Unit
Reference cost (C_B)	6.0	M€
Reference capacity (Q_B)	10.0	MWth
Scaling exponent	0.65	–
Calculated generator cost (C)	8.2	M€

Table B.4: CAPEX estimation for the generator using a scaling law.

Formula used:

$$C_E = C_B \cdot \left(\frac{Q}{Q_B}\right)^M \quad [€] \tag{B.1}$$

where C_B is the base cost, Q_B is the reference capacity, and M is the scaling exponent

OPEX Estimation (Additional Biomass Cost)

Finally, the operational cost associated with the additional biomass required for steam generation was calculated. Assuming continuous operation (8,000 h/y) and a biomass price of 80.6 /€t (Table 4.4), the extra OPEX is estimated at about 3.7 M€/y, as reported in Table B.5.

Parameter	Value	Unit
Additional biomass cost	3 728 047	€/year

Table B.5: Estimated additional OPEX due to biomass consumption, assuming 8,000 operating hours per year and 80.6 €/ton biomass price.

—

In summary, the internal steam generation strategy requires (i) an extra biomass consumption of about 1.7 kg/s, (ii) an additional CAPEX investment of approximately 8.2 M€

for the steam generator, and (iii) an OPEX contribution of 3.7 M€/y due to biomass procurement. These values should be regarded as estimates, meant to provide an order-of-magnitude indication of the economic impact of this configuration.

B.2. Case Assumption – CO_2 Capture and Sale

If the CO_2 stream is assigned an economic value, it is assumed that 85% of the produced emissions ([21]) can be captured and sold to a negative emissions market. This assumption reflects a simplified boundary condition, where the capture rate and selling price are representative of values commonly reported in literature for bioenergy with carbon capture and storage (BECCS) projects. The objective here is not to design a detailed capture system, but to provide an order-of-magnitude estimation of the potential revenues.

Capture and Cost Assumptions

Table B.6 summarizes the key assumptions used in the calculation. Based on the process mass balances, the total CO_2 available for capture corresponds to about 318,400 t/y (Table 4.5). With an assumed capture efficiency of 85% ([21]), this amount is considered the effective stream sold to the market. The cost of capture, compression, transport, and storage was set at 50 €/tCO_2, while the selling price was assumed at 100 €/tCO_2, in line with recent literature values [21].

Parameter	Value	Unit
Amount of CO_2 captured	318,400	t_{CO_2} /y
Capture, transport, and storage cost	50	€/t_{CO_2}
Selling price	100	€/t_{CO_2}
Annual revenue	15.9	M€/y

Table B.6: Assumptions and revenues for the sale of captured CO_2.

Calculation of Net Revenue

The net economic contribution of CO_2 capture is derived by subtracting the capture and storage cost from the selling price. This gives a profit margin of 50 €/t_{CO_2}:

$$\text{Net profit per ton } CO_2 = \text{Selling price} - \text{Capture cost} = 100 - 50 = 50 \text{ €/t}_{CO_2} \quad \text{(B.2)}$$

Multiplying this margin by the annual amount of CO_2 captured provides the total revenue:

$$\text{Total revenue} = 318{,}400\ \text{t}_{CO_2}/\text{y} \times 50\ €/\text{t}_{CO_2} = 15.9\ \text{M}€/\text{y} \tag{B.3}$$

Discussion

This simplified approach shows that, under the assumed market conditions, CO_2 capture and sale can contribute nearly 16 M€/y to the project's economics. These values should be regarded as indicative: the actual profitability would depend on market dynamics for negative emissions, transport logistics, and long-term storage availability. Nevertheless, the estimation highlights the significant potential of CCUS in improving the economic competitiveness of biomass-to-hydrogen pathways.

List of Figures

List of Tables

Acronyms

AWE	Alkaline Water Electrolysis
BECCS	Bioenergy with Carbon Capture and Storage
BFBG	Bubbling Fluidized Bed Gasifier
CAPEX	Capital Expenditure
CCS	Carbon Capture and Storage
CCUS	Carbon Capture, Utilization, and Storage
CFBG	Circulating Fluidized Bed Gasifier
CH_4	Methane
CO	Carbon Monoxide
CO_2	Carbon Dioxide
DR	Direct Reduction
DRI	Direct Reduced Iron
EAF	Electric Arc Furnace
GHG	Greenhouse Gas
H_2	Hydrogen
H_2S	Hydrogen Sulfide
HBI	Hot Briquetted Iron
HDRI	Hot Direct Reduced Iron
HTWGS	High-Temperature Water-Gas Shift
LCOH	Levelized Cost of Hydrogen
LTWGS	Low-Temperature Water-Gas Shift

LHV Lower Heating Value

OPEX Operating Expenditure

PG Plasma Gasification

POX Partial Oxidation

PSA Pressure Swing Adsorption

SMR Steam Methane Reforming

STCR Steam-to-Carbon Ratio

STCOR Steam-to-CO Ratio

SATS Sulfidric Acid Thermal Splitting

TCI Total Capital Investment

TEA Techno-Economic Assessment

TRL Technology Readiness Level

WGS Water-Gas Shift

Acknowledgements

I would like to express my sincere gratitude to all the professors and supervisors who have guided and supported me throughout the development of this thesis.

First and foremost, I would like to thank Prof. Flavio Manenti (Politecnico di Milano) for his guidance and continuous support as my official supervisor at Politecnico di Milano. His availability and encouragement have been essential in the preparation and presentation of this work within my Master's degree.

I am especially grateful to Marita Nilsson (Stegra), who selected me for this project and gave me the opportunity to get to know the company and its inspiring work environment. Thanks to her, I was introduced to the industrial world and had the chance to actively participate in several company meetings, including those specifically arranged to connect me with external partners who supported my thesis work. She also made it possible for me to meet many people within Stegra and to present my final results directly to the company. Her guidance and support have been invaluable throughout this journey.

I wish to thank Prof. Klas Engvall (KTH Royal Institute of Technology), who supervised me throughout the project at KTH and also served as my examiner during the thesis presentation in Stockholm. I am grateful for the many meetings and discussions we had, as well as for the opportunity to present my work and results to his research team at the Division of Process Technology. His feedback and expertise have been invaluable in shaping this thesis.

I would also like to thank Prof. Joakim Lundgren (Luleå University of Technology), who supported this work by providing essential documentation and valuable input on the techno-economic assessment. His contribution was particularly helpful in addressing the economic aspects of the study.

Finally, I would like to thank Dr. Simone Caspani and Dr. Nicolas Iannotta (Politecnico di Milano) for their valuable technical support with the SATS and GASDS simulations, which were crucial for the process analysis. In particular, I am grateful to Simone for his availability and constructive feedback during the final stages, which greatly helped refine

and improve this thesis.

Above all, I am truly grateful for the opportunity to work on this thesis, which has been not only a valuable academic challenge but also a unique professional experience, allowing me to grow both as a student and as an engineer.

Laura Pesaresi

Milan, October 2025